Cosmological SPH simulations

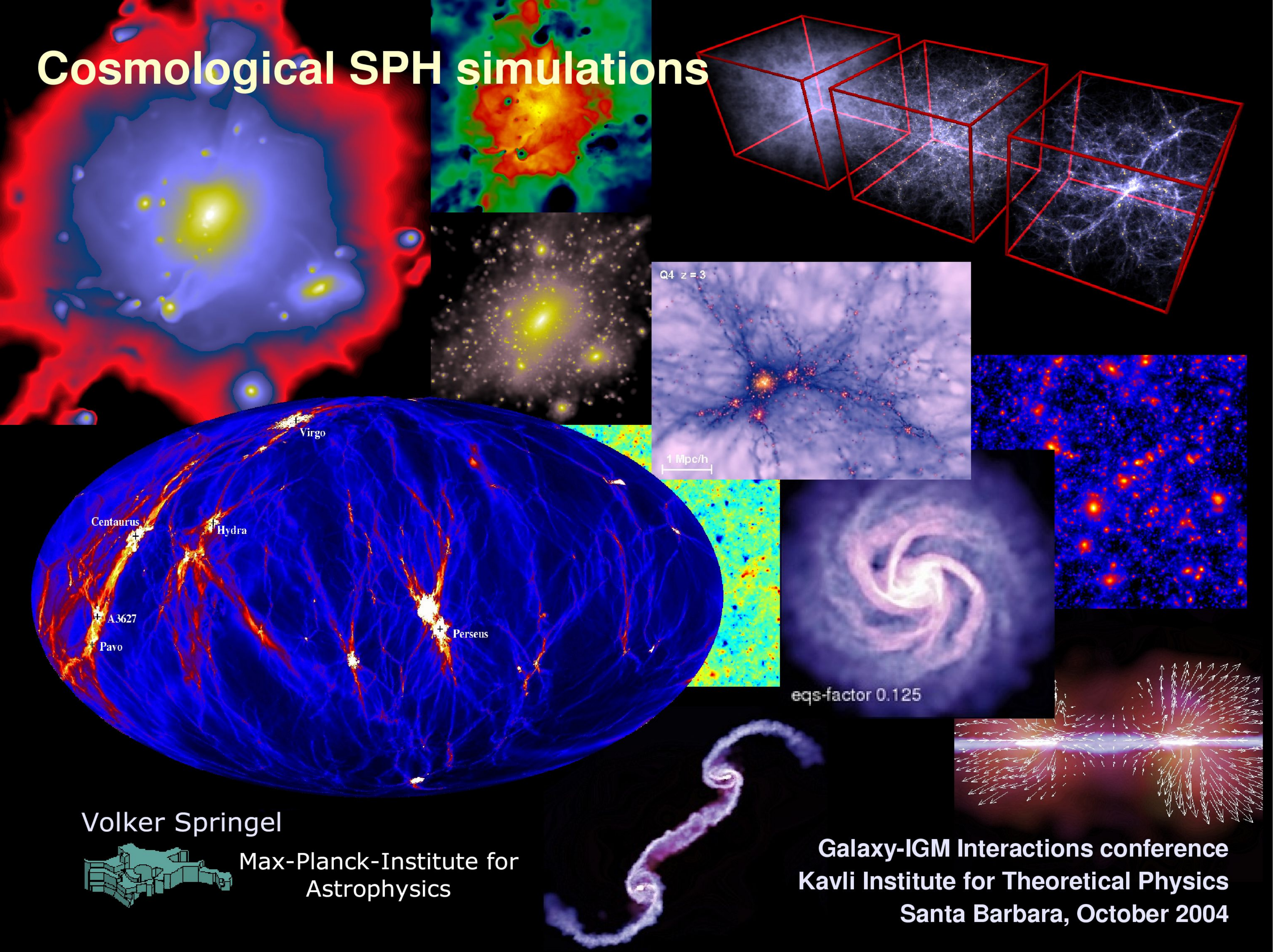

Volker Springel

Max-Planck-Institute for
Astrophysics

Galaxy-IGM Interactions conference
Kavli Institute for Theoretical Physics
Santa Barbara, October 2004

Cosmological SPH simulations

Volker Springel

- **Growth of supermassive black holes**
  - Mergers of disk galaxies with accreting black holes
  - M_B-σ relationship
  - Remnant properties

Di Matteo, Hernquist

- **Ly-alpha forest**
  - Heating of the IGM by galactic winds
  - Doppler-parameter, column densities, flux power spectrum, etc.
  - Metal enrichment of the IGM

Hernquist
Haehnelt, Viel, Bolton
Schaye, Aguirre, Furlanetto

- **Magnetic fields**
  - Cosmic magnetic field in the Local Universe
  - Deflection of UHECR

Dolag, Grasso, Tkachev

A faithful representation of cosmic structure formation requires large simulation volumes

BARYONIC DENSITY IN SIMULATIONS WITH RADIATIVE COOLING, STAR FORMATION AND FEEDBACK

Springel & Hernquist (2003)

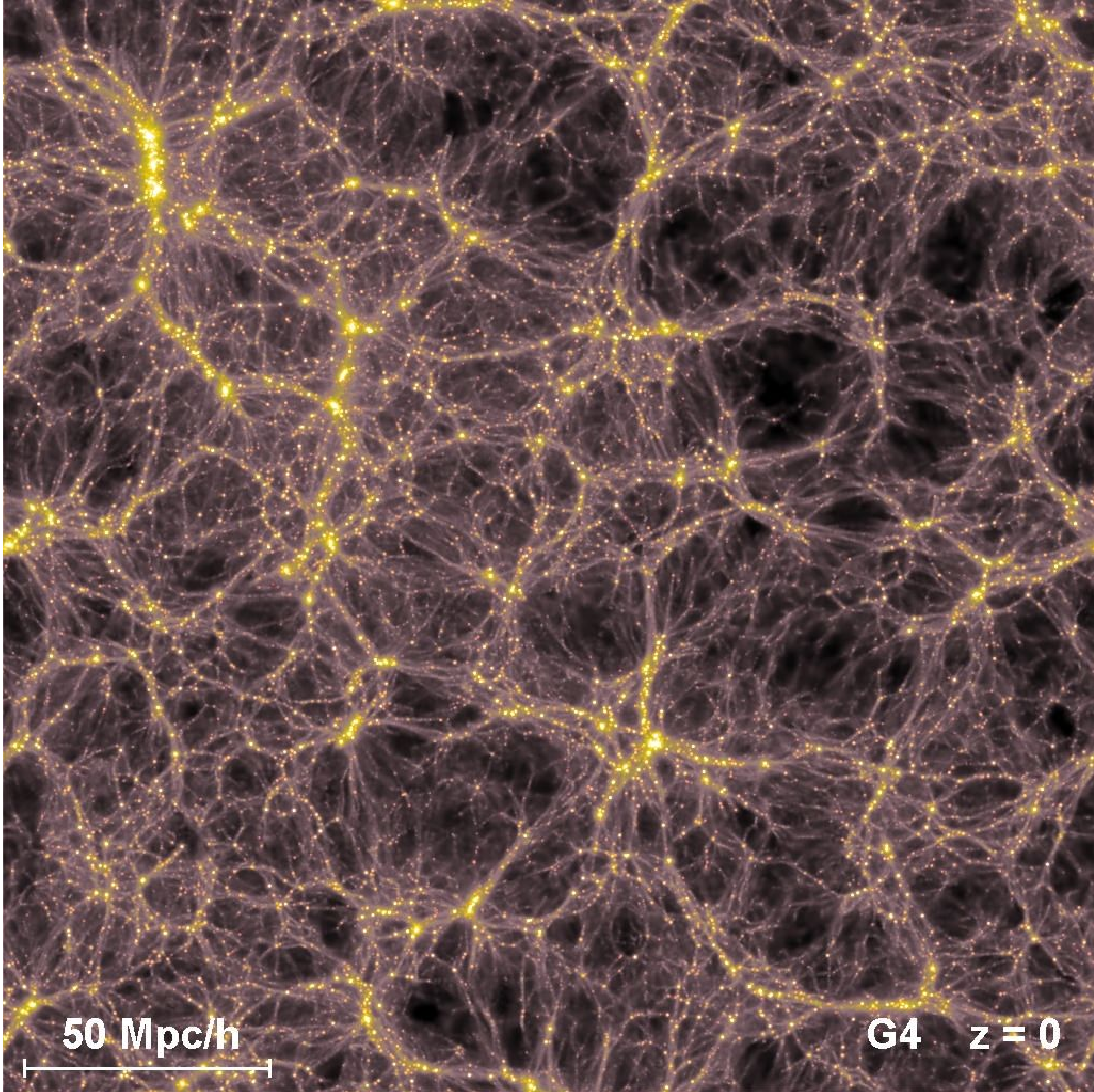

Direct simulations of star formation in cosmological volumes are very difficult

COMMON HEADACHES OF SIMULATORS OF GALAXY FORMATION

- Cooling catastrophe & overproduction of stars
- Thermal supernova-feedback fails to regulate star formation, and fails to explain metal enrichment of the IGM
- Collapse of gas halted by numerical resolution not by physics
- The real structure of the ISM is known to be multi-phase

→ *Sub-resolution multi-phase model for the ISM*
Inclusion of galactic winds

- **Required dynamic range is huge**

→ *Comprehensive set of simulations on interlocking scales*

Multi-phase subresolution model for the ISM (Springel & Hernquist 2003)

Describes cloud formation, star formation out of clouds, and evaporation of clouds by supernova explosions.

Works with an **effective equation of state** for the star-forming ISM.

Successes:

- Numerically converged prediction for the cosmic star formation history
- Moderation of the cooling catastrophy, ~10% of baryons end up in stars
- Metal enrichment of the IGM can be accounted for

But:

- Luminosity functions has steep faint-end
- Clusters have strong cooling flows

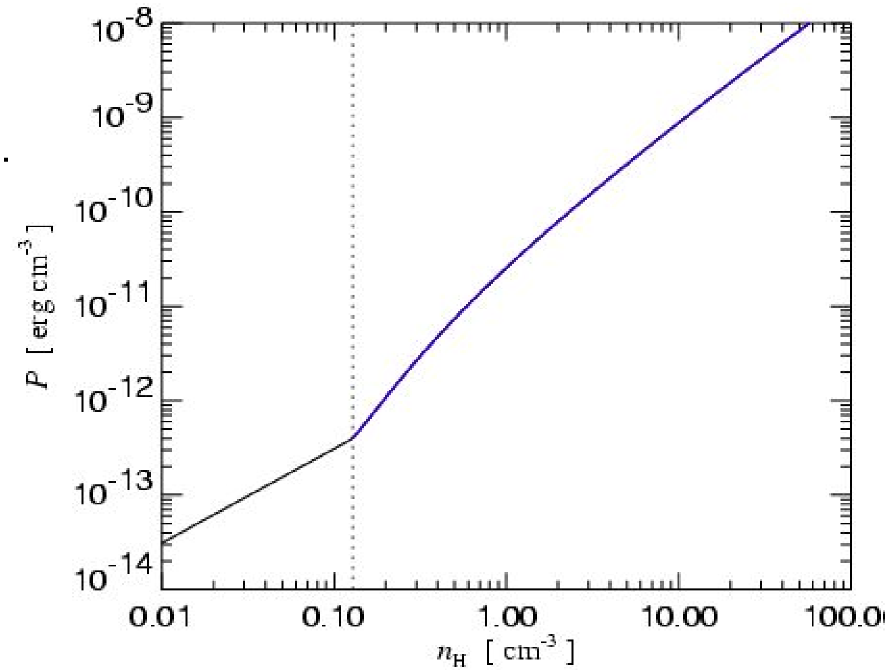

To study the star formation history, we have run a program of simulations on a set of interlocking scales and resolutions

SIMULATION PROGRAM

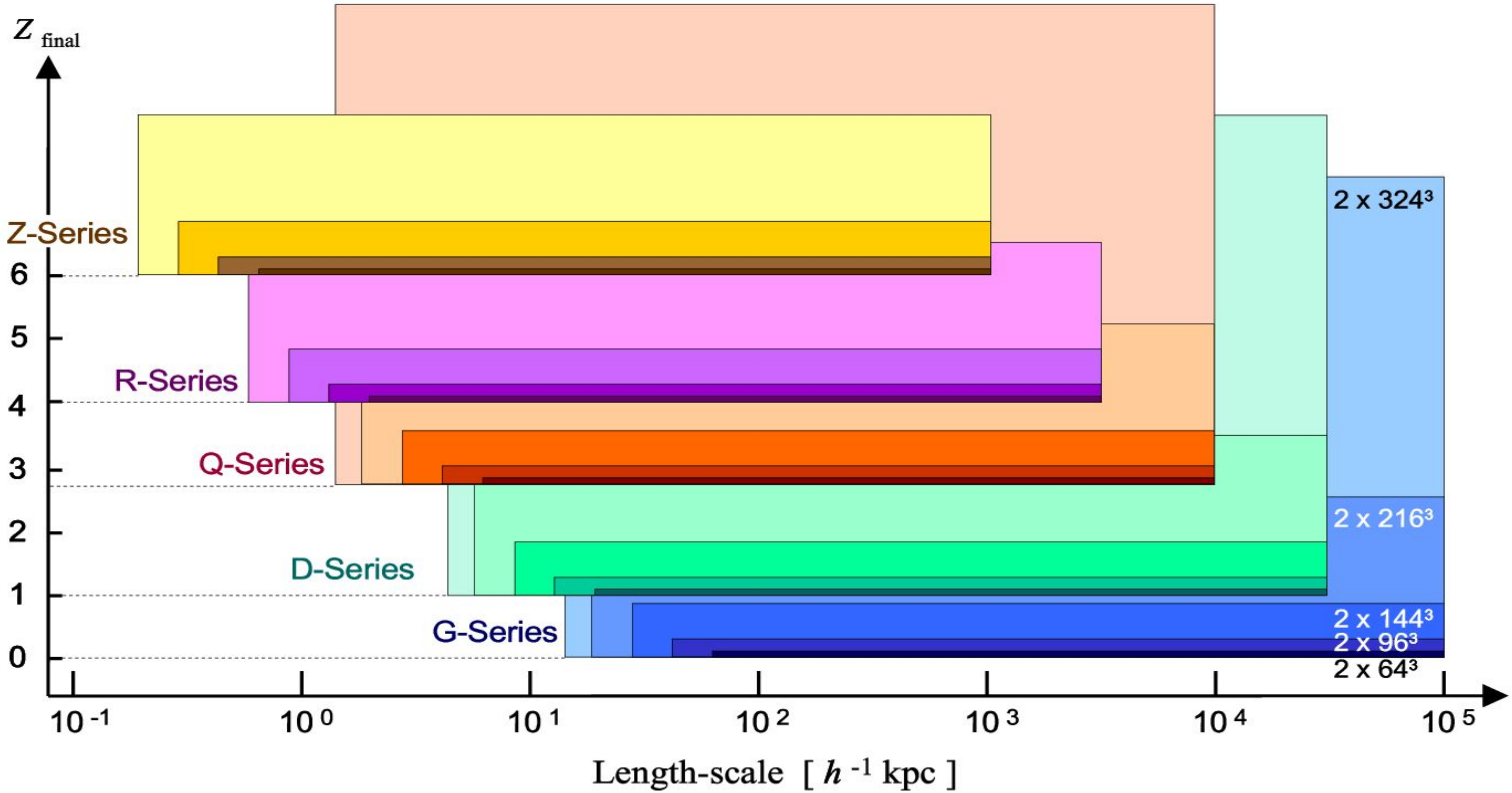

Beowulf-class computer

Configuration:

256 Athlon MP (1.6 GHz) arranged in 128 double-processor SMP nodes with 1 GB RAM each, 100 Base-T switched Ethernet, Linux

Separate frontend and 2 big fileservers

Galaxy formation and accretion on supermassive black holes appear to be closely related

BLACK HOLES MAY PLAY AN IMPORTANT ROLE IN THEORETICAL GALAXY FORMATION MODELS

Observational evidence suggests a link between BH growth and galaxy formation:

- M_B-σ relation
- Similarity between cosmic SFR history and quasar evolution

Theoretical models often assume that BH growth is self-regulated by **strong** feedback:

- Blow out of gas in the halo once a crtitical M_B is reached
  Silk & Rees (1998), Wyithe & Loeb (2003)

Feedback by AGN may:

- Solve the cooling flow riddle in clusters of galaxies
- Explain the cluster-scaling relations, e.g. the tilt of the L_x-T relation
- Explain why ellipticals are so gas-poor
- Drive metals into the IGM by quasar-driven winds
- Help to reionize the universe and surpress star formation in small galaxies

Galaxy formation models need to include the growth and feedback of black holes !

This also applies to simulations !

Sink-particles and a simple parameterization of the accretion rate are used to model the growth of black holes

THE IMPLEMENTED BLACK HOLE ACCRETION MODEL

Growth of Black Holes

Bondi-Hoyle-Lyttleton type accretion rate parameterization:

$$\dot{M}_{\rm B} = \alpha \times 4\pi R_{\rm B}^2 \, \rho \, c_s \simeq \frac{4\pi \alpha G^2 M_\bullet^2 \, \rho}{(c_s^2 + v^2)^{3/2}}$$

Limitation by the Eddington rate:

$$\dot{M}_\bullet = \min(\dot{M}_{\rm B}, \dot{M}_{\rm Edd})$$

Feedback by Black Holes

Standard radiative efficiency:

$$L_{\rm bol} = 0.1 \times \dot{M}_\bullet \, c^2$$

Thermal coupling of some fraction of the energy output to the ambient gas:

$$\dot{E}_{\rm feedback} = f \times L_{\rm bol} \qquad f \simeq 5\%$$

Implementation in SPH simulation code

Additions in the parallel GADGET-2 code:

- BH sink particles swallow gas stochastically from their local neighbourhoods, in accordance with the estimated BH accretion rate
- Feedback energy is injected locally into the thermal reservoir of gas
- On-the-fly FOF halo finder detects emerging galaxies and provides them with a seed black hole
- BHs are merged if they reach small separations and low enough relative speeds

We construct compound disk galaxies that are in dynamical equilibrium

STRUCTURAL PROPERTIES OF MODEL GALAXIES

Components:

- Dark halo (Hernquist profile matched to NFW halo)
- Stellar disk (expontial)
- Stellar bulge
- Gaseous disk (expontial)
- Central supermassive black hole (small seed mass)

We compute the exact gravitational potential for the axisymmetric mass distribution and solve the Jeans equations

Gas pressure effects are included

The gaseous scale-height is allowed to vary with radius

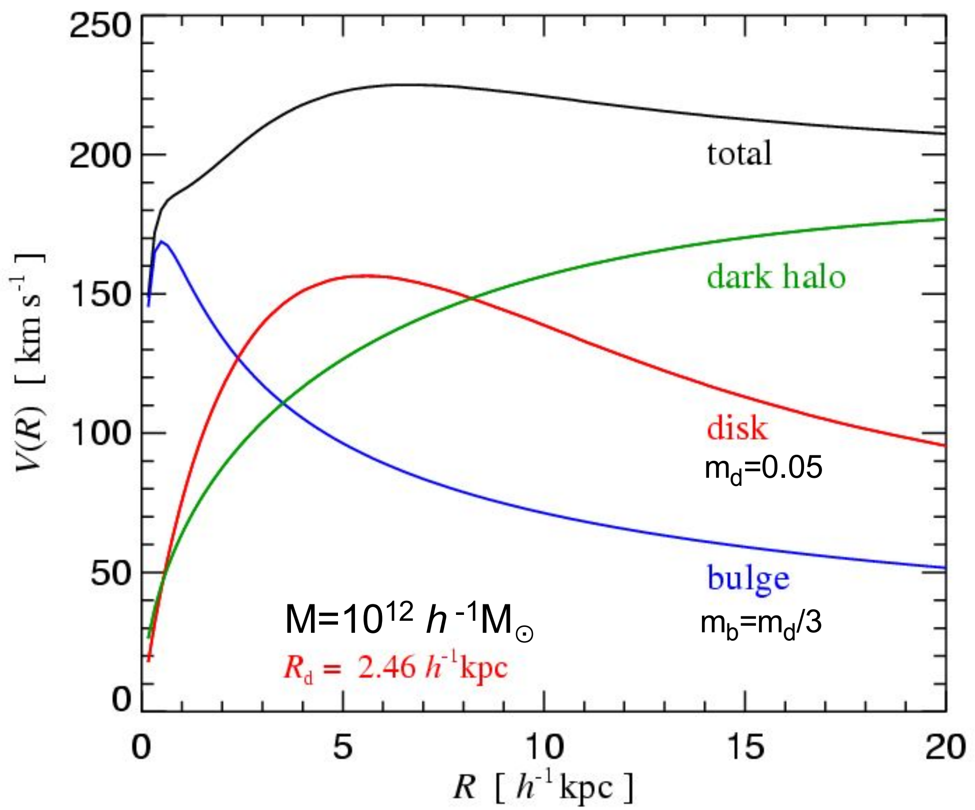

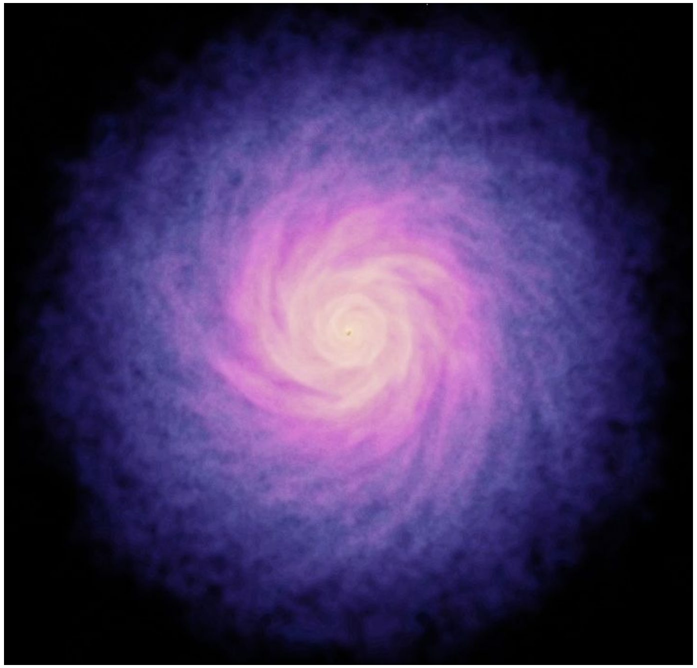

The multiphase-model allows stable disk galaxies even for very high gas surface densities

STABILITY OF DISKS AS A FUNCTION OF GAS FRACTION AND EQUATION OF STATE

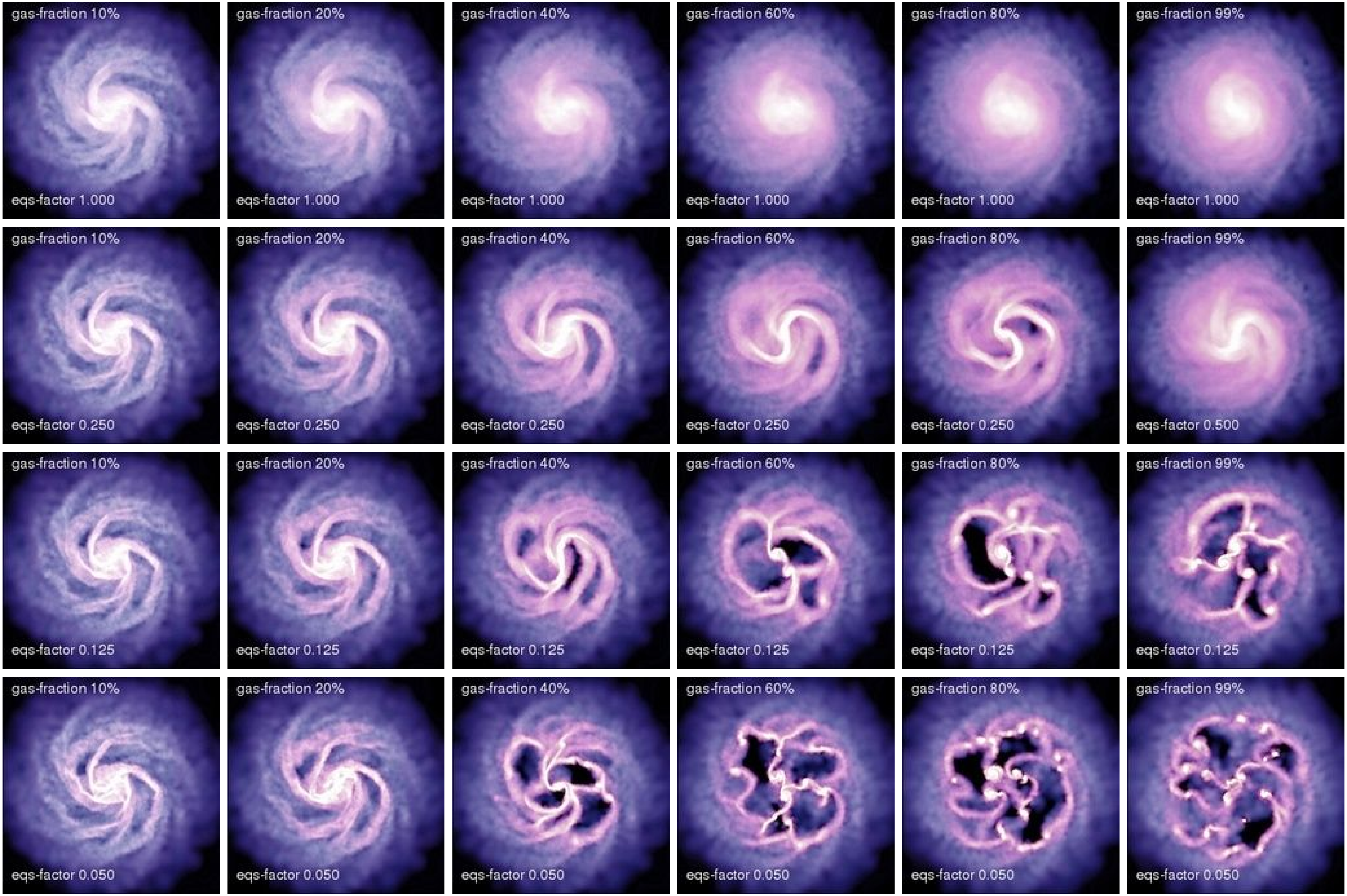

Growth rate of black holes in isolated galaxies

THREE PHASES OF BLACK HOLE GROWTH

Bondi-growth:

$$\dot{M}(t) = \frac{M_0}{1 - 4\pi\alpha\rho G^2 M_0 t/c^3}$$

Eddington-growth:

$$\dot{M}(t) = M_0 \exp\left(\frac{t}{t_\mathrm{S}}\right)$$

Slow, feedback regulated growth:

$$\frac{\mathrm{d}E_\mathrm{cool}}{\mathrm{d}t} = \Lambda(T)\,\rho\,M_\mathrm{gas}$$

$$\frac{\mathrm{d}E_\mathrm{heat}}{\mathrm{d}t} = 0.1 f \dot{M} c^2 \propto \frac{\rho M_\mathrm{B}^2}{T^{3/2}}$$

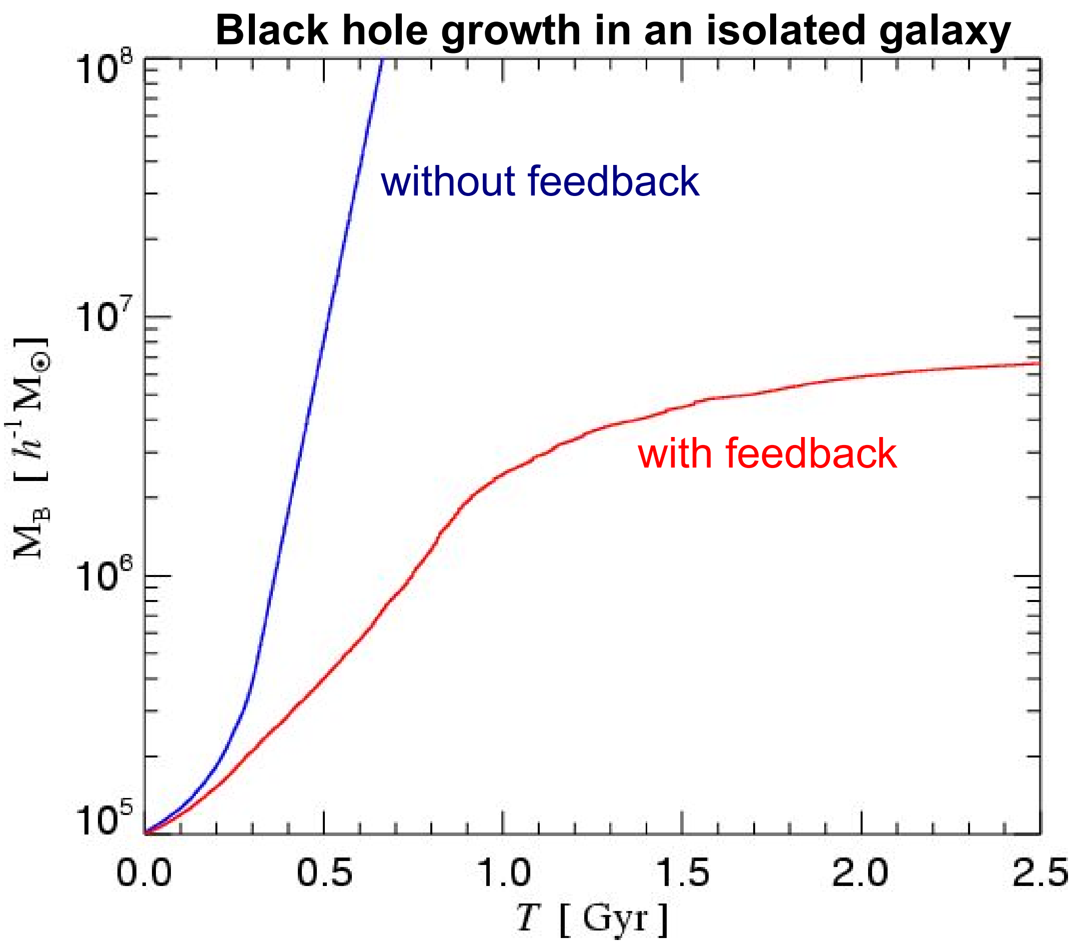

- **T_{equal}** independent of density
- for: $T_\mathrm{equal} \simeq T_\mathrm{vir}, \;\; M_\mathrm{gas} \propto M_\mathrm{halo}$

$$M_\mathrm{B} \propto V_\mathrm{vir}^{7/2}$$

- If **T_{equal} >> T_{vir}**, the hole is too big for the halo. It can blow gas out of the halo until there is none left.

In larger galaxies, black holes grow to progressively larger sizes before feedback throttles the growth rate

GROWTH OF BLACK HOLES IN ISOLATED GALAXIES AS A FUNCTION OF GALAXY SIZE

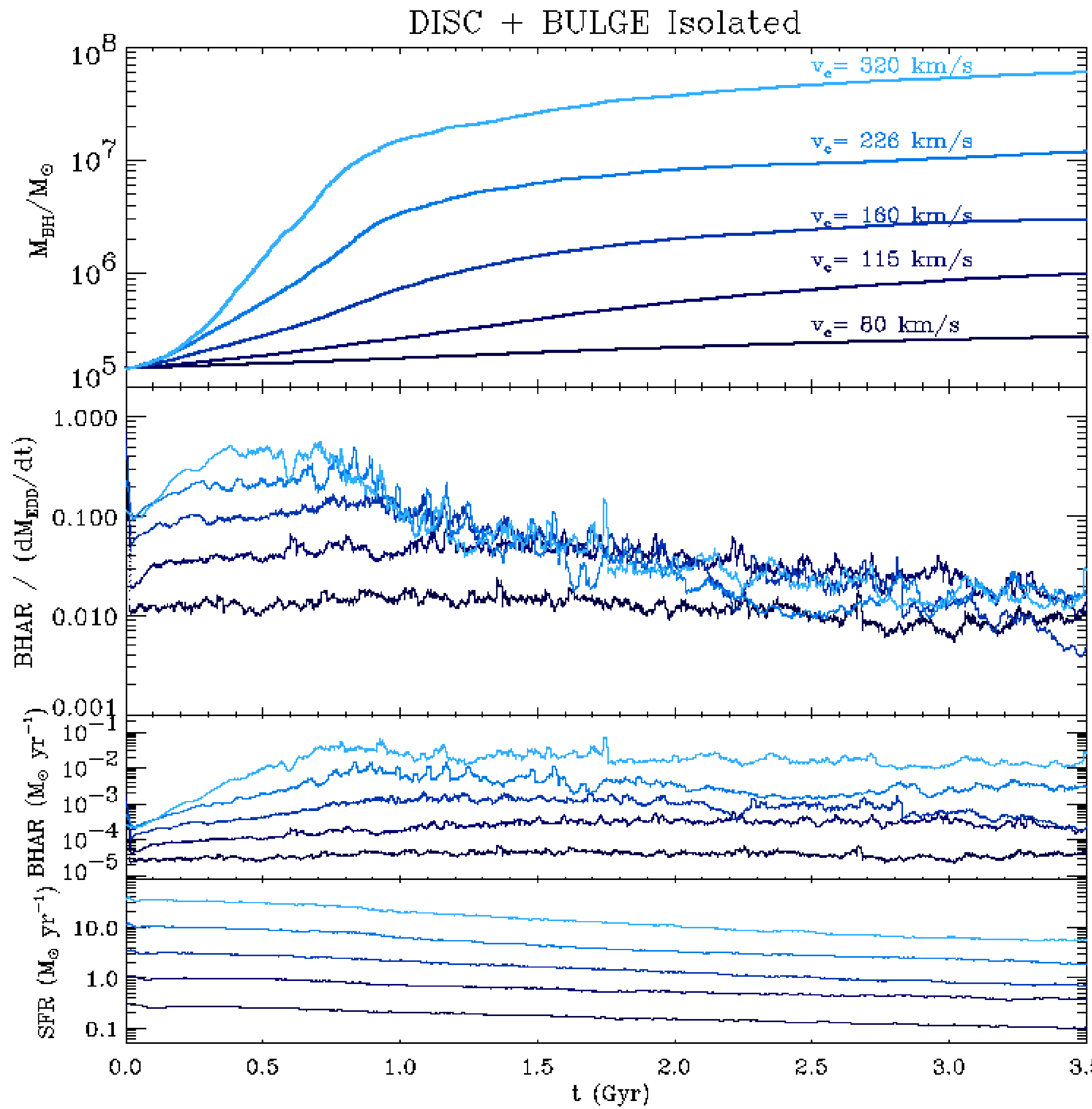

In major-mergers between two disk galaxies, tidal torques extract angular momentum from cold gas, providing fuel for nuclear starbursts

TIME EVOLUTION OF A PROGRADE MAJOR MERGER

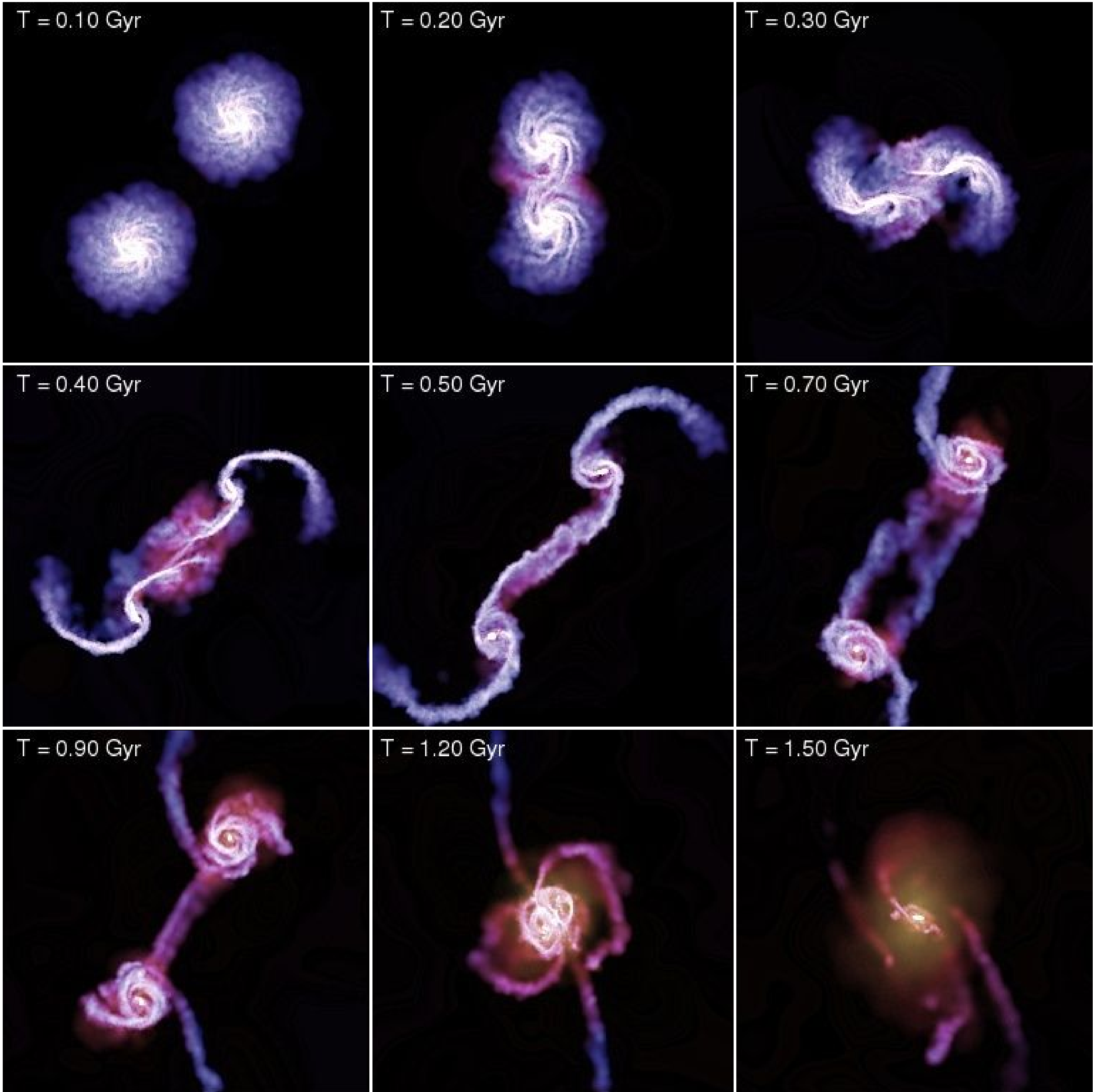

This may also fuel a central AGN !

In mergers with supermassive black holes, simultaneous feeding of nuclear starbursts and central AGN activity occurs

TIME EVOLUTION OF A MERGER WITH CENTRAL BLACK HOLE ACCRETION

A movie of the merger of two gas rich sprirals with central black holes

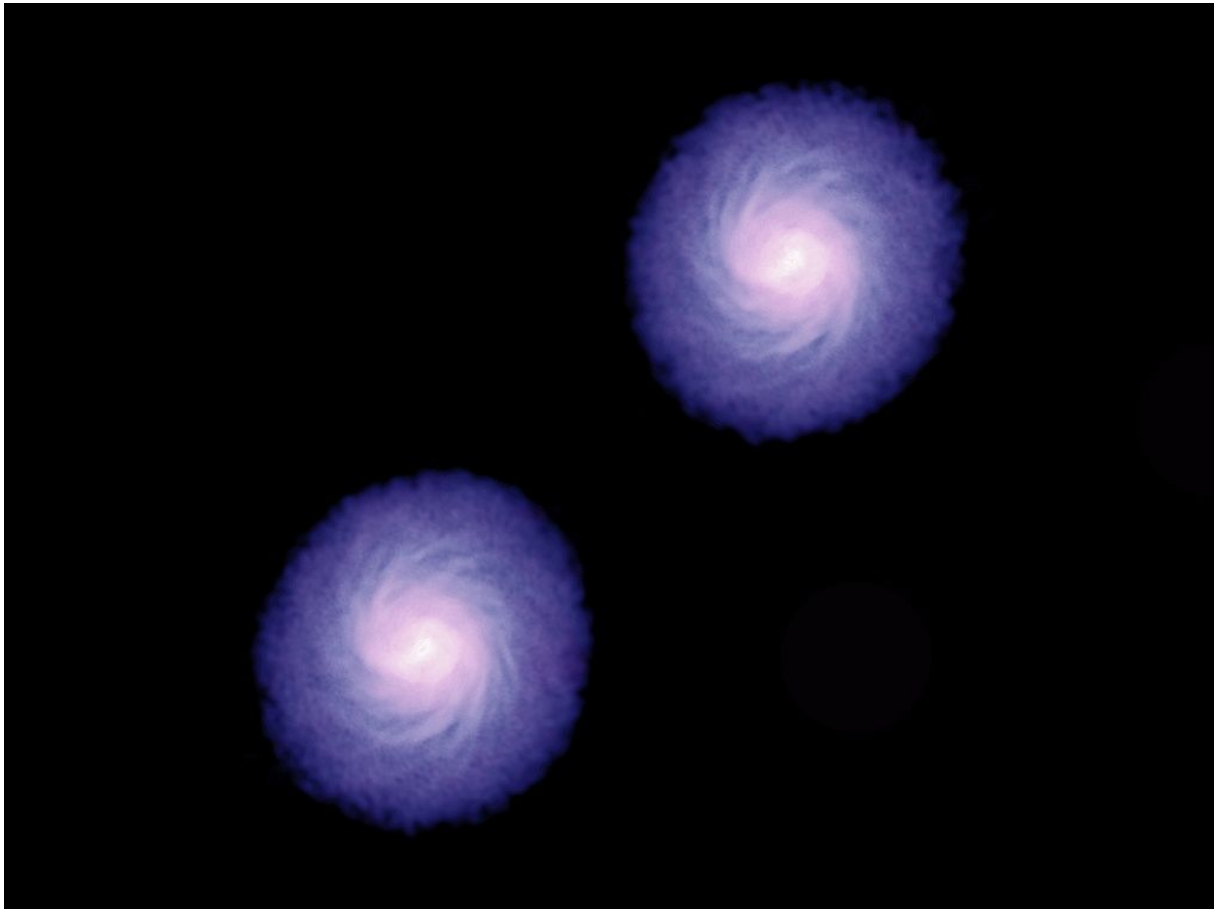

Mergers of disk galaxies trigger starburts and ignite central AGN activity

TIME EVOLUTION OF STAR FORMATION RATE AND BLACK HOLE GROWTH IN A MERGER

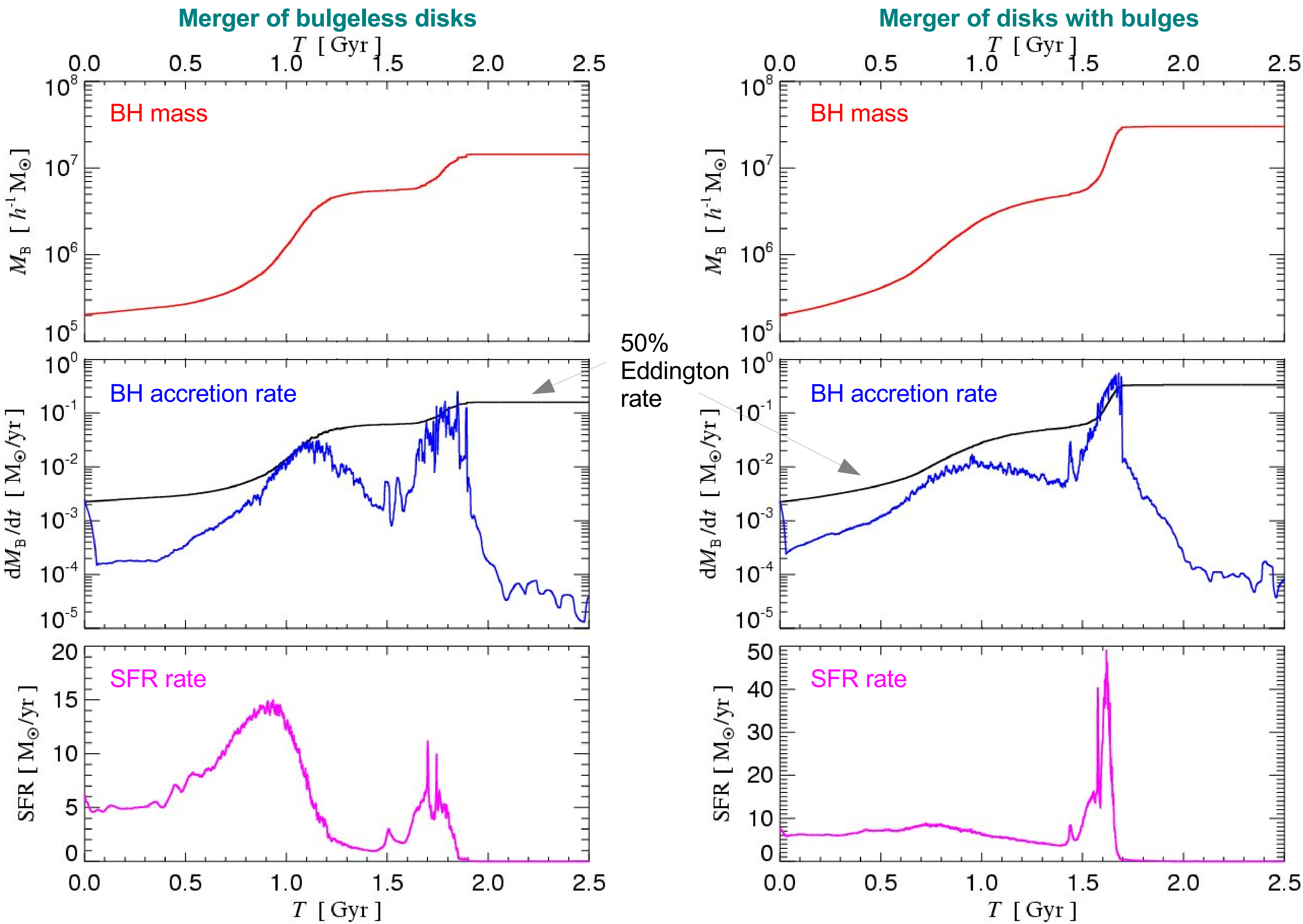

The relation between final black hole mass and stellar velocity dispersion follows a Magorrian-type relationship

BLACK HOLE MASSES IN MERGER REMNANTS

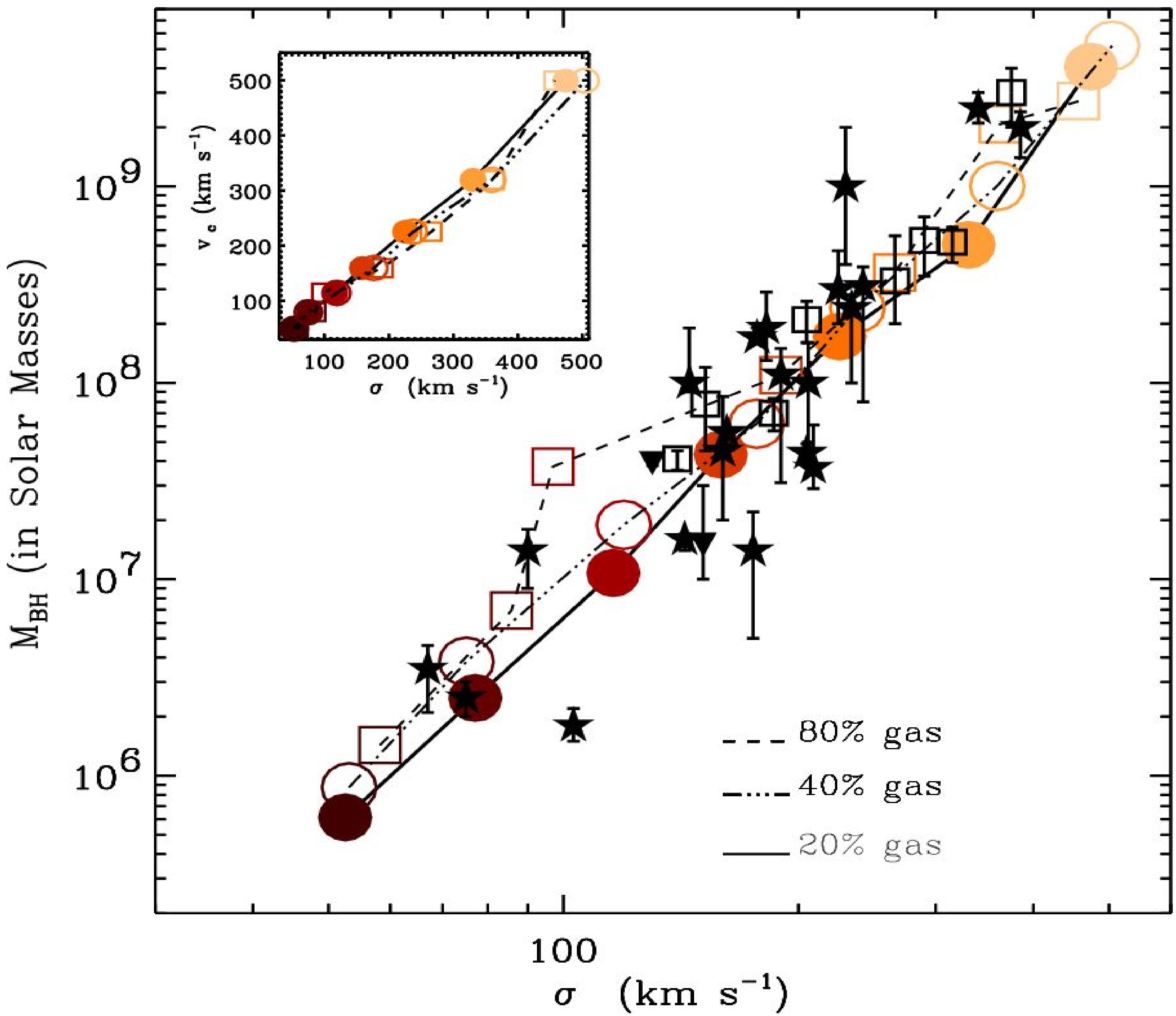

At low accretion rates, feedback by the central black hole activity may blow a weak wind into the halo

GAS FLOW INTO THE HALO

Isolated disk galaxy with bulge

Generated hot halos holds 1-2% of the gas

(dynamic range in gas surface density ~10^6)

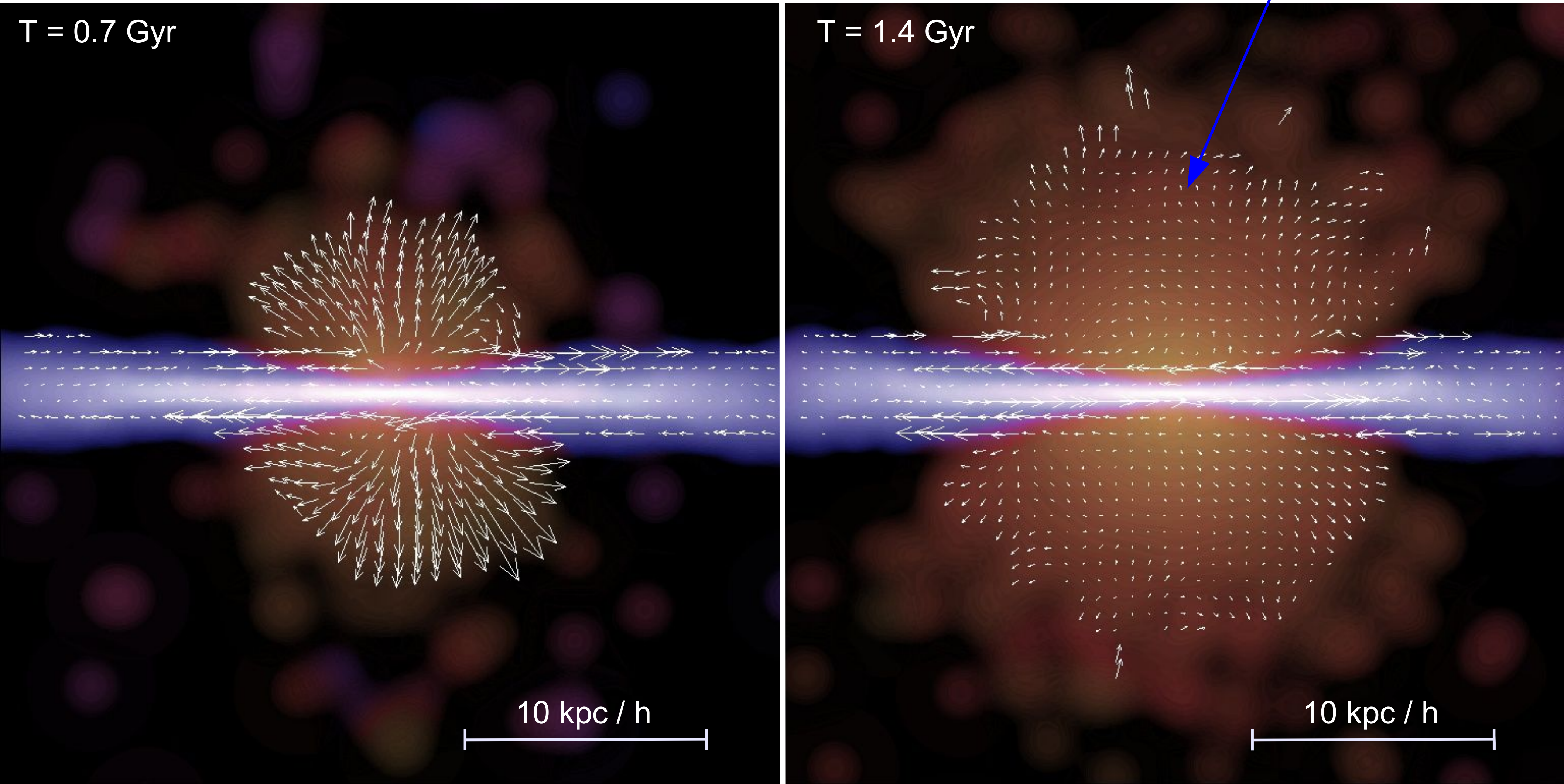

The feedback by the central black activity may drive a strong quasar wind

GAS OUTFLOW BY AGN FEEDBACK

(outflow reaches speeds of up to ~1800 km/sec)

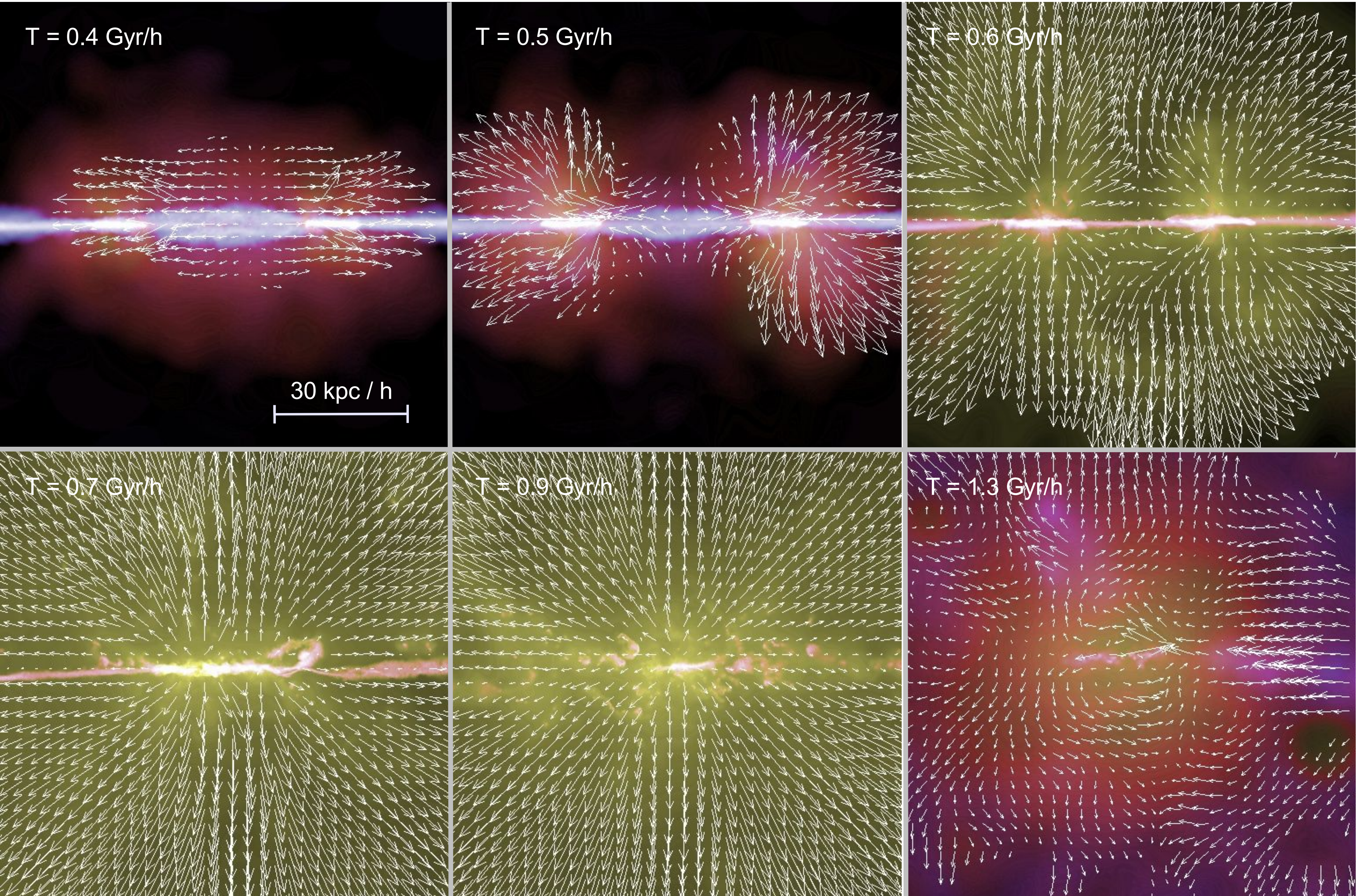

A series of merger simulations is used to test how sensitive the black hole feeding is to the orbital geometry

ENCOUNTER GEOMETRIES

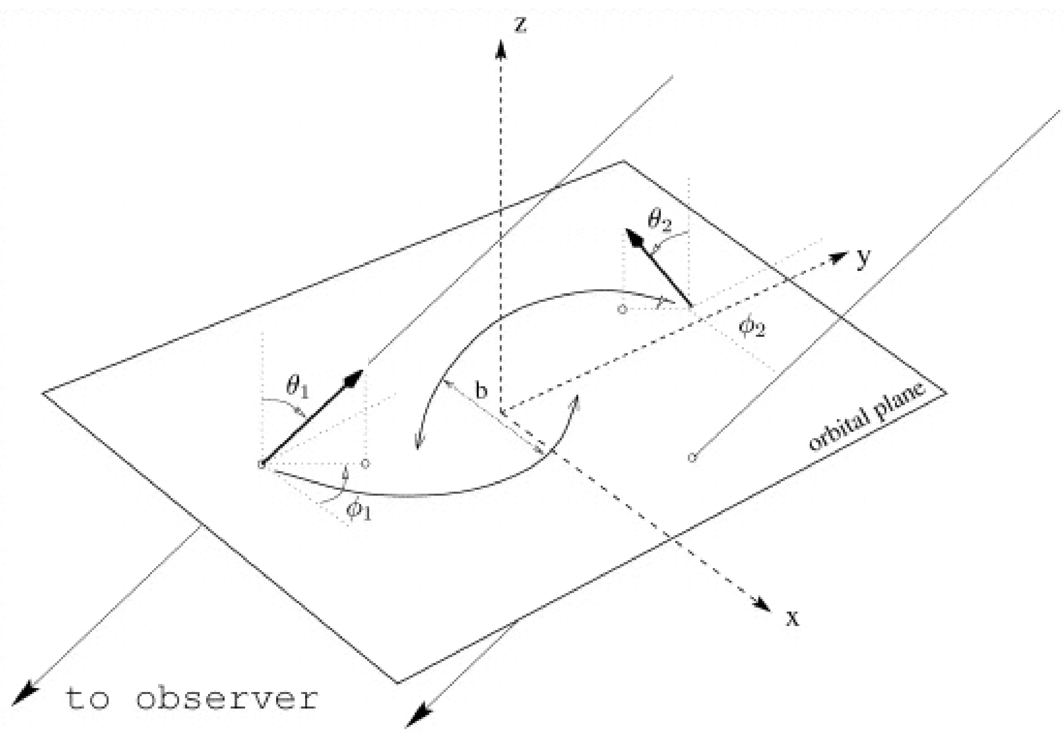

run	θ_1	ϕ_1	θ_2	ϕ_2
0	180.0	0.0	0.0	0.0
1	180.0	0.0	180.0	0.0
2	93.2	123.9	150.5	246.3
3	85.5	135.2	133.2	37.2
4	61.7	167.3	33.8	158.0
5	128.6	47.2	141.8	35.1
6	9.2	282.9	81.9	229.5
7	86.5	88.3	46.5	290.7
8	147.5	118.5	36.8	357.6
9	57.4	162.0	50.9	19.0
10	120.3	196.6	95.5	224.5
11	162.5	126.6	128.8	192.4

The orientation of the galaxies in the merger affects the accretion pattern

BLACK HOLE ACCRETION RATE FOR DIFFERENT GALAXY ORIENTATIONS

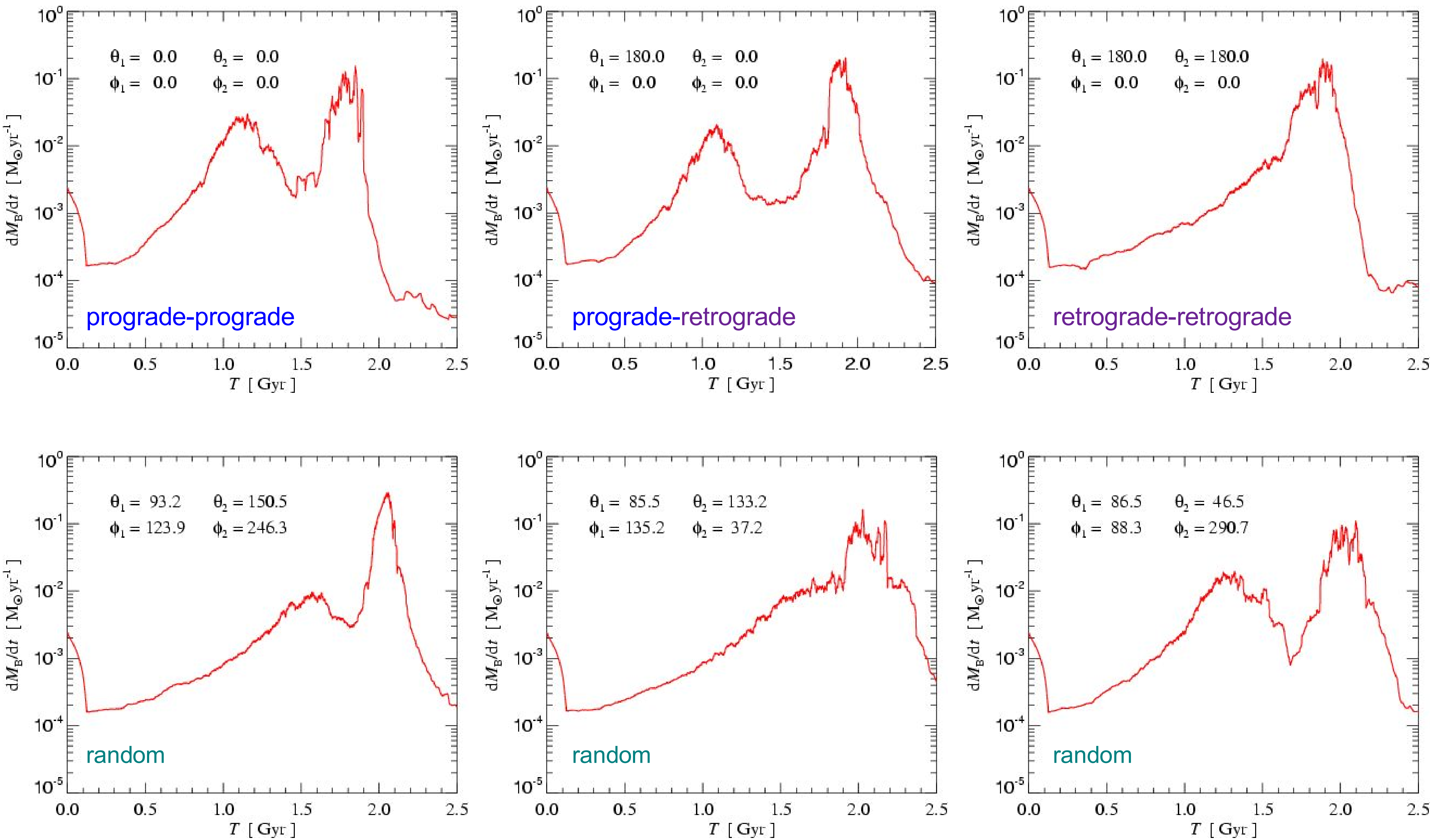

The final black hole mass in the merger remnant is not very sensitive to details of the orbit of the collision

BLACK HOLE MASS FOR DIFFERENT GALAXY ORIENTATIONS

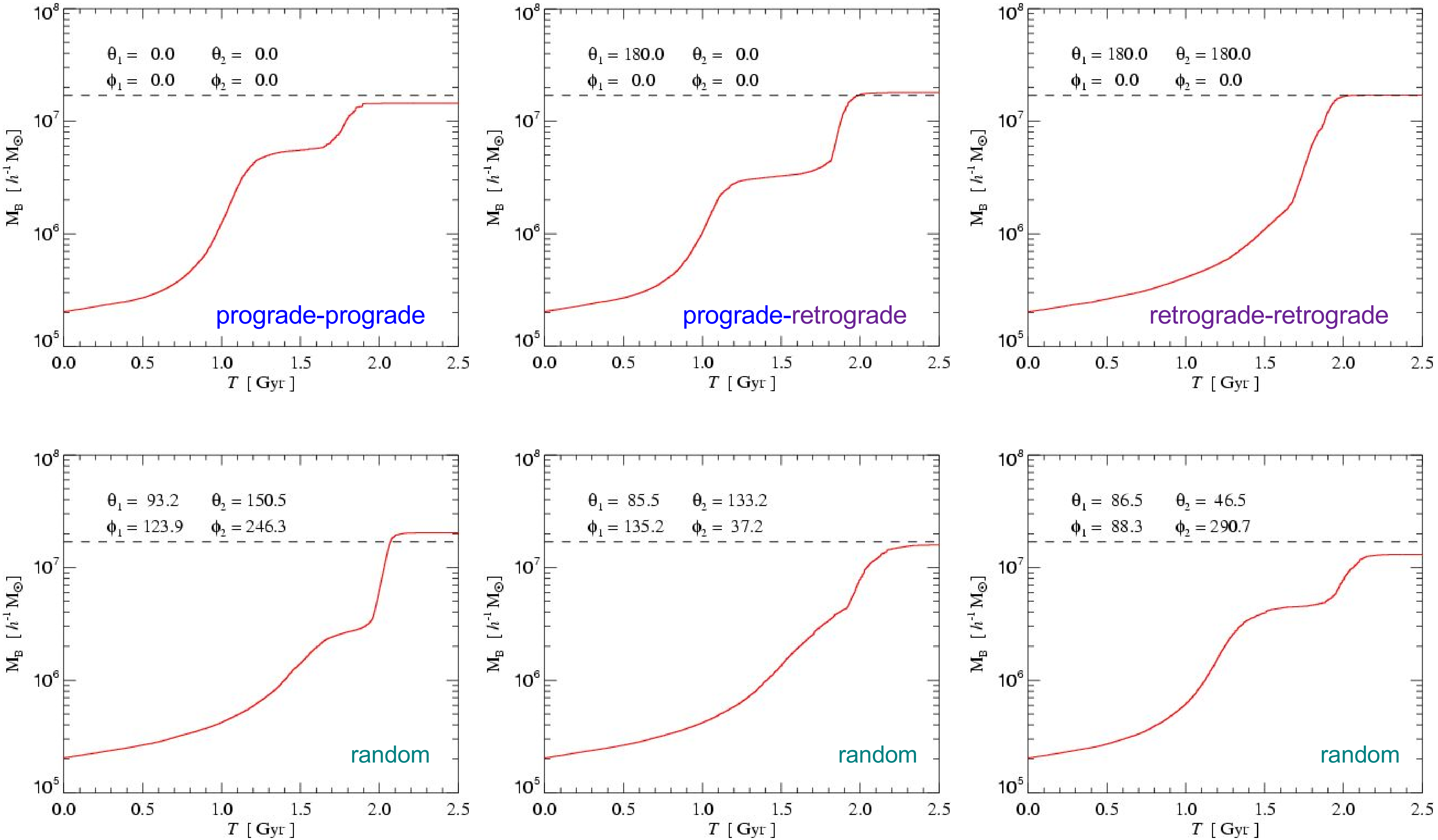

The properties of merger remnants are altered by the AGN activity

THE FATE OF THE GAS IN A MERGER WITH AND WITHOUT BLACK HOLES

Merger without black hole:

initial gas mass: $1.56 \times 10^{10}\ h^{-1} M_\odot$

- 89.0% turned into stars
- 0.05% expelled from halo
- 1.2% cold, star forming gas
- 9.8% diffuse gas in halo

X-ray luminosity

$\sim 9.5 \times 10^{39}$ erg s^{-1}

Residual star formation rate

$\sim 0.13\ M_\odot yr^{-1}$

(1 Gyr after galaxy coalesence)

Merger with black hole:

initial gas mass: $1.56 \times 10^{10}\ h^{-1} M_\odot$

- 51.9% turned into stars
- 35.3% expelled from halo
- 0% cold, star forming gas
- 11.1% diffuse gas in halo
- 1.6% swallowed by BH(s)

X-ray luminosity

$\sim 4.8 \times 10^{38}$ erg s^{-1}

Residual star formation rate

$0\ M_\odot yr^{-1}$

(1 Gyr after galaxy coalesence)

The feedback by the AGN can reduce the strength of the starburst

COMPARISON OF STAR FORMATION IN MERGERS WITH AND WITHOUT BLACK HOLE

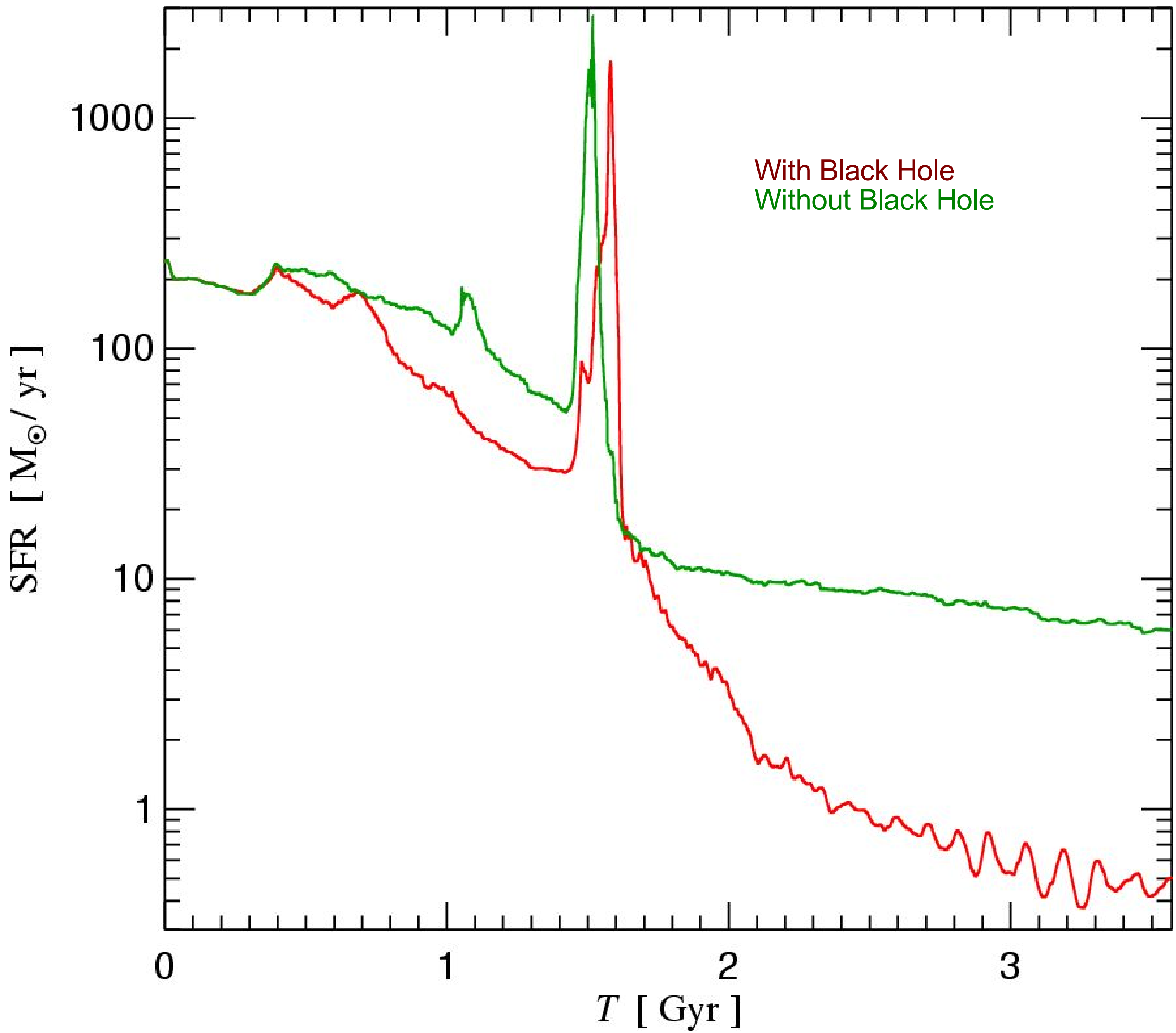

Remnants in mergers with black holes redden more quickly due to efficient truncation of star formation

COLOR EVOLUTION IN MERGER SIMULATIONS

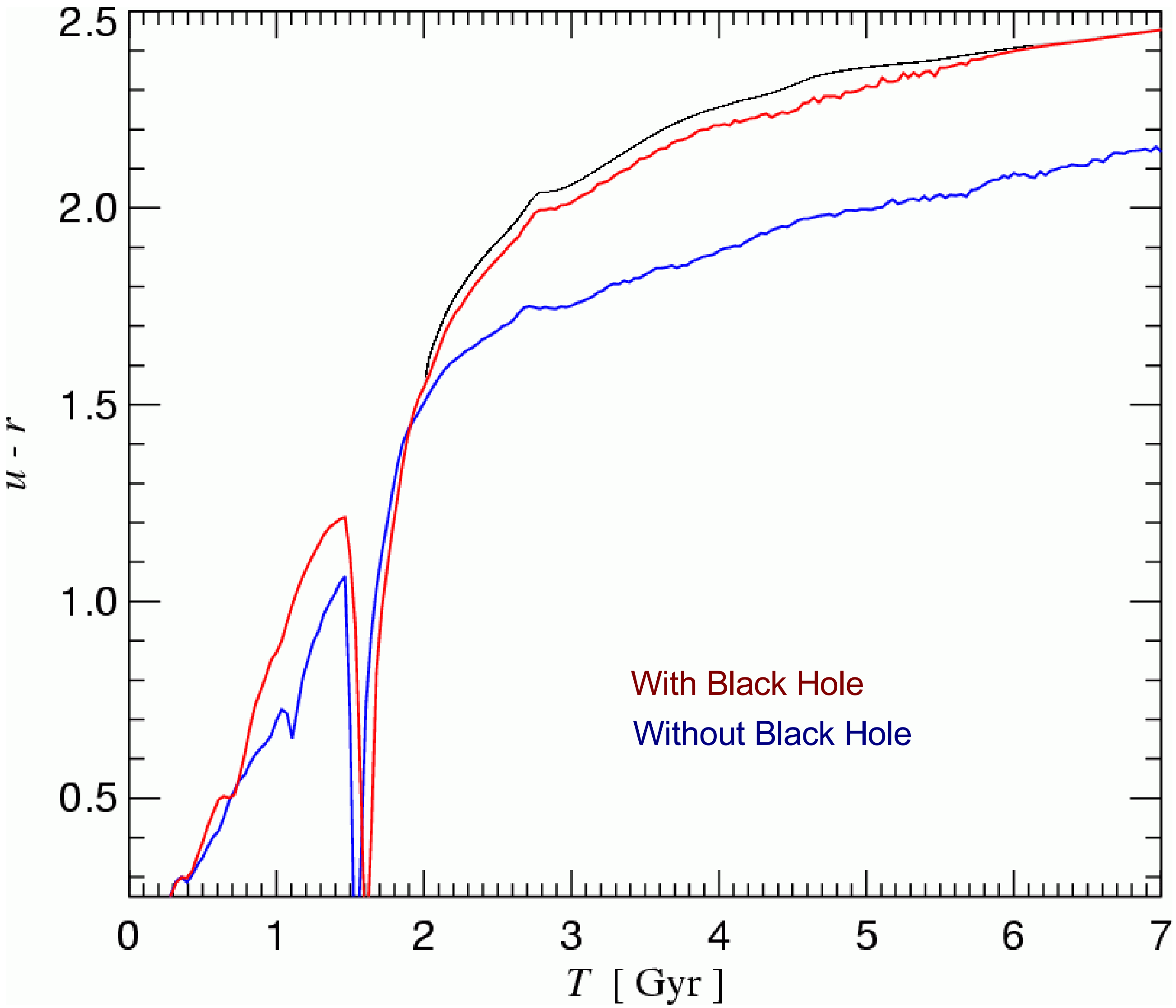

AGN feedback may help in shaping the observed bimodal color distribution of galaxies

COLOR-MAGNITUDE TRACKS OF MERGERS OF DIFFERENT MASS

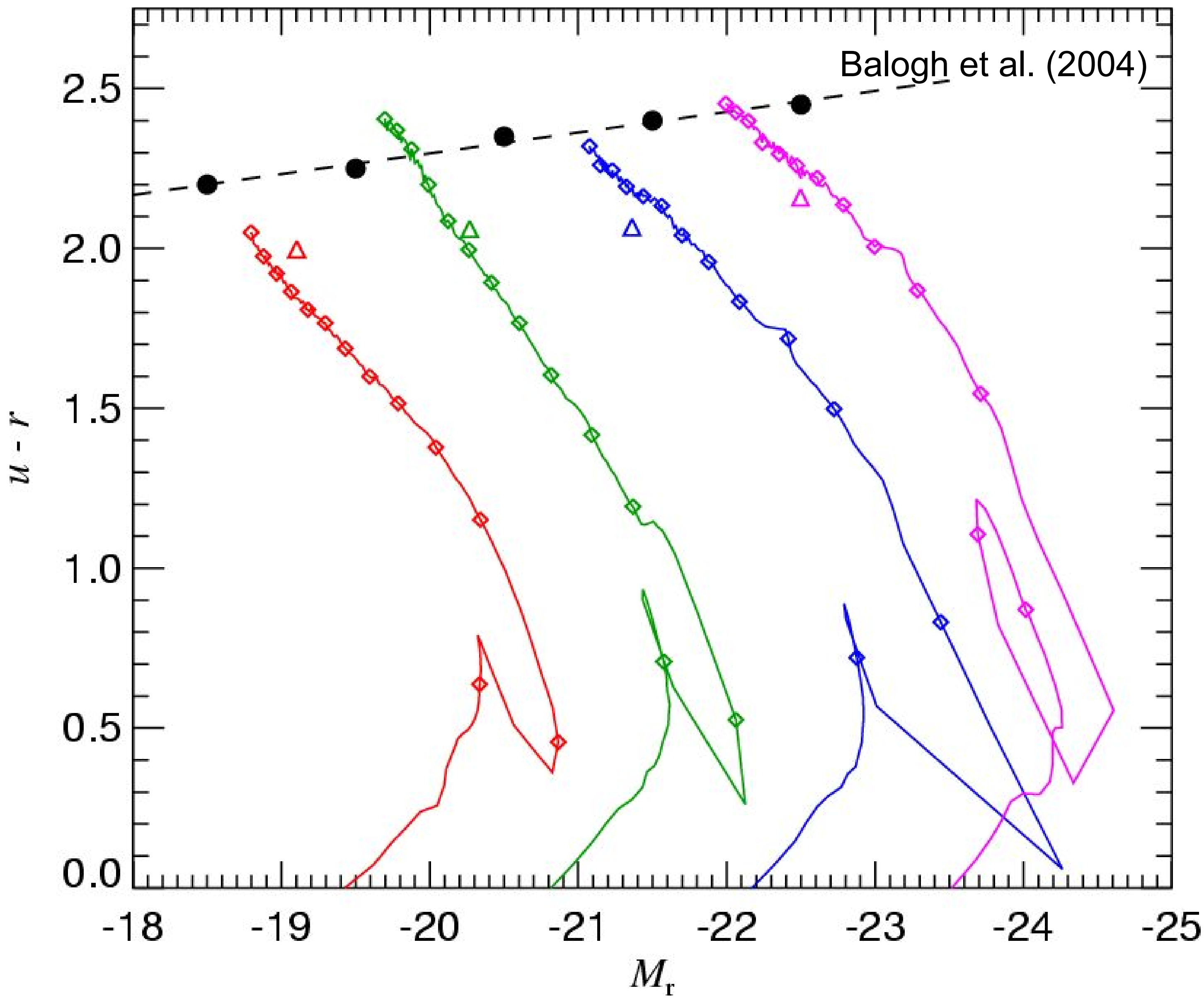

Galaxy mergers bring their central supermassive black holes quickly to separations less than ~100 pc

APPROACH OF THE BLACK HOLES IN MERGER SIMULATIONS

Note: The actual formation of a black hole binary, and the hardening of it, cannot presently be addressed by our simulations in an adequate way, due to lack of spatial dynamic range.

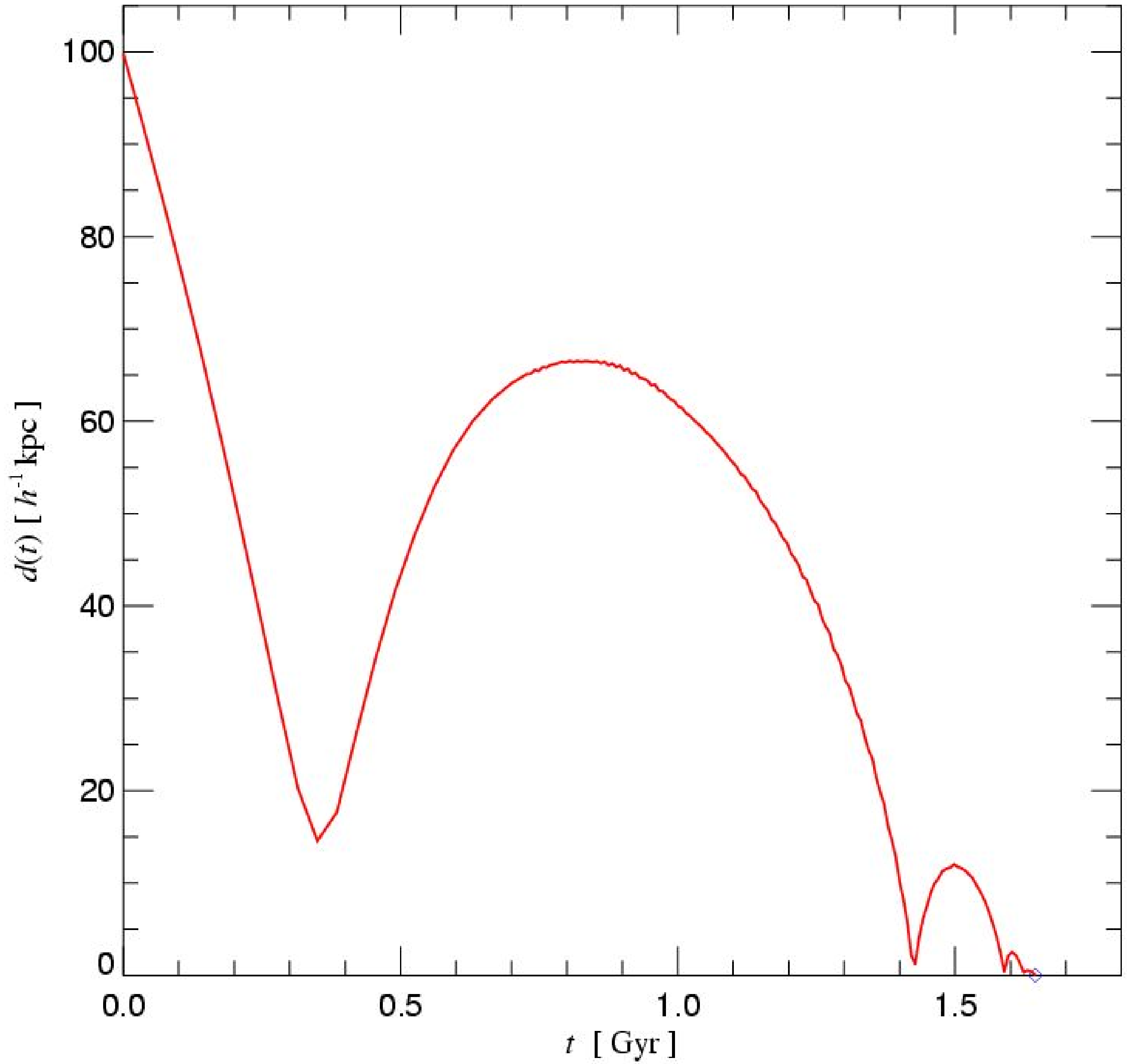

Strong nuclear starbusts may leave behind a central luminosity spike in the merger remants

STELLAR PROFILES OF MERGER REMNANTS WITH ISOTHERMAL ISM

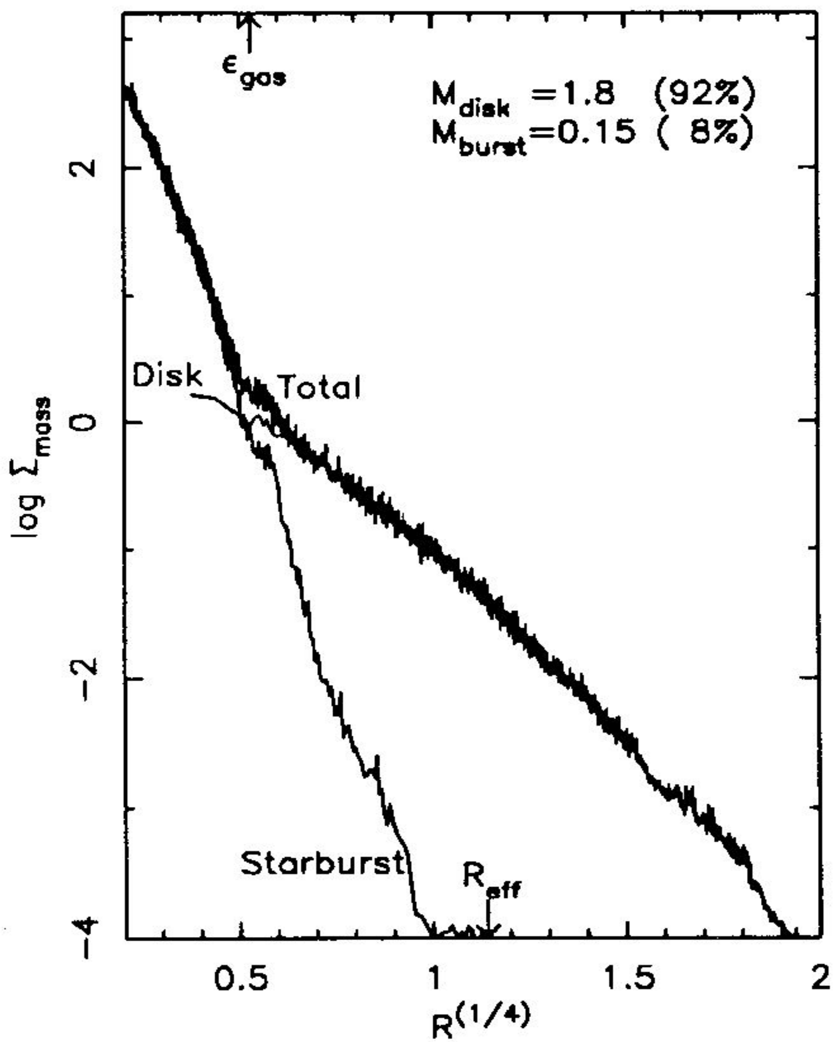

FIG. 1*a*

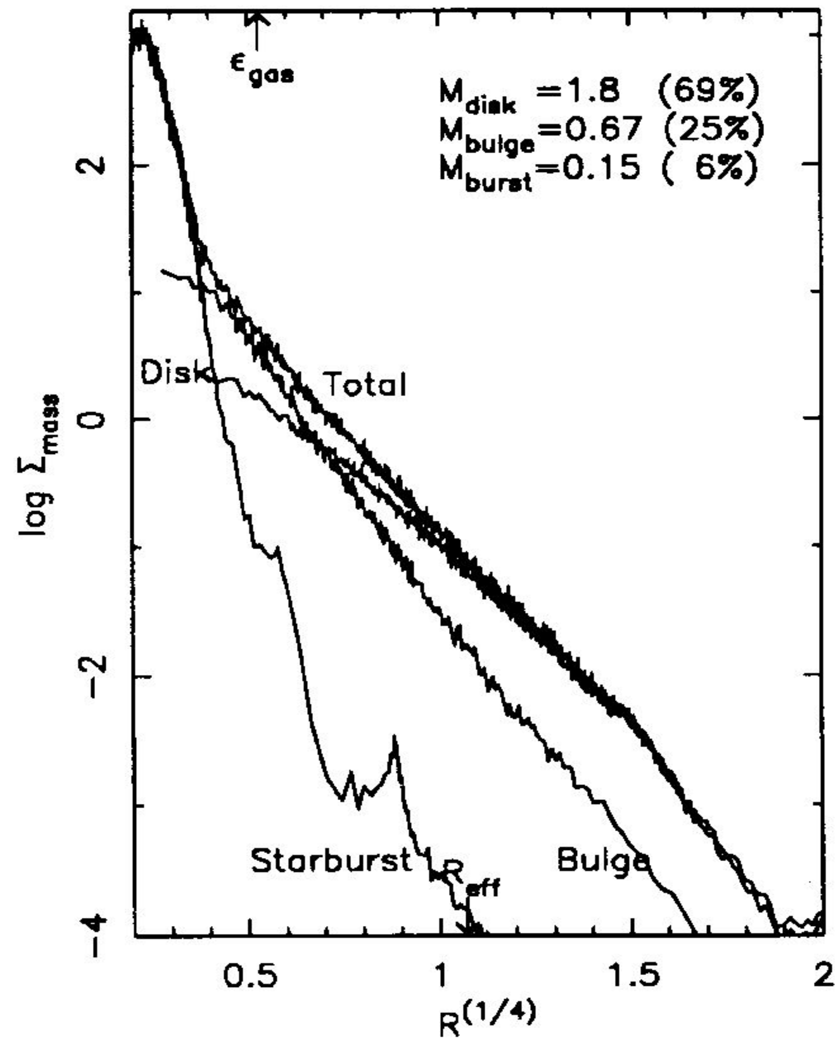

FIG. 1*b*

Mihos & Hernquist (1994)

The stellar surface brightness profiles of merger remnants with black holes follow $r^{1/4}$ profiles

STELLAR SURFACE DENSITY PROFILES OF MERGER REMNANTS

remnant at “low” resolution

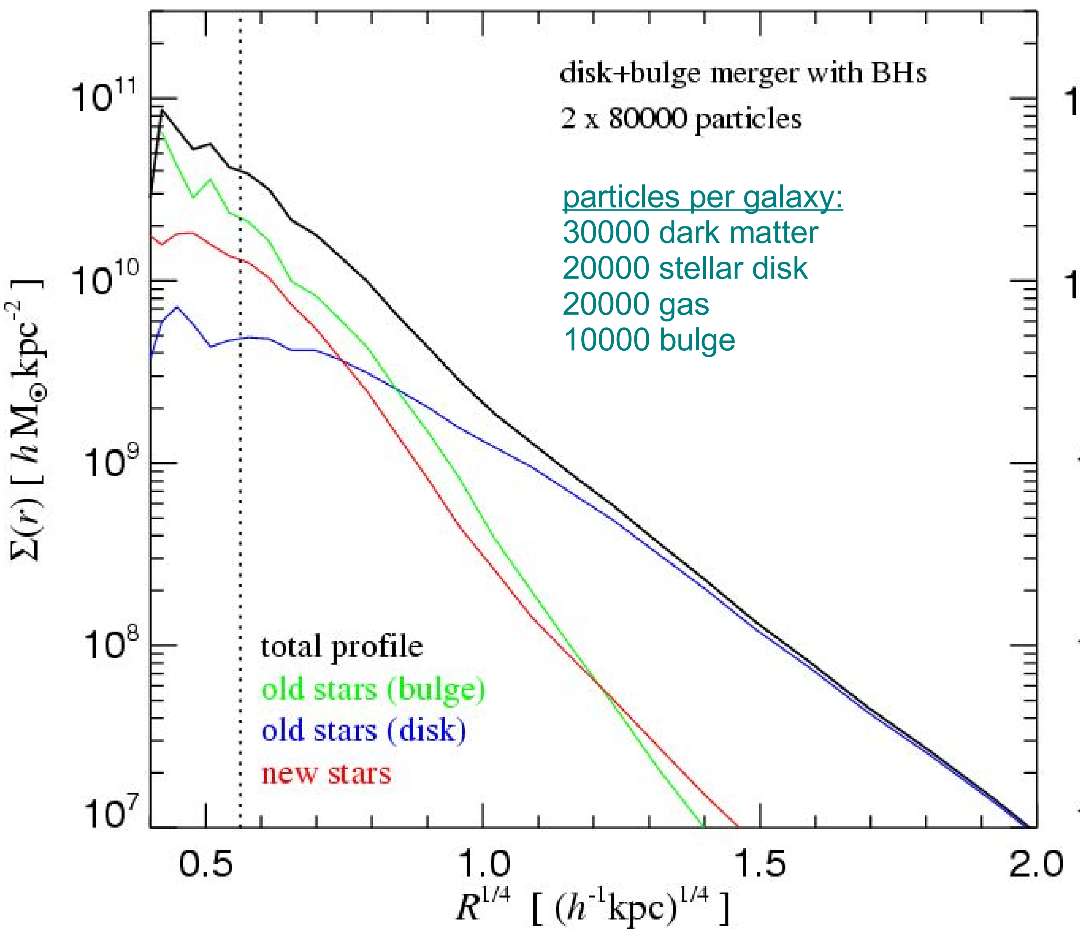

remnant at high resolution

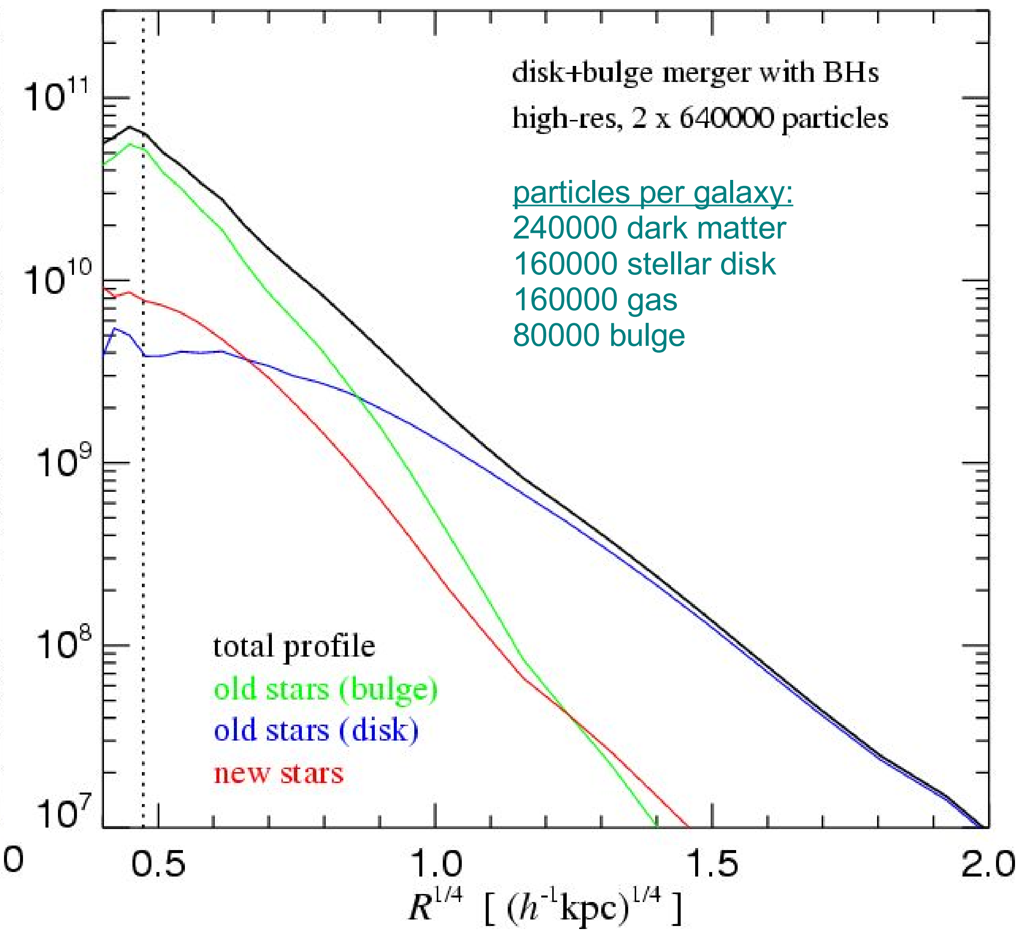

→ quite reasonable convergence

The total black hole mass density in the simulations grows to values consistent with observational estimates

TIME EVOLUTION OF BLACK HOLE MASS DENSITY IN THE D4 RUN

Yu & Tremaine (2002)

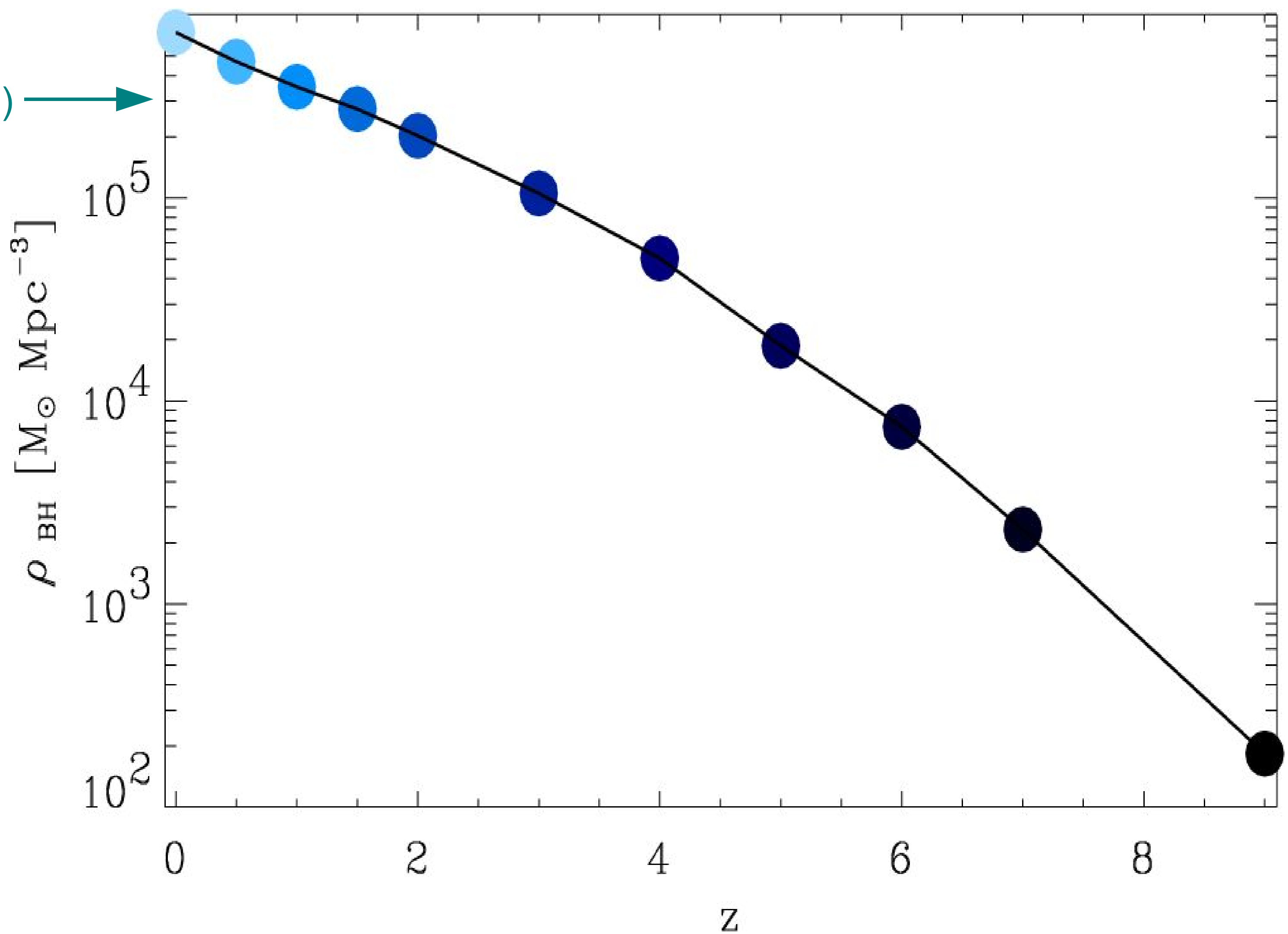

The cosmological simulations allow a detailed tracking of quasar activity of each blach hole

HISTORY OF AN INDIVIDUAL BLACK HOLE IN THE D4 SIMULATION

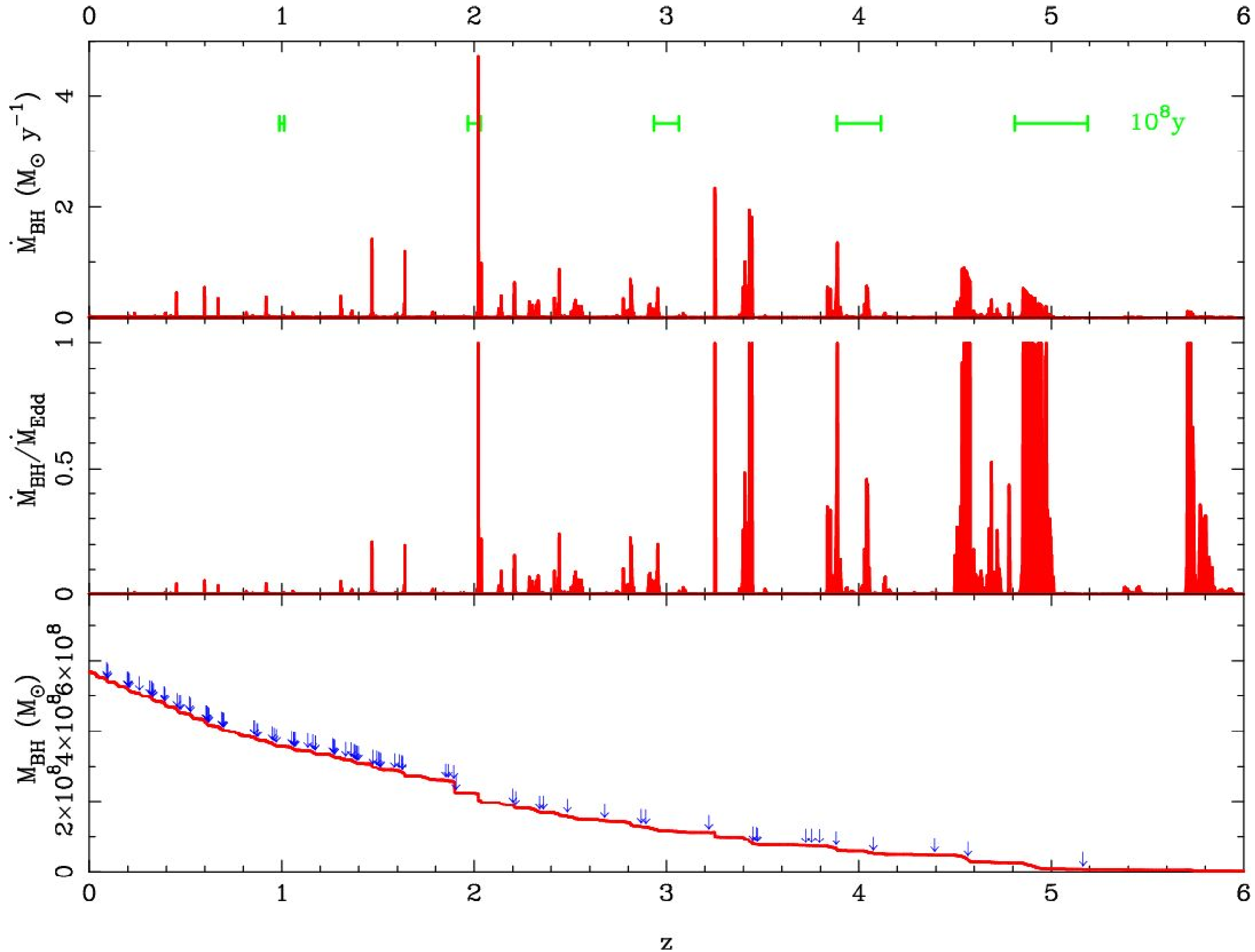

Higher mass resolution can resolve smaller galaxies

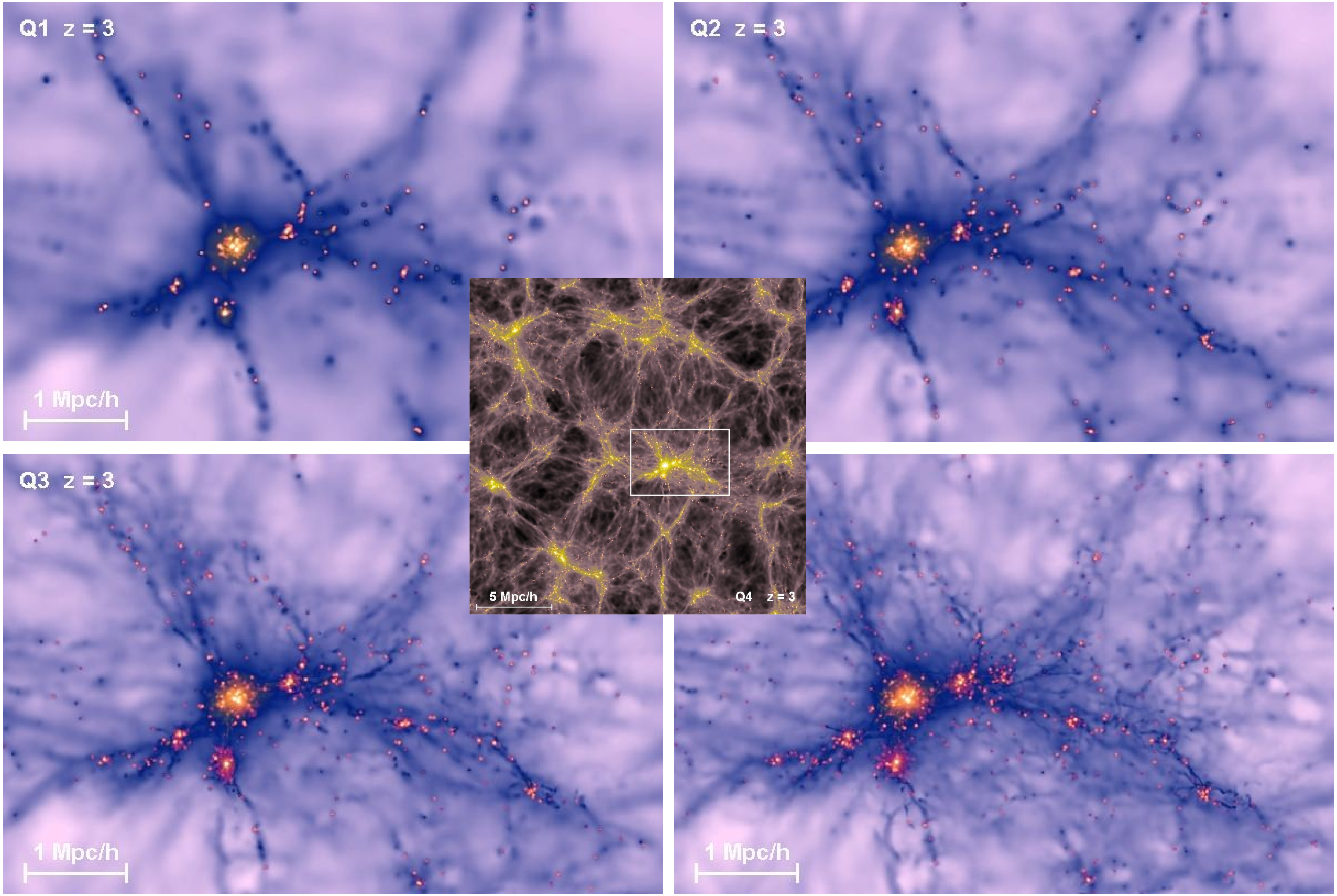

The "large-scale" structure seen at high redshift superficially resembles the morphology of structure seen at low redshift

GAS DISTRIBUTION SEEN IN A SMALL PERIODIC BOX AT REDSHIFT z=6

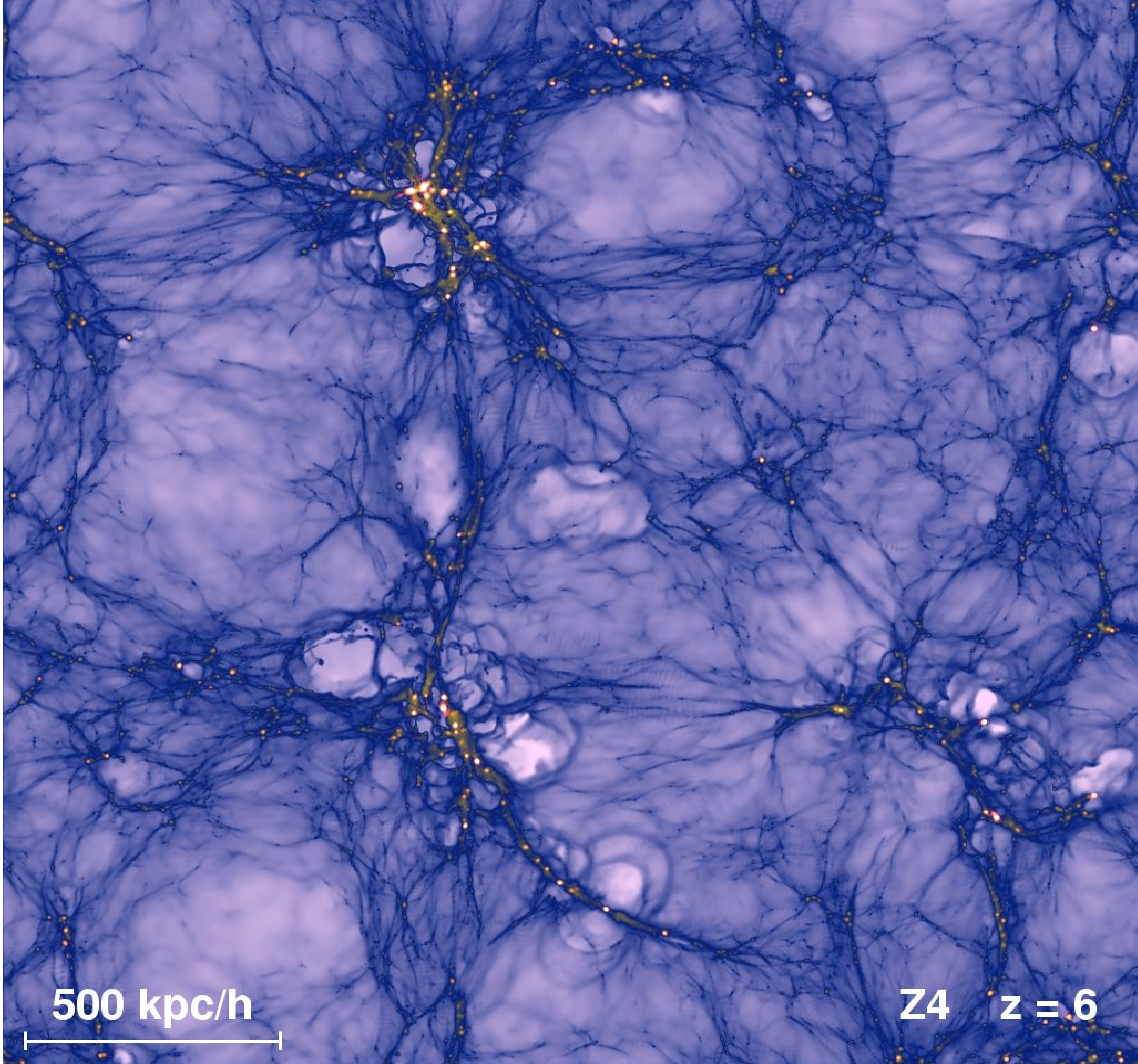

Galactic winds that escape from galaxies are producing shocks in the IGM, dissipating their kinetic energy into heat

HOT BUBBLES IN THE IGM GENERATED BY WINDS

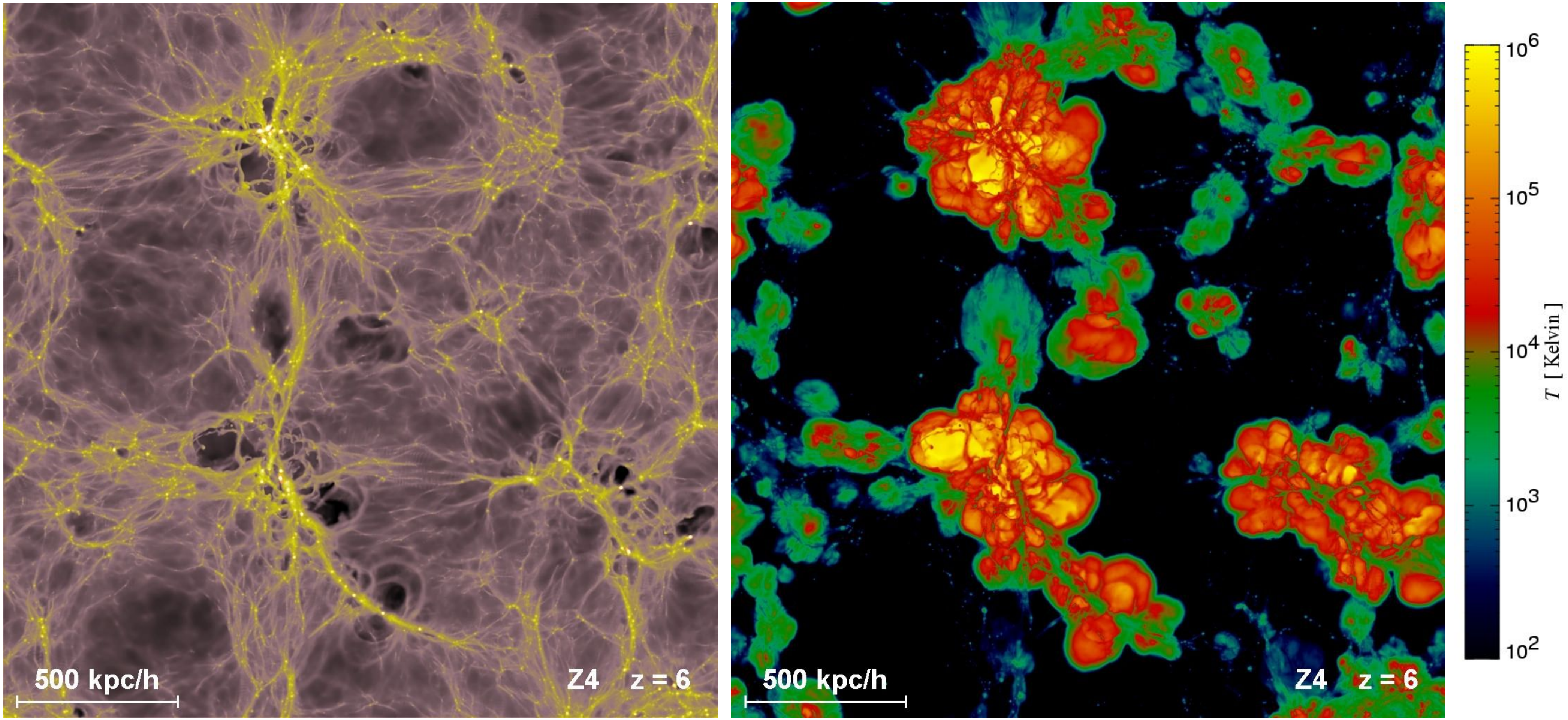

Even though galactic winds heat parts of the IGM significantly, most of the volume still follows the ordinary "equation of state"

VOLUME-WEIGHTED PHASE-SPACE DIAGRAMS

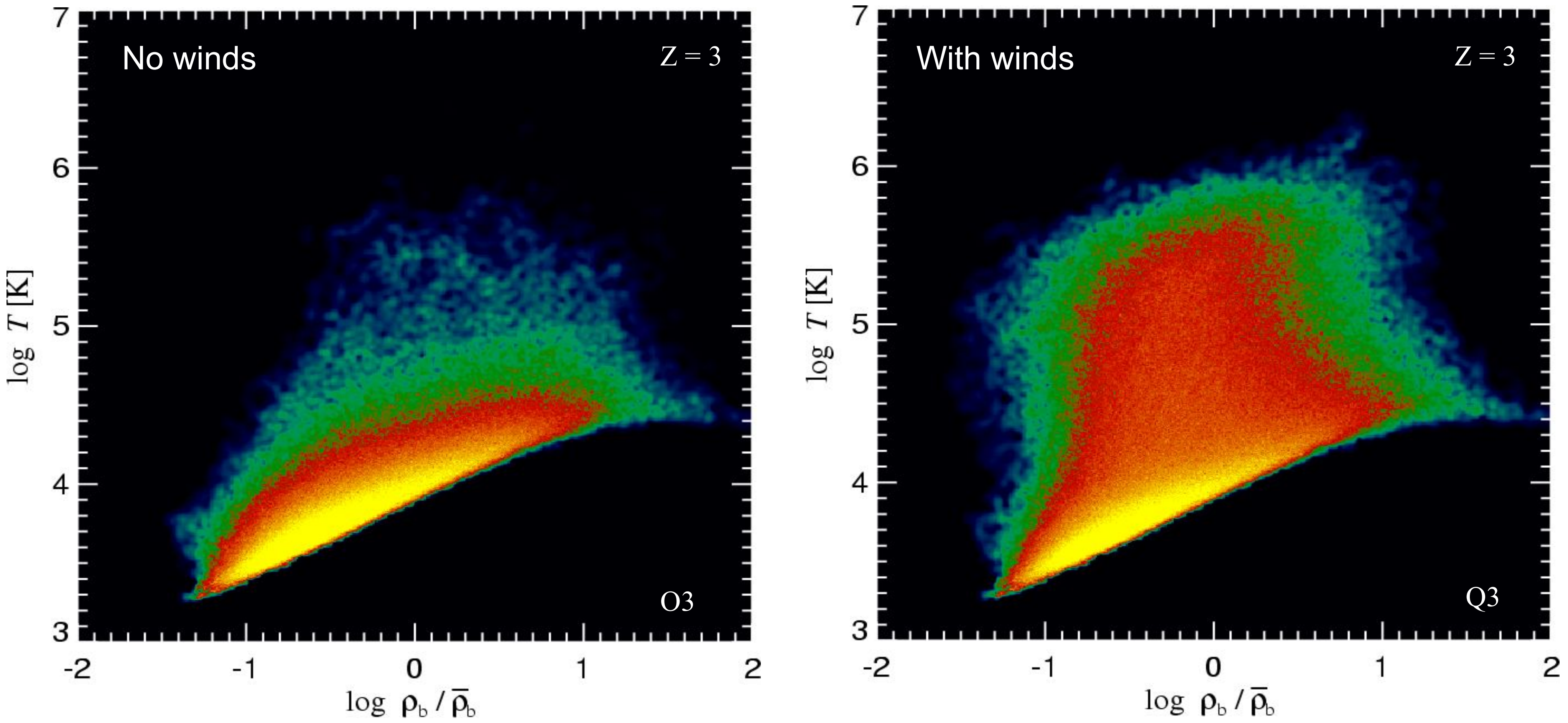

Only a small volume fraction of the IGM is heated by galatic winds

DIFFERENTIAL DISTRIBUTION OF VOLUME AS A FUNCTION OF TEMPERATURE

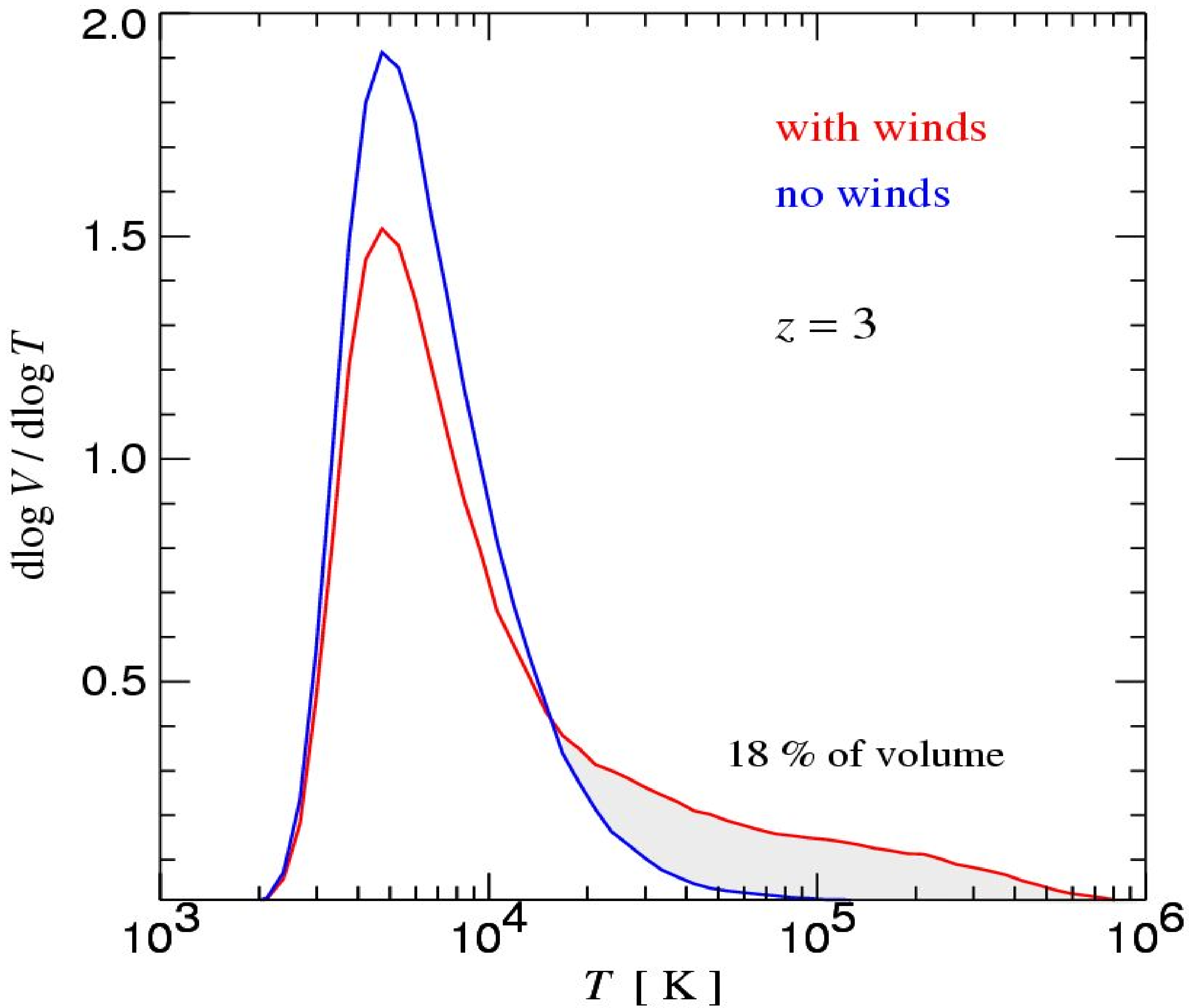

The Lyman alpha forest appears to survive nicely even for strong winds

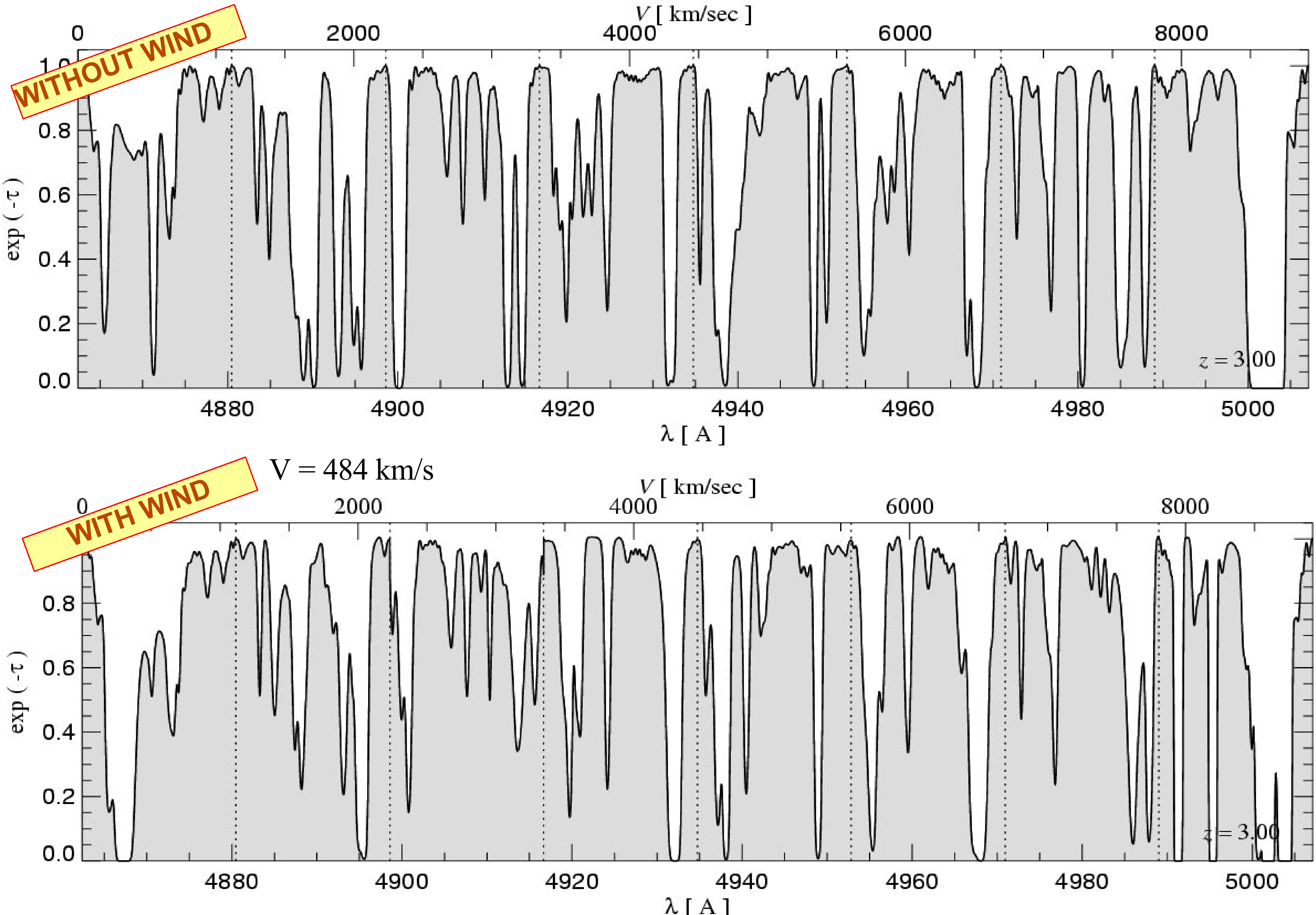

Winds induce differences in transmission

IDENTICAL LINES OF SIGHT

Without wind:

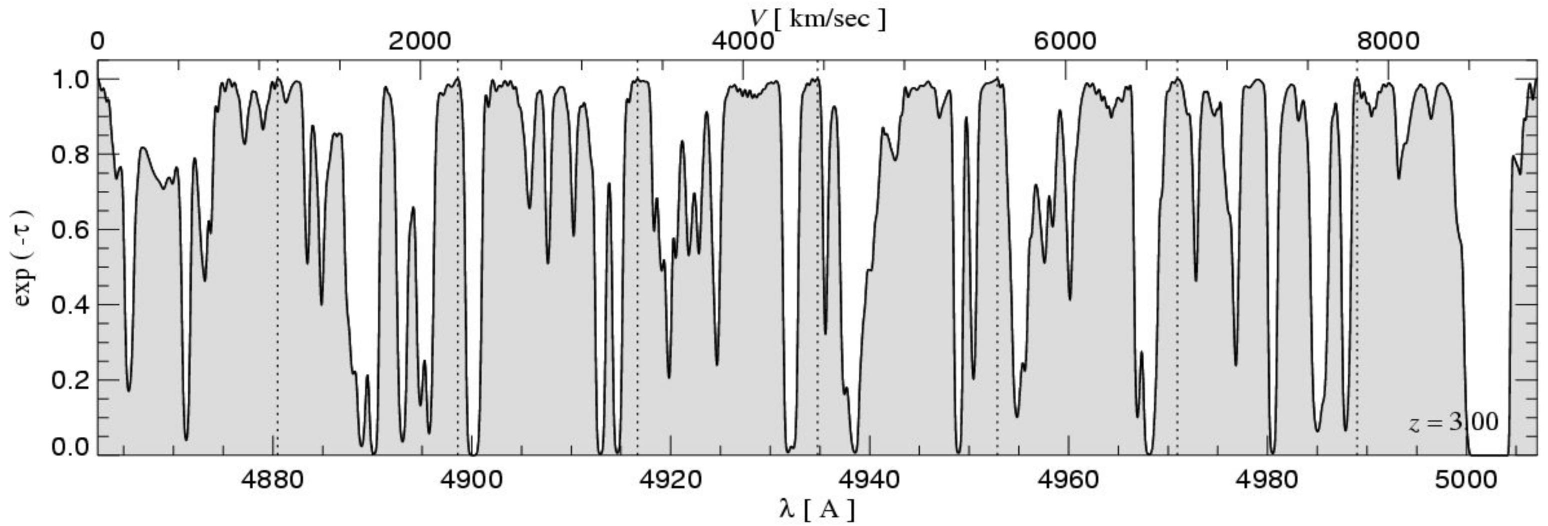

With wind:

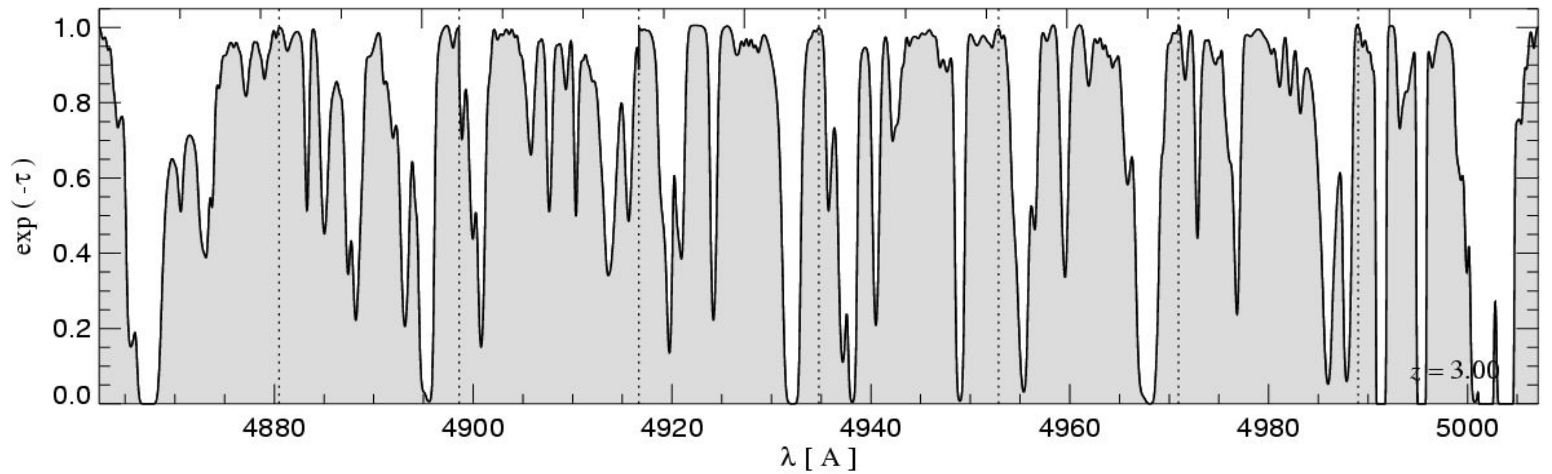

Difference in transmission:

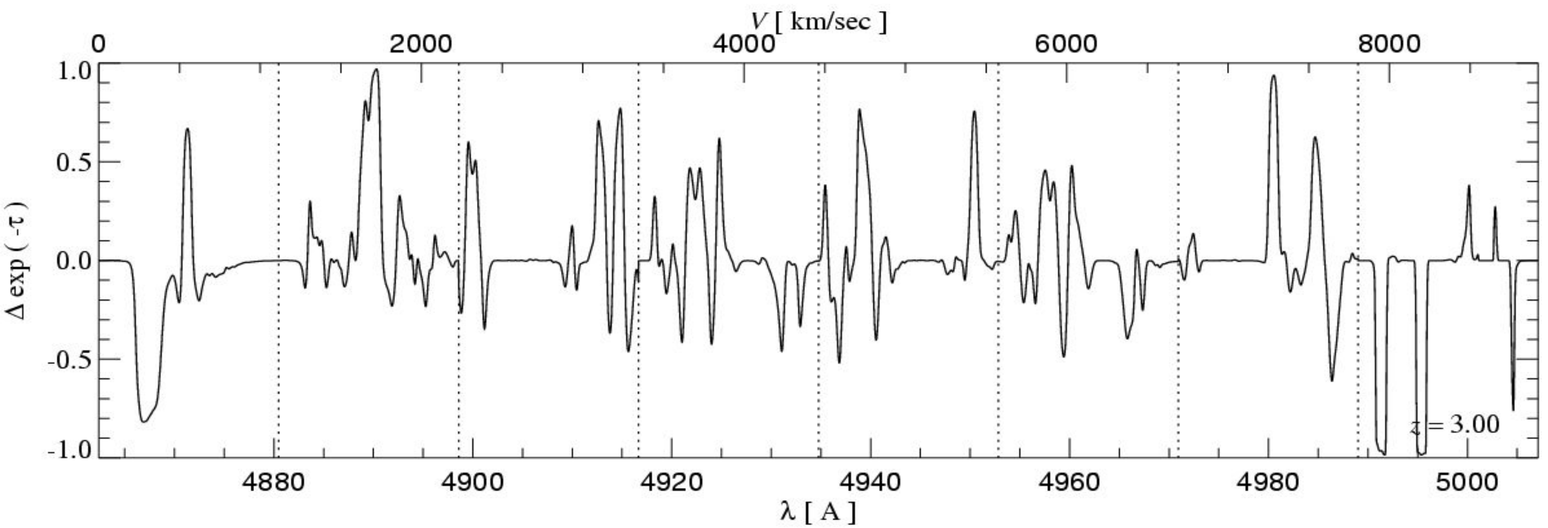

(maximum difference selection)

Difference in **velocity**:

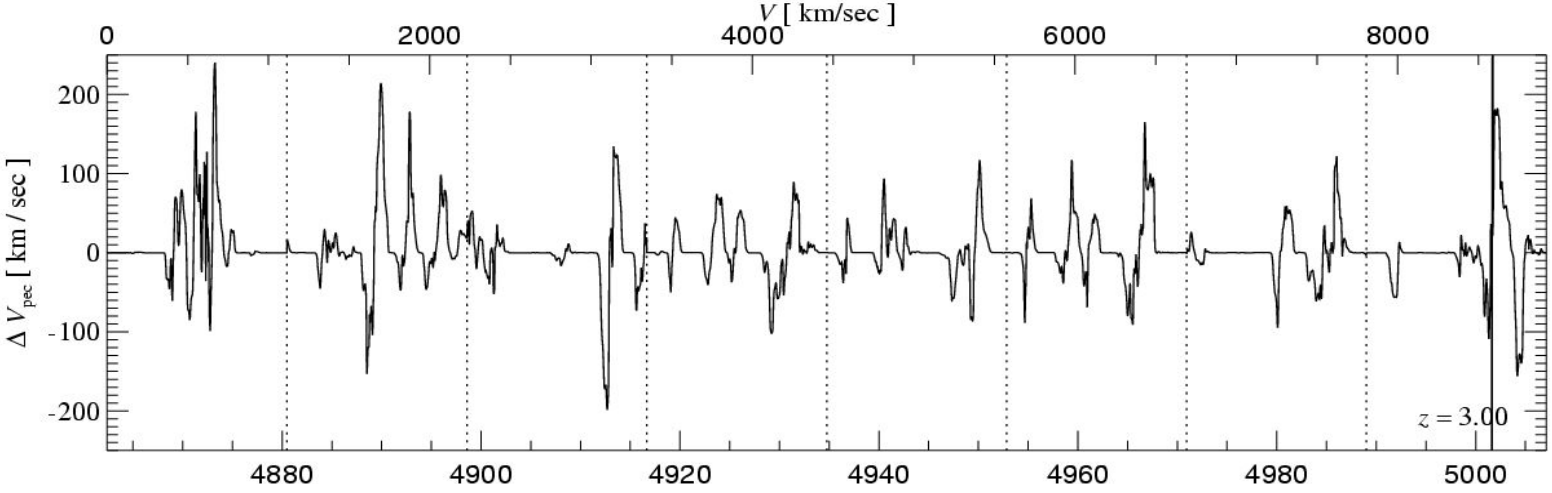

Difference in **temperature**:

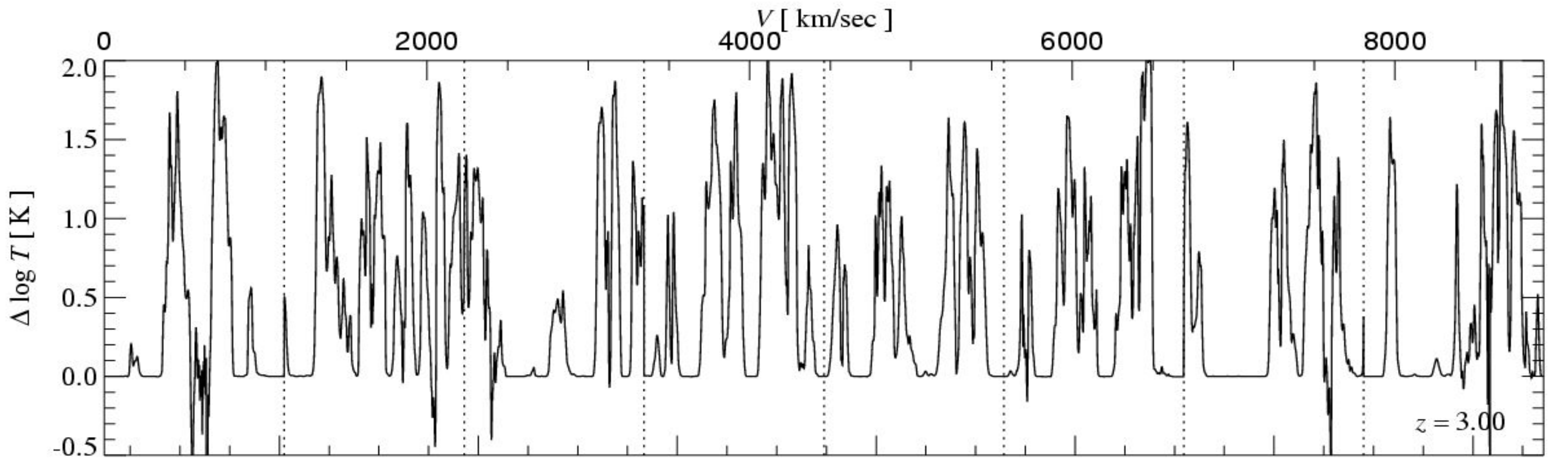

Difference in **metallicity**:

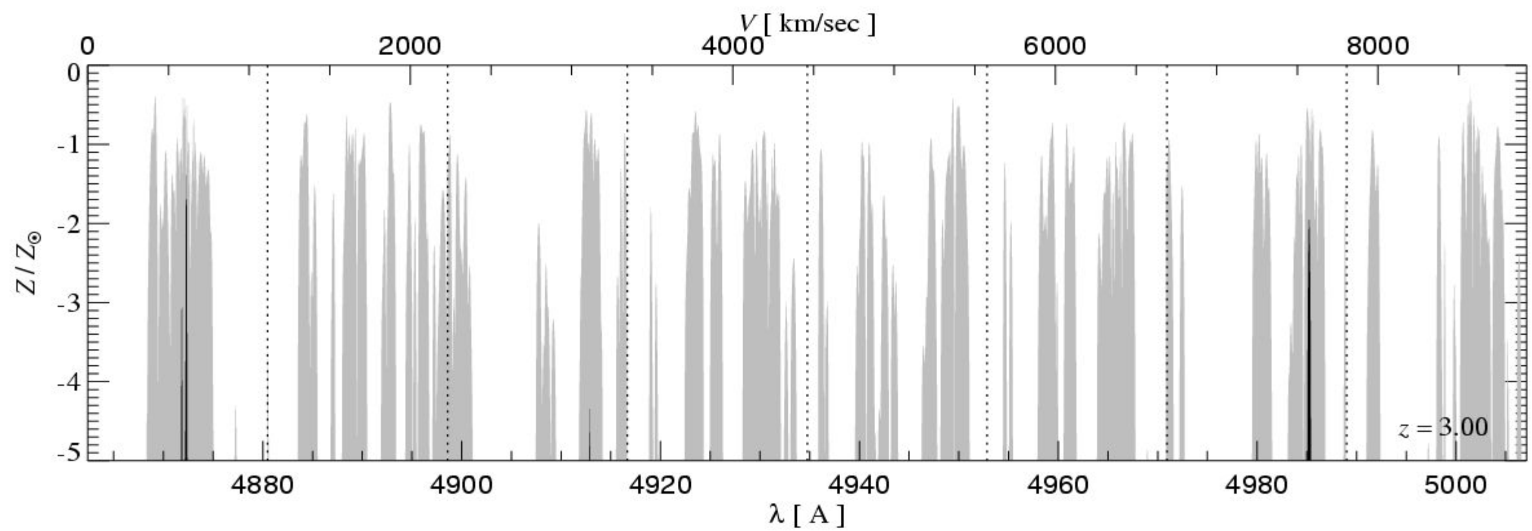

(maximum difference selection)

Random lines of sight are only mildly affected by winds

IDENTICAL RANDOM LINES OF SIGHT

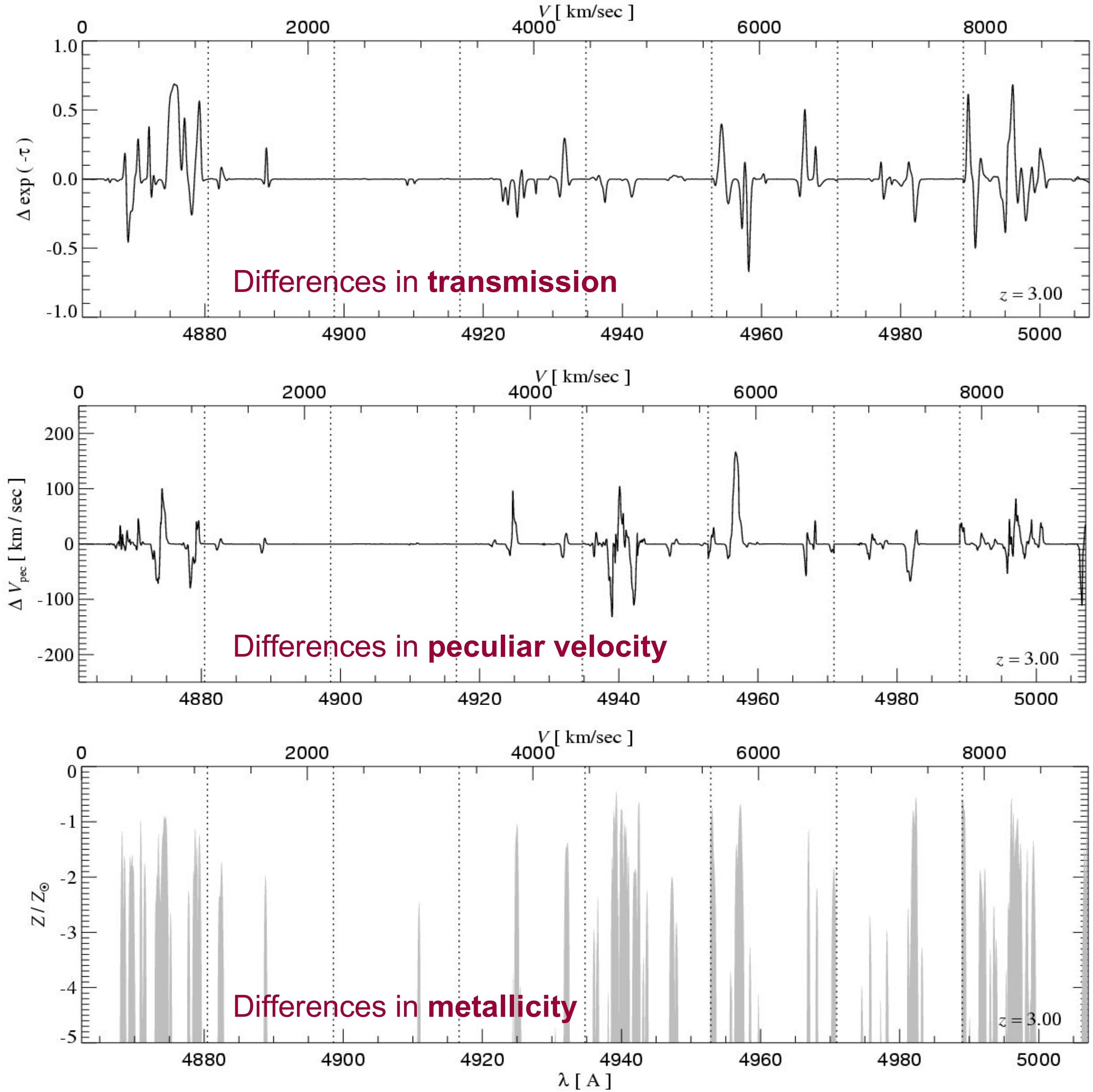

Our simulation technique provides good convergence for the *b*-parameter distribution

COMPARISON OF LINE-WIDTH DISTRIBUTIONS

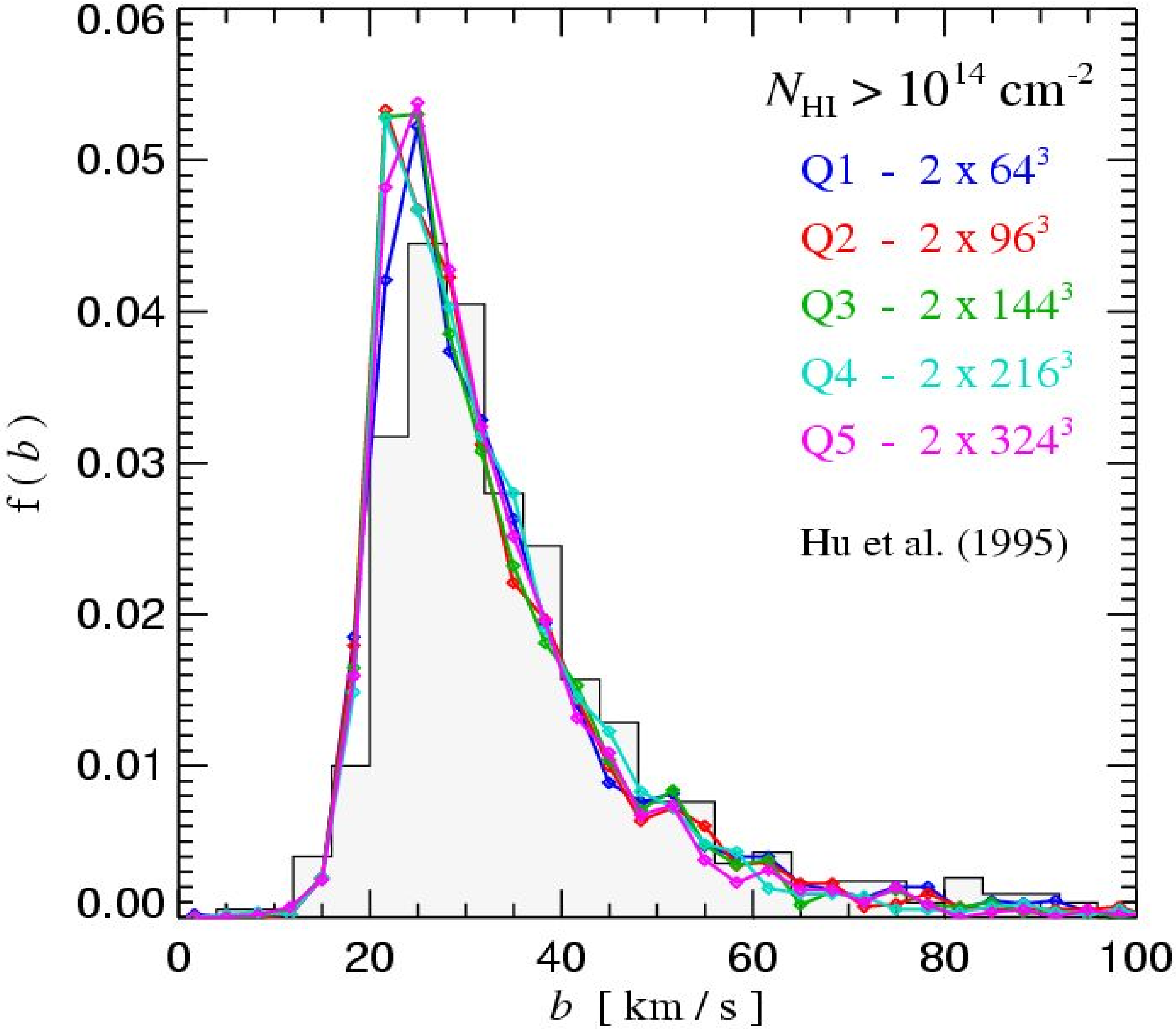

Theuns et al. (1998)

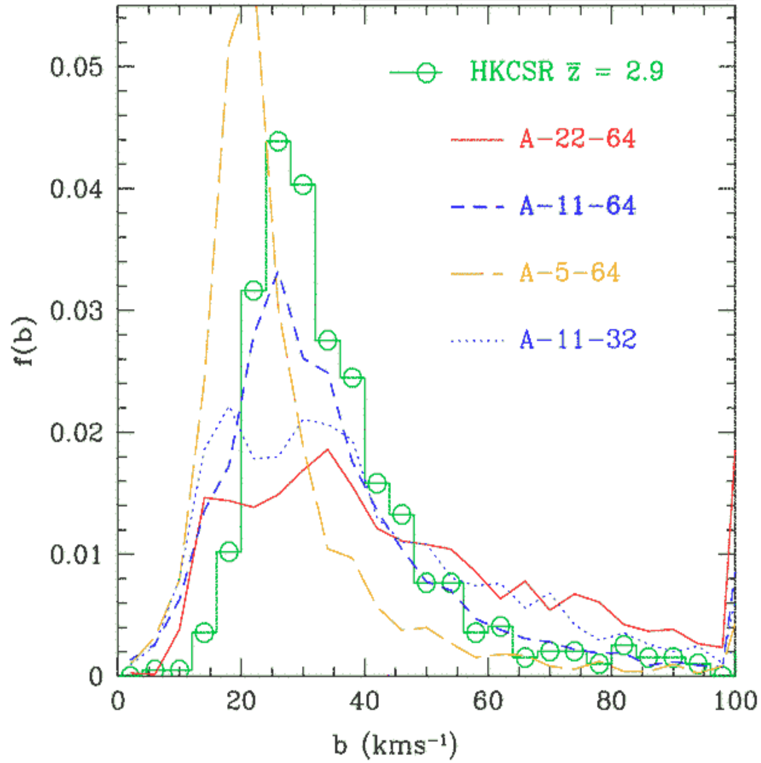

Bryan et al. (1999)

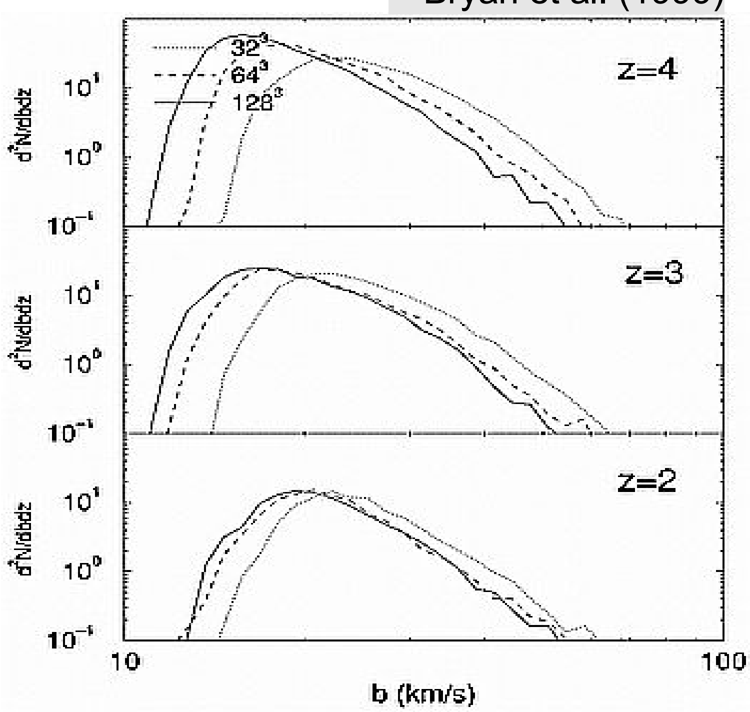

The column density distribution provides a good fit to data and is hardly affected by galactic winds

NUMBER DENSITY OF LINES AS A FUNCTION OF COLUMN DENSITY

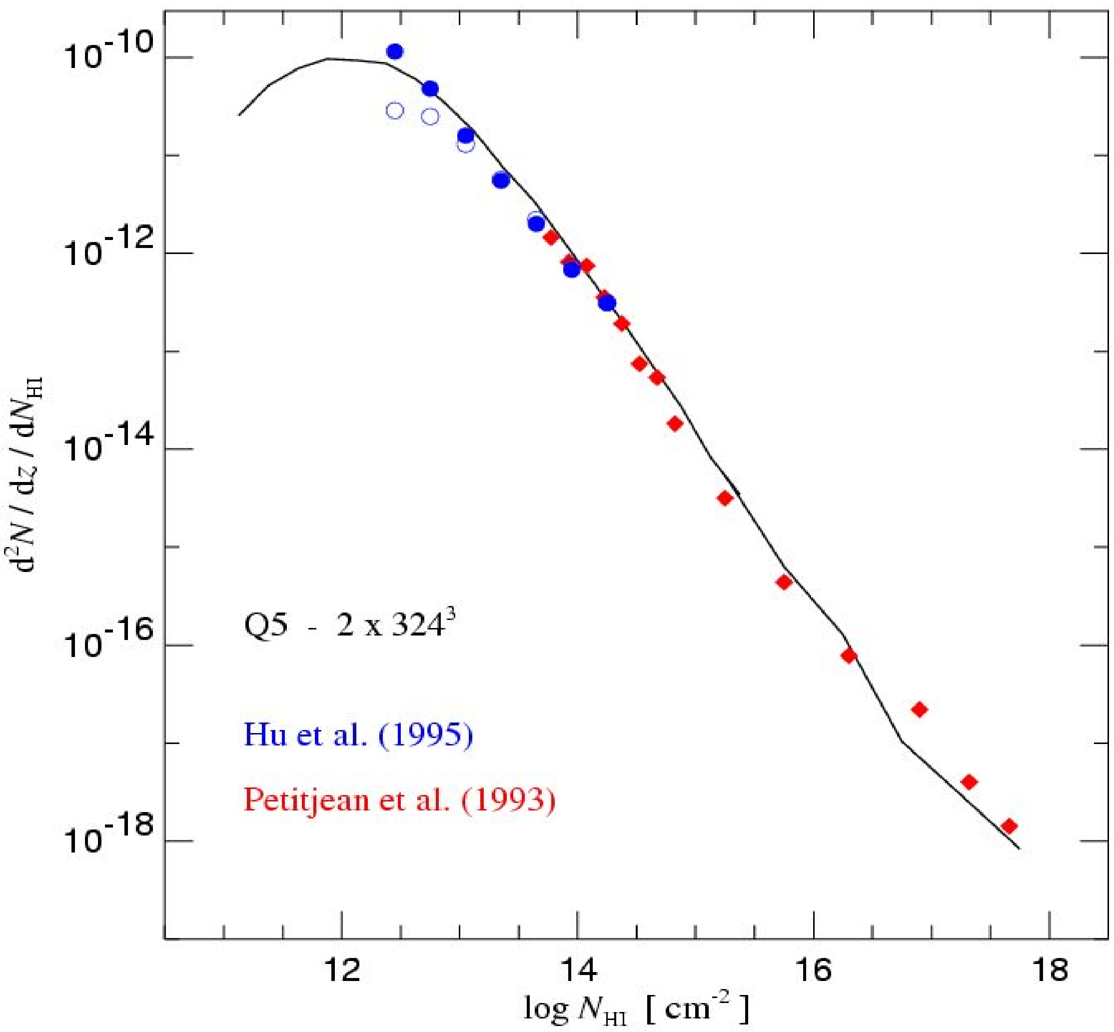

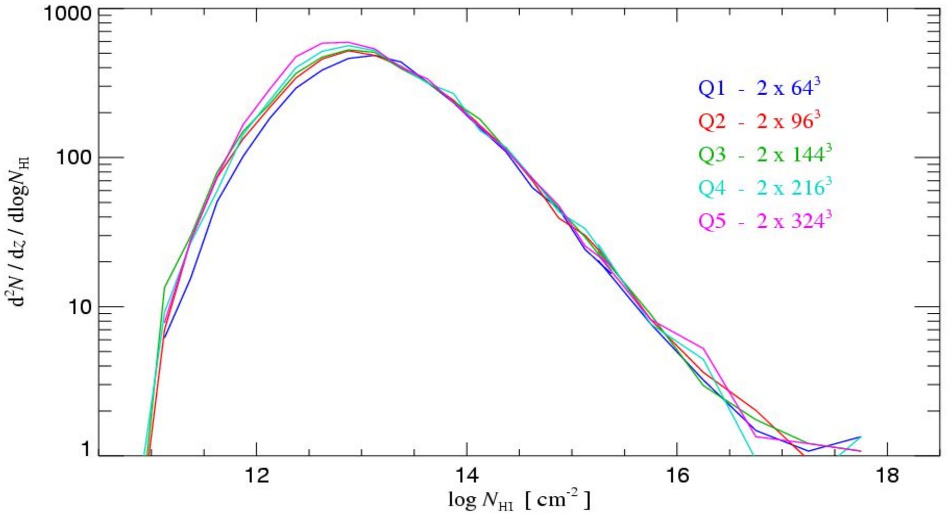

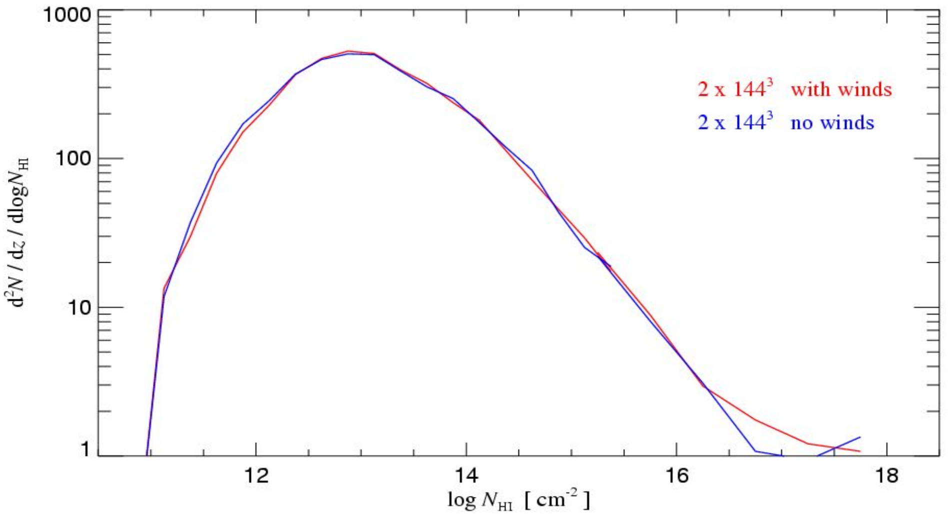

Feedback has been predicted to have a major impact on lines with N_{HI}~10^{16} cm $^{-2}$ (e.g. Theuns, Mo & Schaye 2001) → Not the case in our models

The one-point function of the flux is insensitive to resolution, and to the presence of galactic winds

PROBABILITY DISTRIBUTION OF TRANSMITTED FLUX

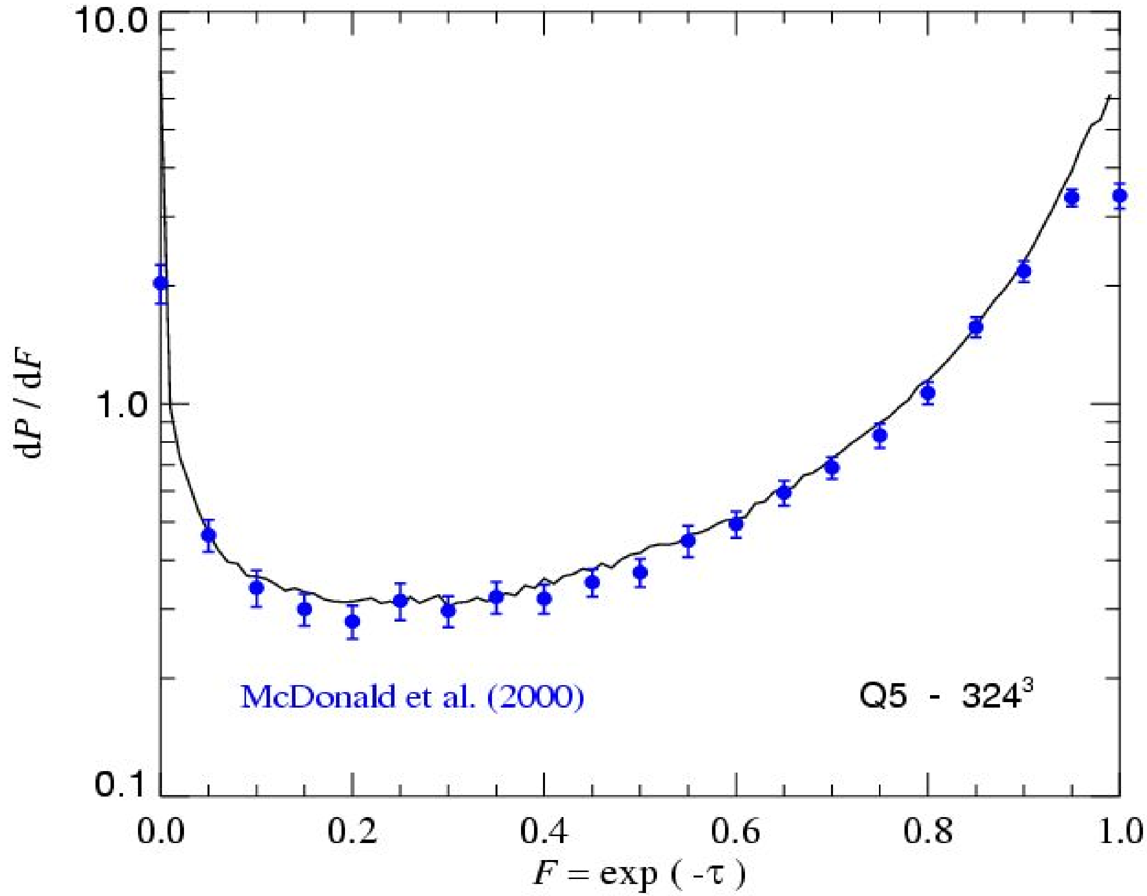

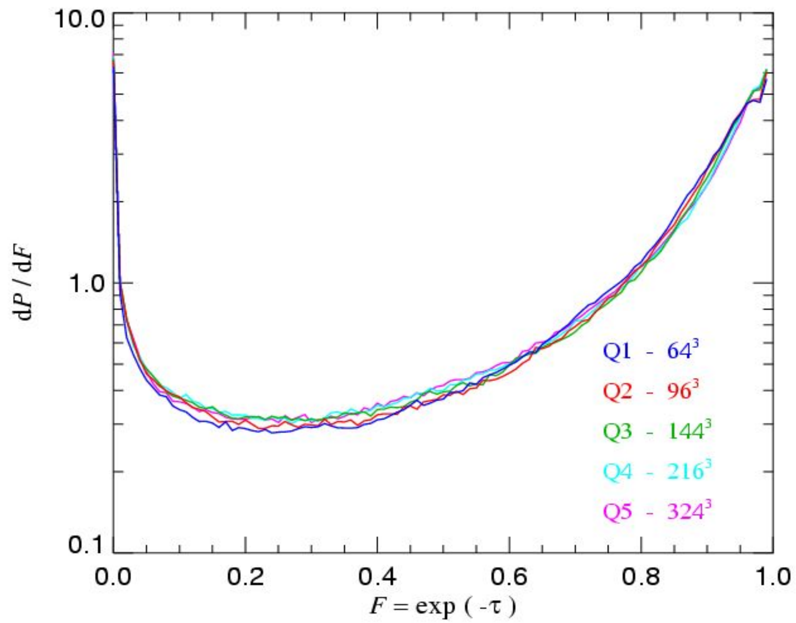

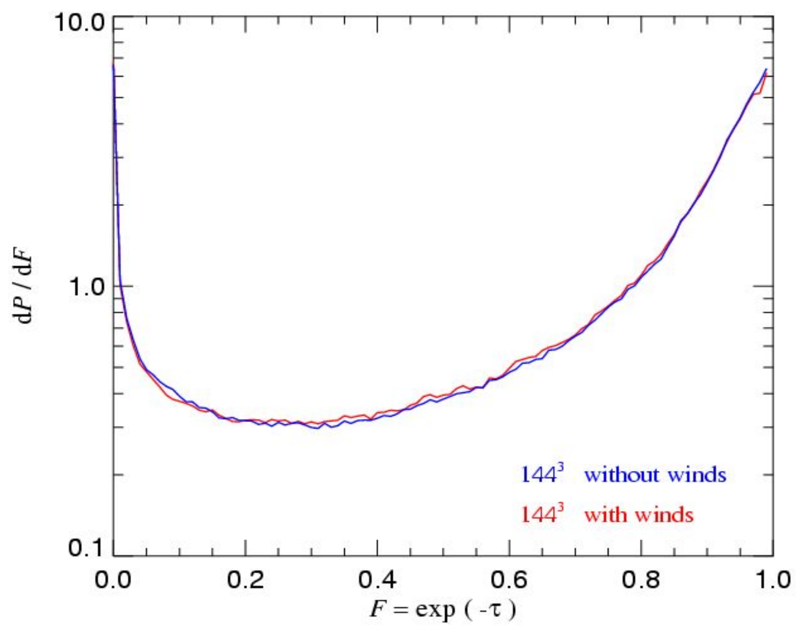

The amount of small-scale power measured in the flux power spectrum is slightly reduced by galactic winds

COMPARISON OF FLUX POWER SPECTRA WITH AND WITHOUT WINDS

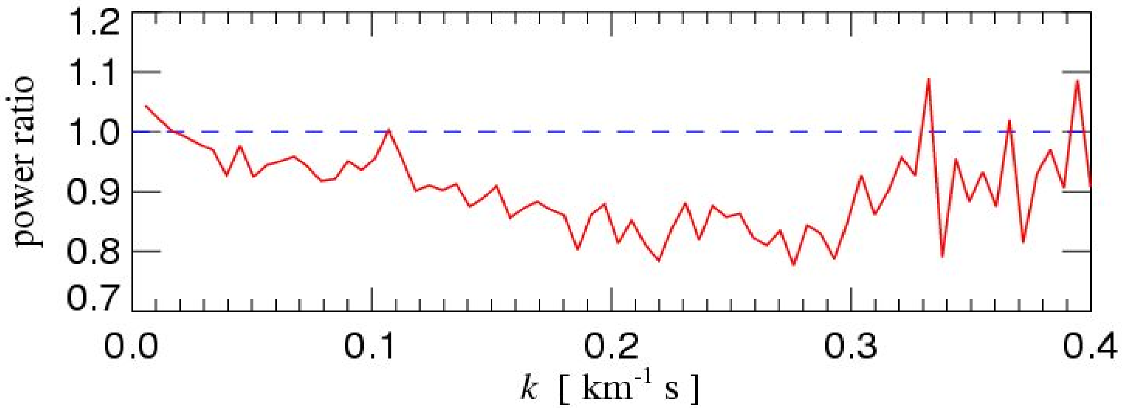

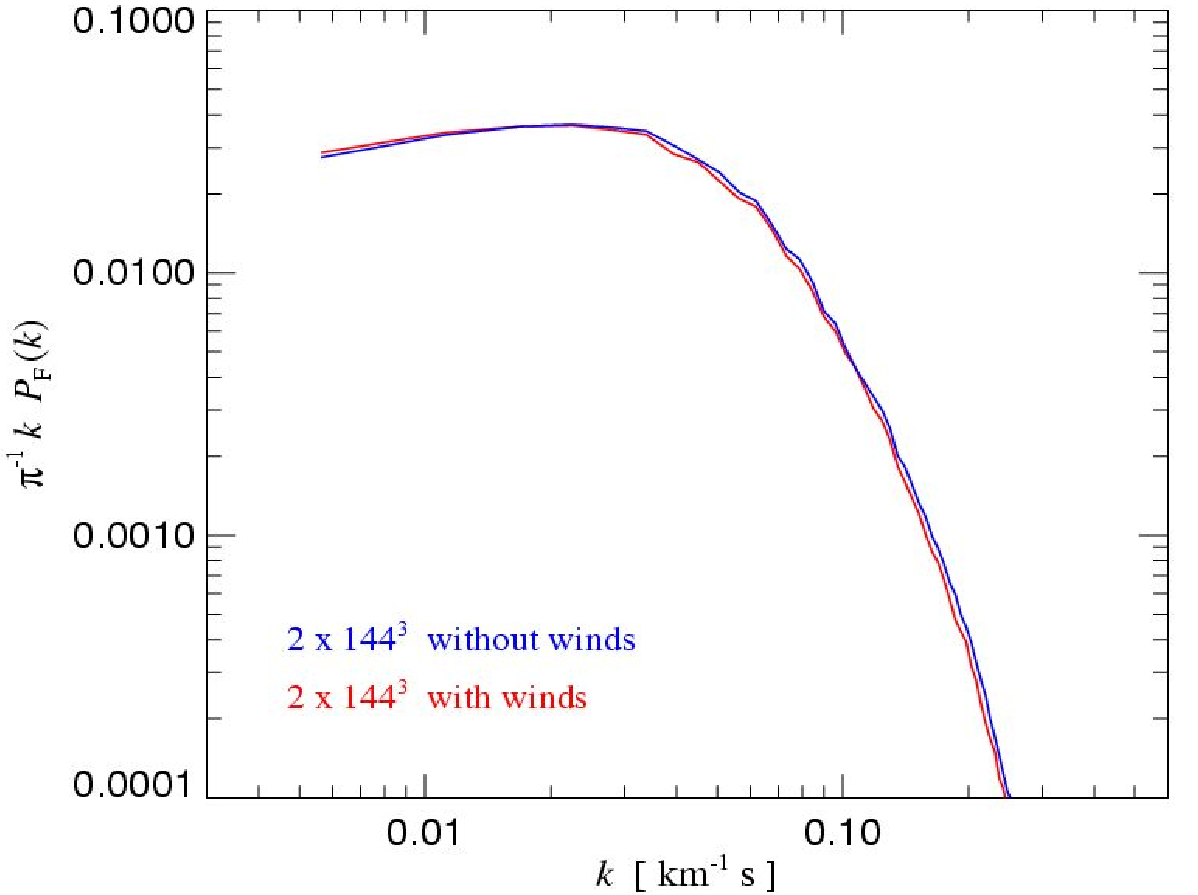

The flux power spectrum matches observational data well, but depending on the correction for meta-line regions, there may be slightly too much small-scale power

FLUX POWER SPECTRUM COMPARED TO OBSERVATIONAL DATA

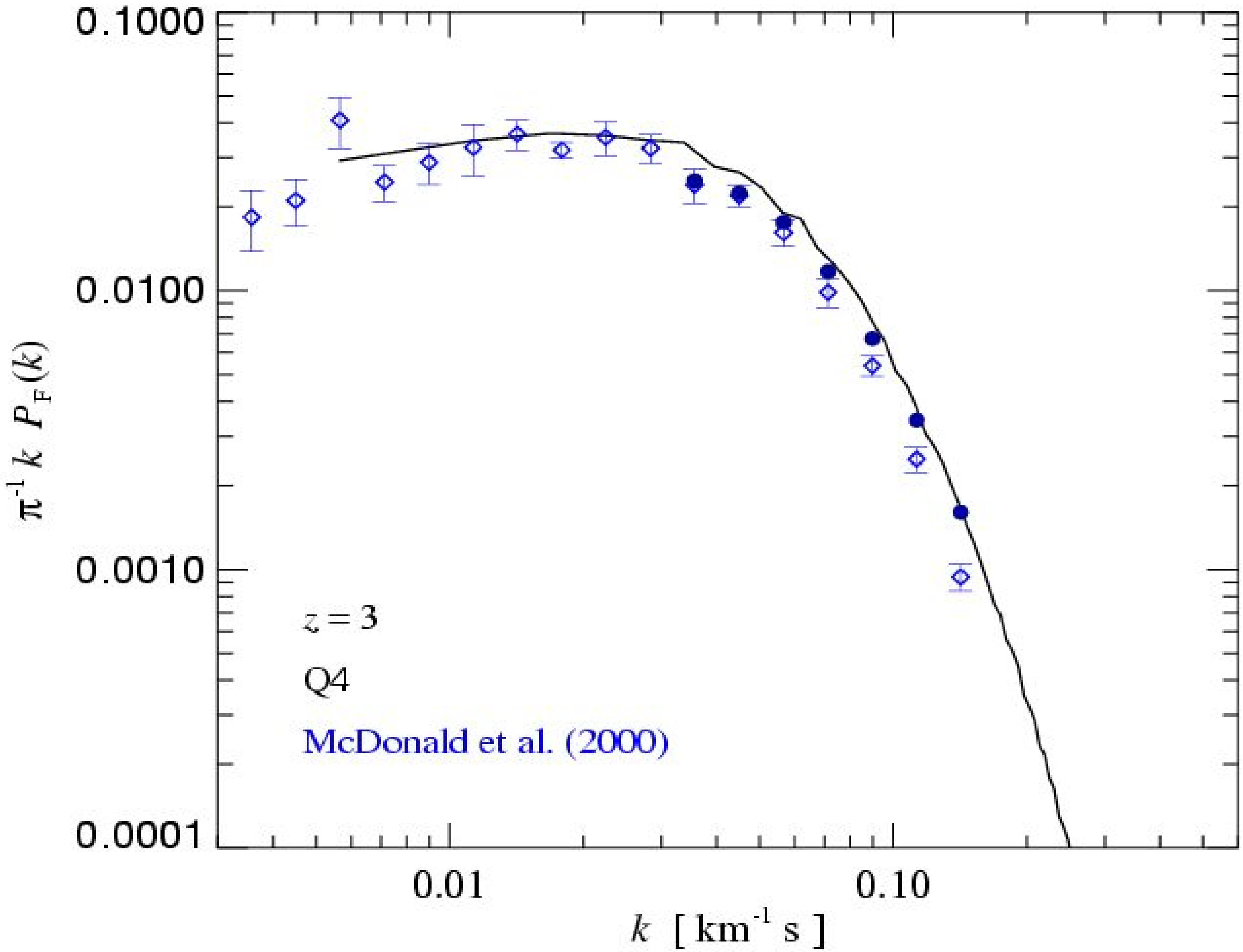

Projected metallcity maps reveal a highly non-uniform enrichment pattern

PROJECTED MEAN GAS METALLICITY

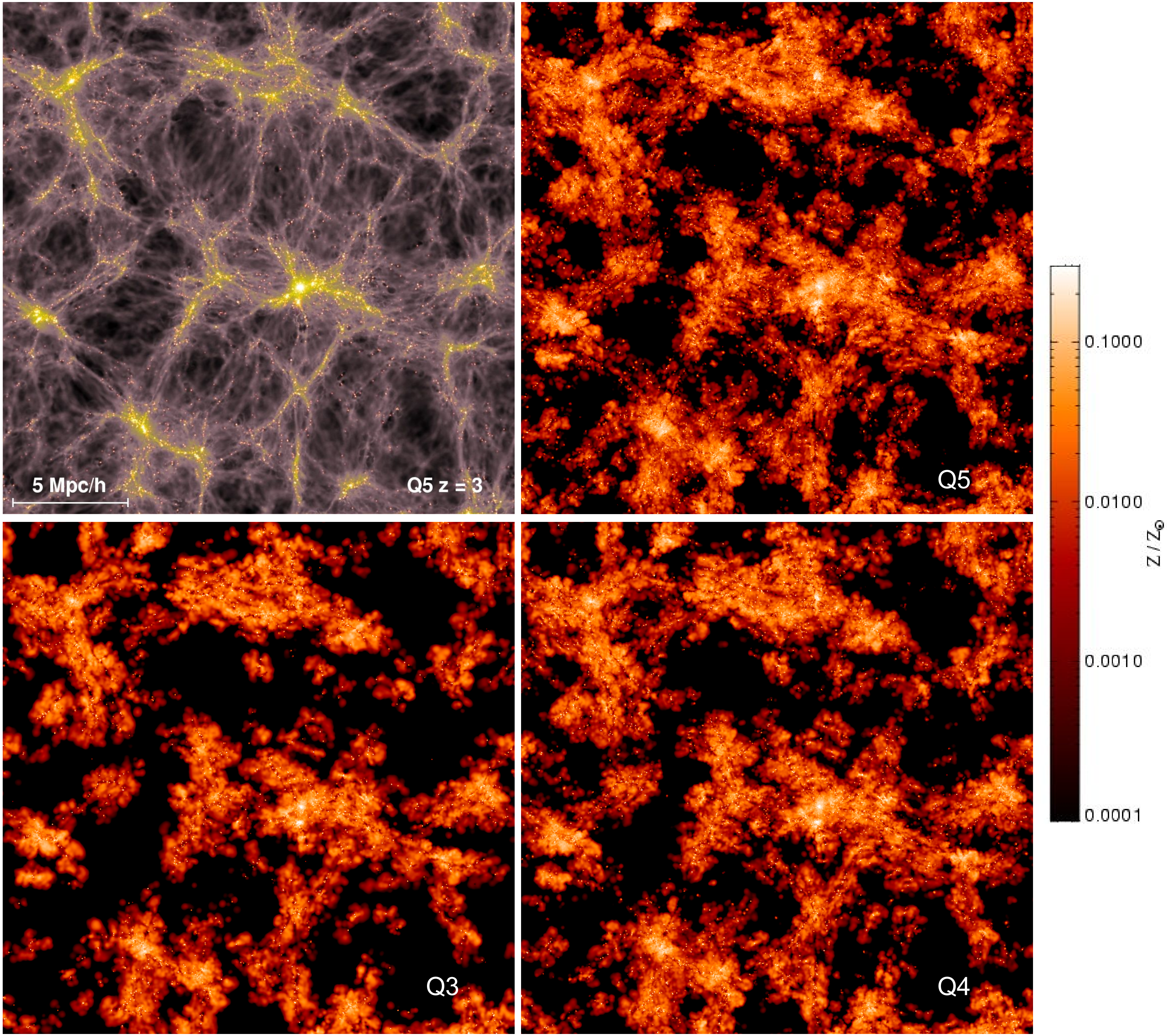

Metal enrichment by winds establishes a bimodal metallicity-density distribution

METAL ABUNDANCE AS A FUNCTION OF GAS OVERDENSITY

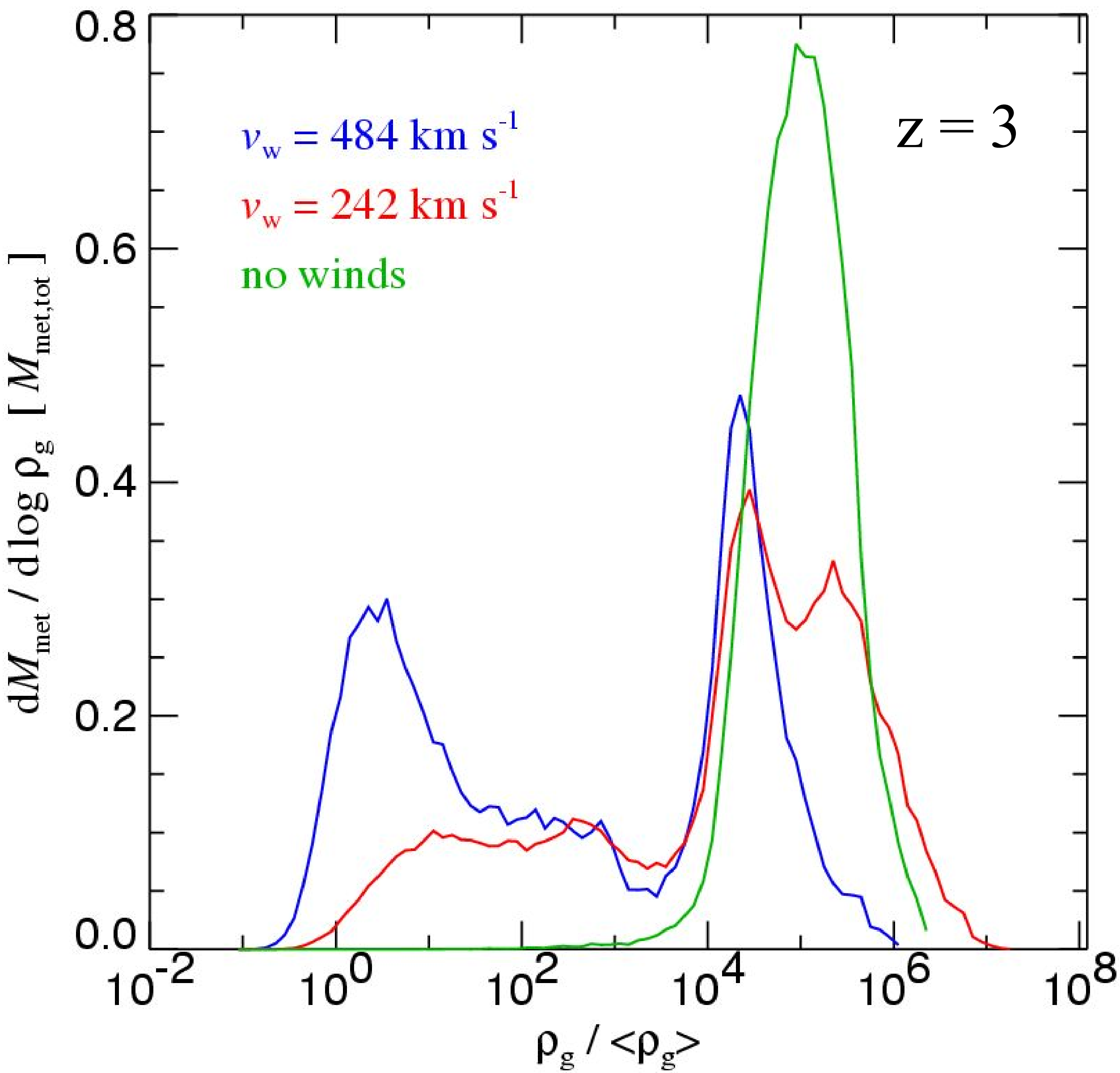

The transport of metals by winds appears to be well resolved by our simulation technique, but full convergence requires high resolution

METAL ABUNDANCE VERSUS GAS OVERDENSITY AT DIFFERENT RESOLUTIONS

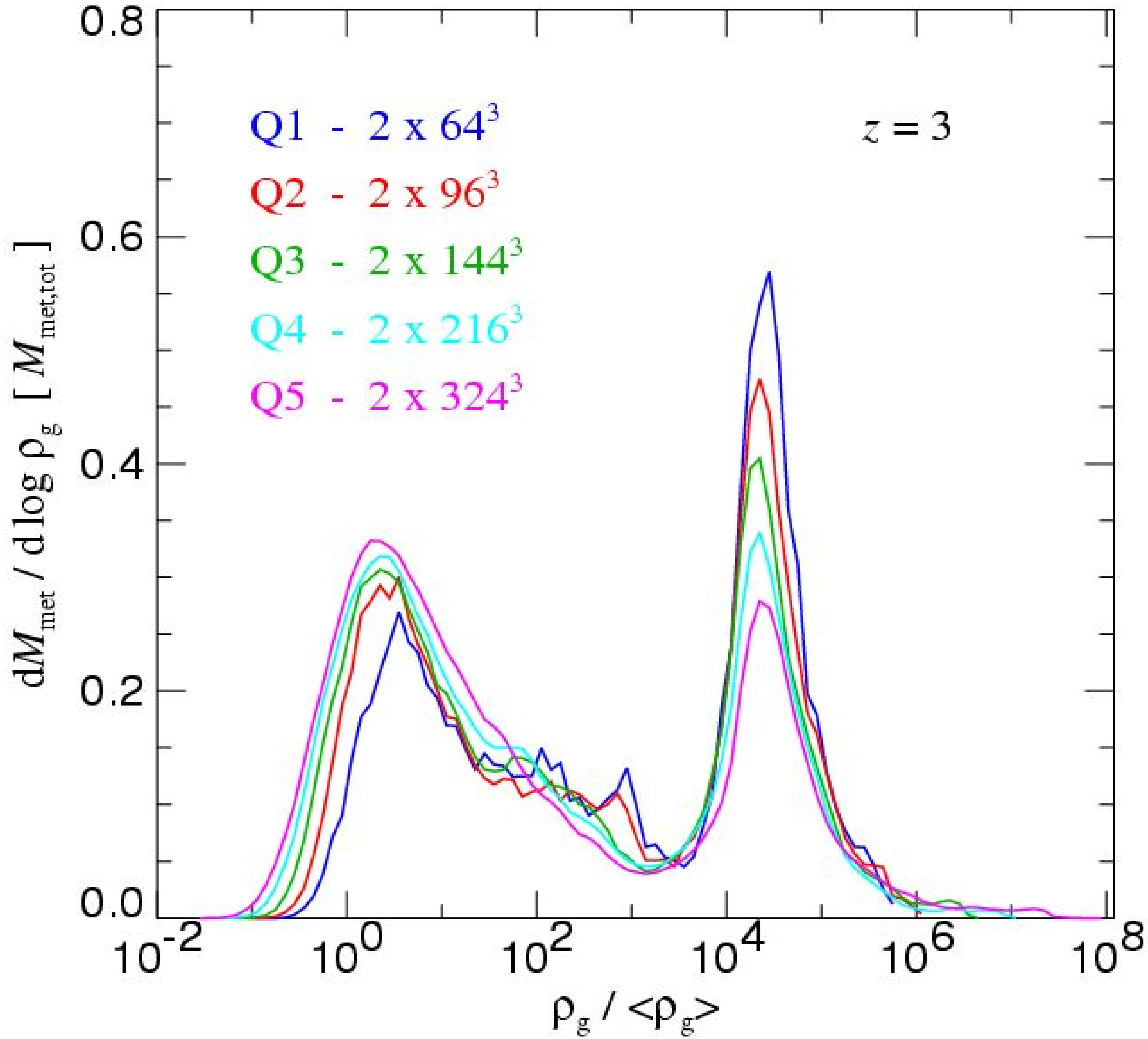

Similarly, it is challenging to obtain a numerically converged result for the volume fraction heated by galactic winds

DIFFERENTIAL VOLUME DISTRIBUTION AS A FUNCTION OF TEMPERATURE

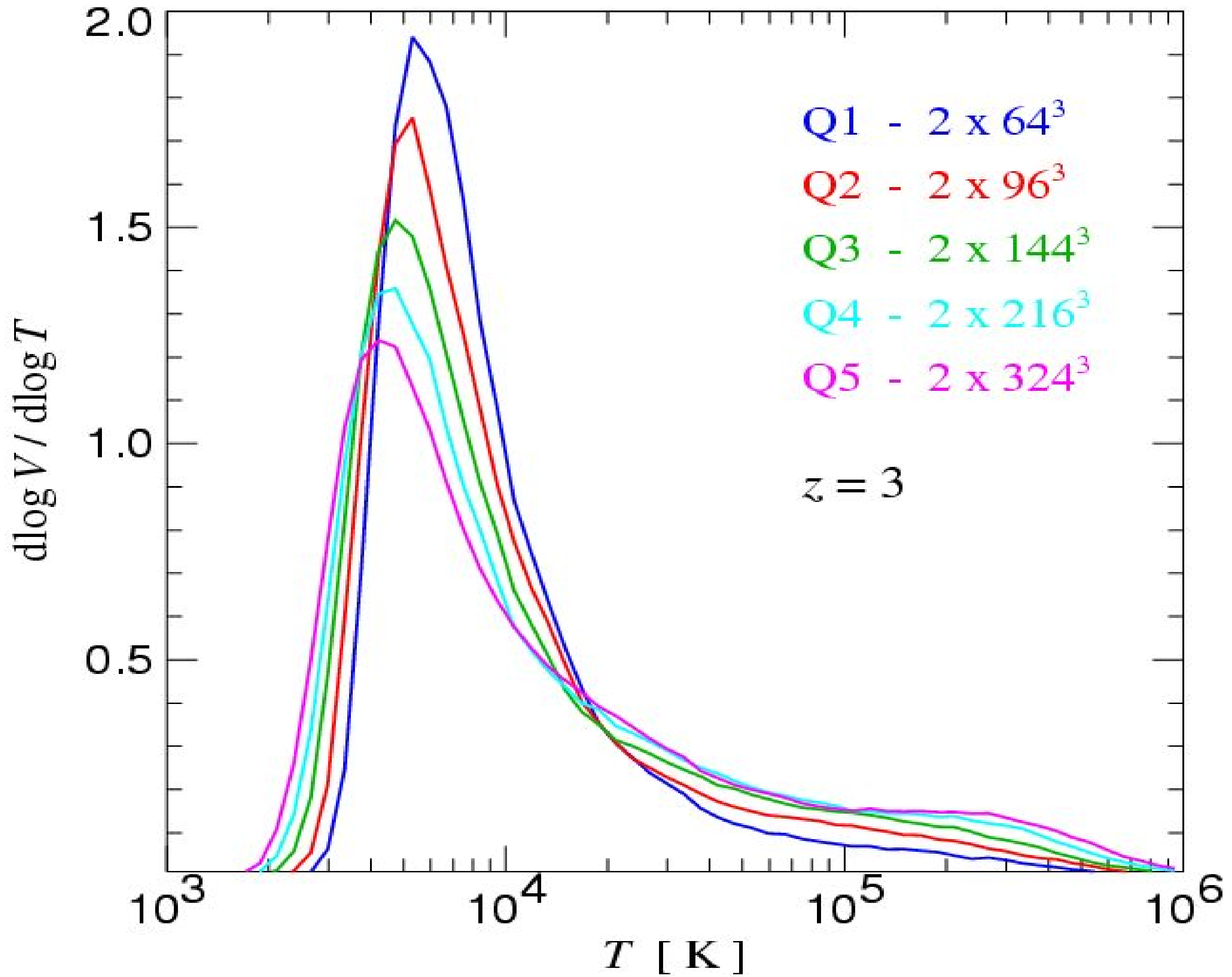

Galactic winds may enrich a sizable fraction of the total volume, while without them the IGM remains completely pristine

POLUTED VOLUME FRACTION

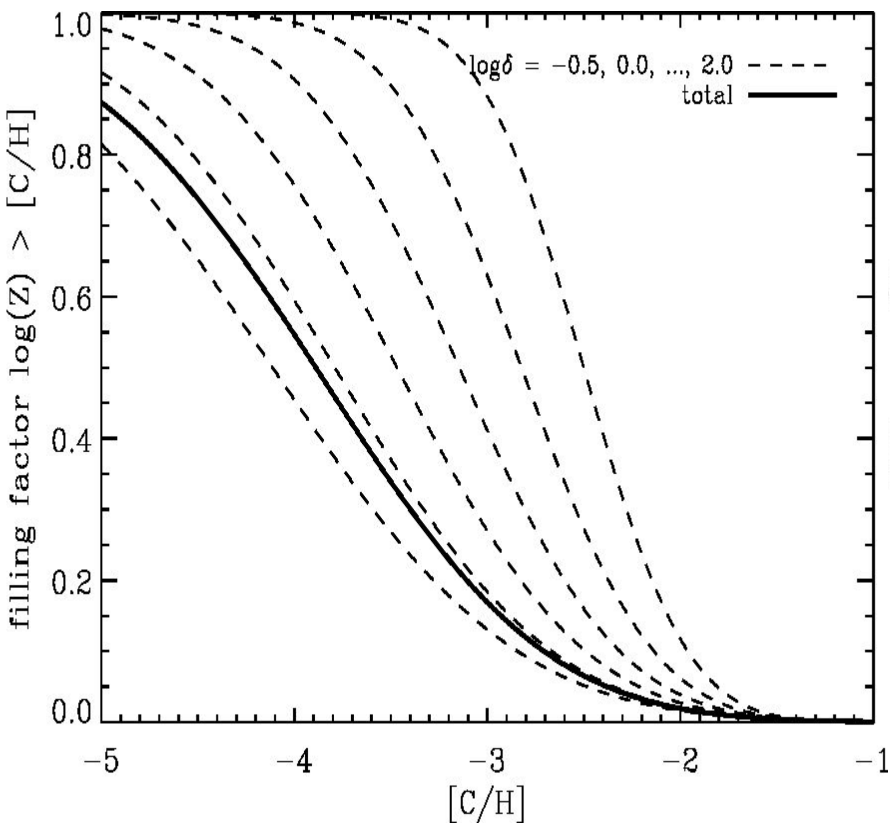

Schaye et al. (2003)

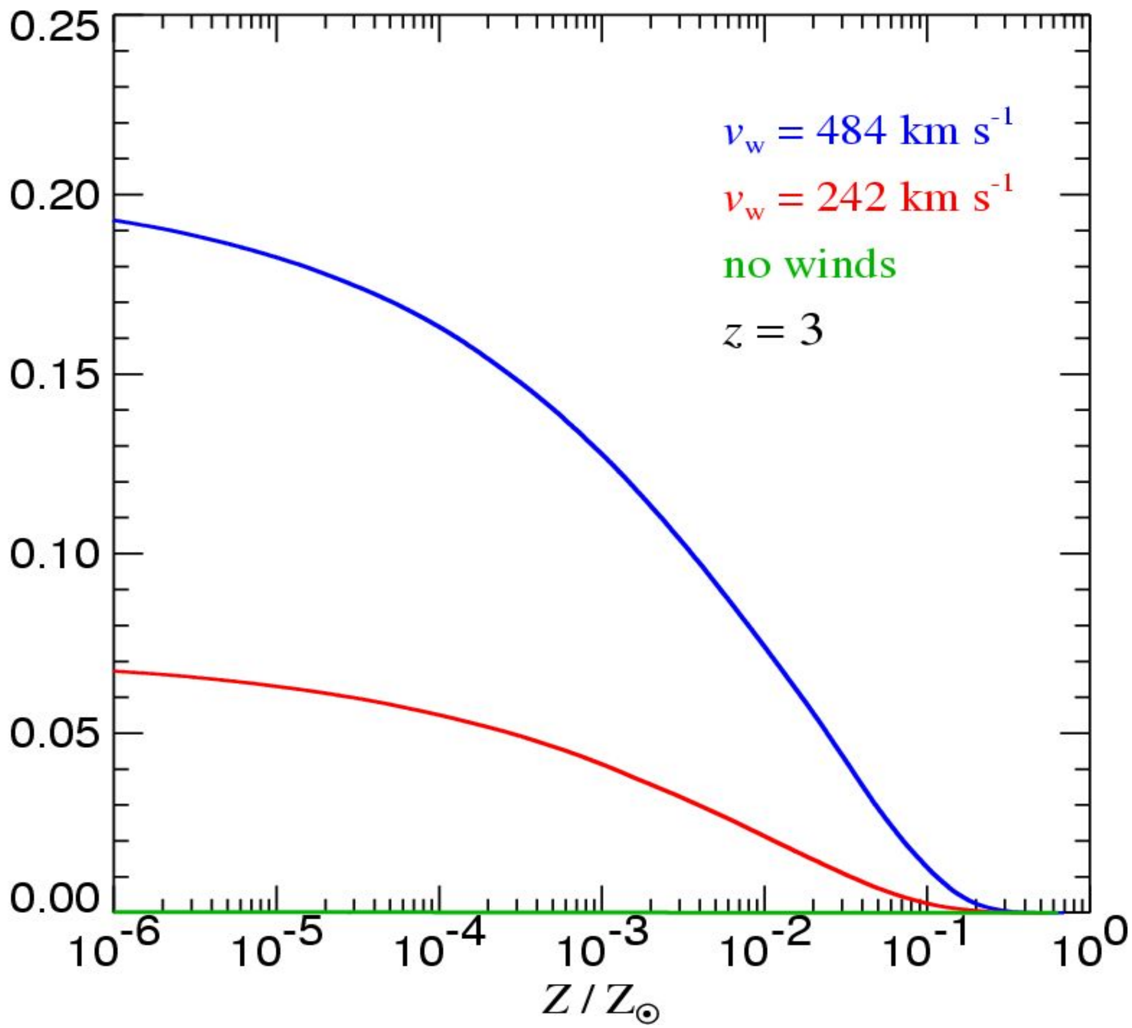

Winds can enrich the low-density IGM to levels suggested by obervations of the Lyman-α forest

MEAN NEUTRAL-WEIGHTED METALLICITY AS A FUNCTION OF OVERDENSITY

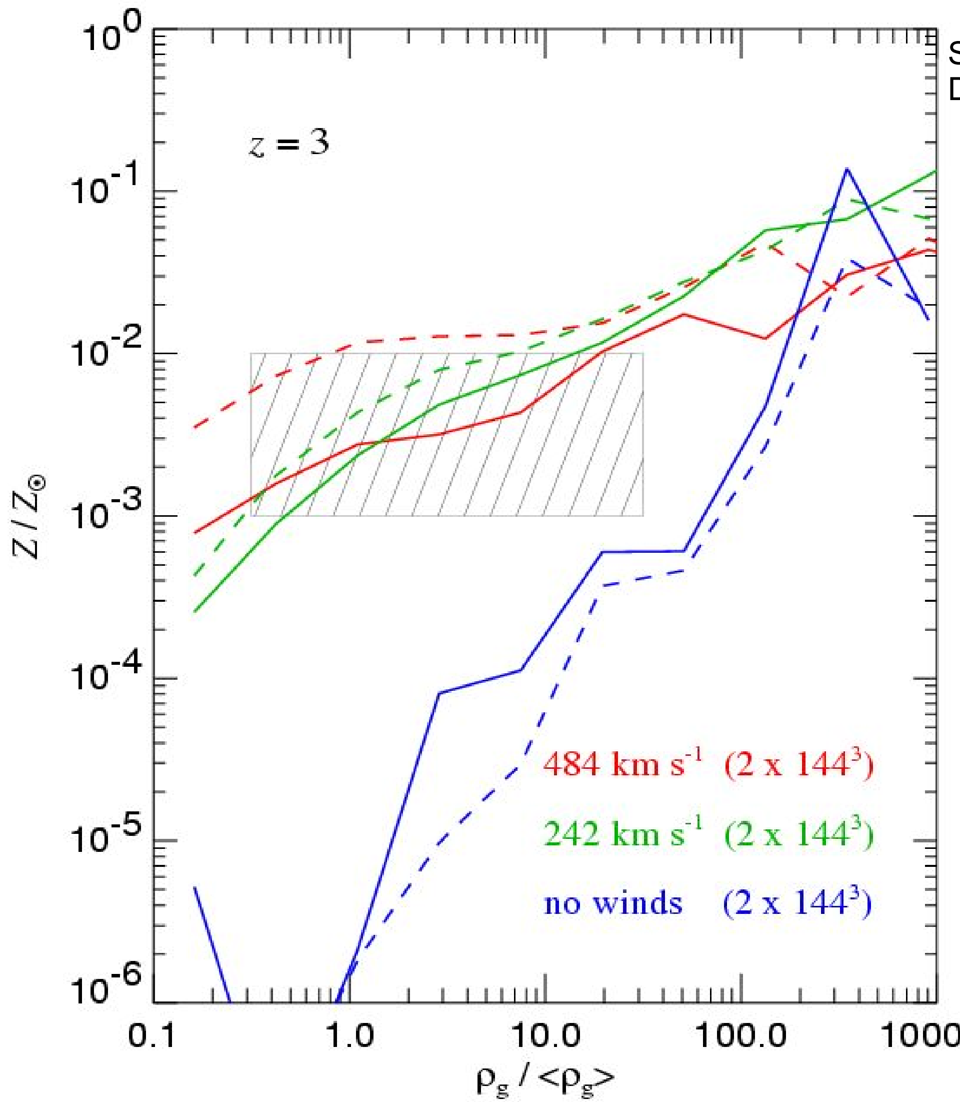

Solid lines: weighted by neutral gas mass
Dashed lines: weighted by full gas mass

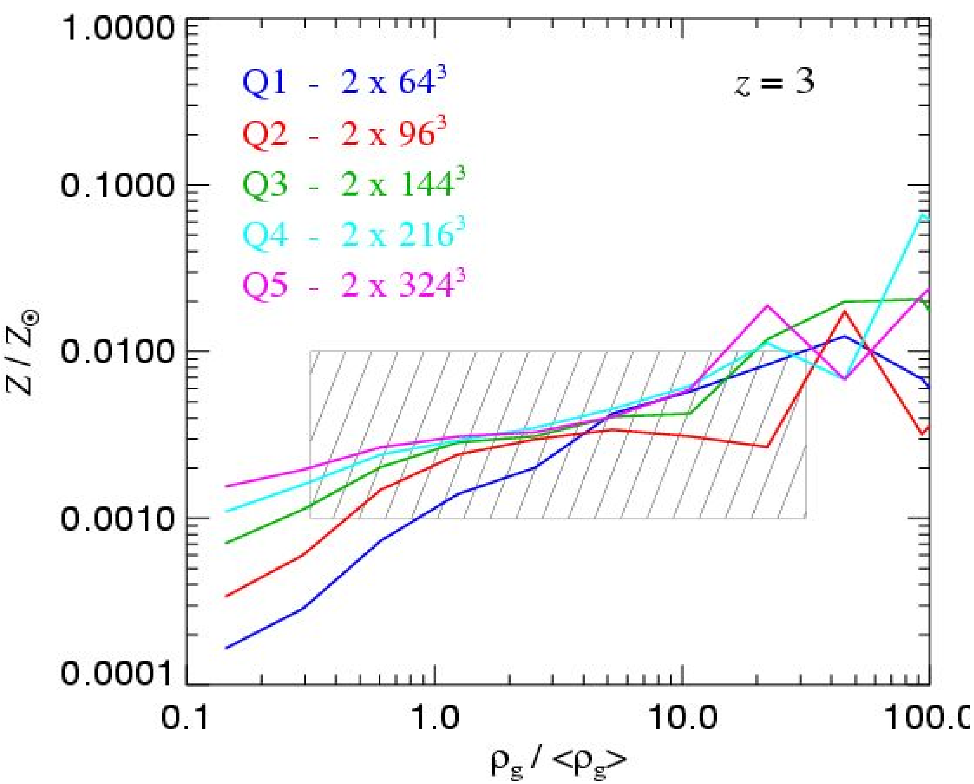

Weak magnetic fields are ubiquitious in clusters of galaxies

EVIDENCE FOR MAGNETIC FIELDS IN CLUSTERS

- The **synchrotron emission** of relativistic electrons in radio halos provides direct evidence for magnetic fields of 0.1-1 μG
- **Faraday rotation measurements** of polarized radio sources in or behind clusters provide significant evidence for fields up to 1-10 μG in the cores of non-cooling flow clusters
- **Outside clusters**, only upper limits for the EGMF strength are available. They are at the level of 10^{-9} – 10^{-8} G for field extending over cosmological distances (coherence length 50 to 1 Mpc)

The origin of intracluster magnetic fields is unknown.

Three classes of models have been proposed to explain their origin:

- **Magnetic field produced at low redshift** locally in galaxies and AGN, and then **expelled** with galactic winds or outflows. EGMF should be concentrated in clusters in this model.
- **Magnetic seed field is generated earlier at high redshift** (either by dwarf galaxies/early quasars, or cosmological origin), and the strength of MF clusters is largely determined by **amplification during cluster formation**.
- **Biermann battery process** at merger shocks. Problem: Can only produce ~10^{-21} G. Only works when a susequent highly efficient boost by a **turbulent dynamo** is invoked.

Magnetic fields can be studied with cosmological SPH simulations

MAGNETIC FIELD FORMED FROM A HOMOGENEOUS SEED FIELD AT HIGH Z

Contrained Simulation of the Local Universe

ideal MHD, run with P-Gadget2

Seed field: 10^{-9} G at z=20,
corresponds to 2×10^{-12} G at z=0

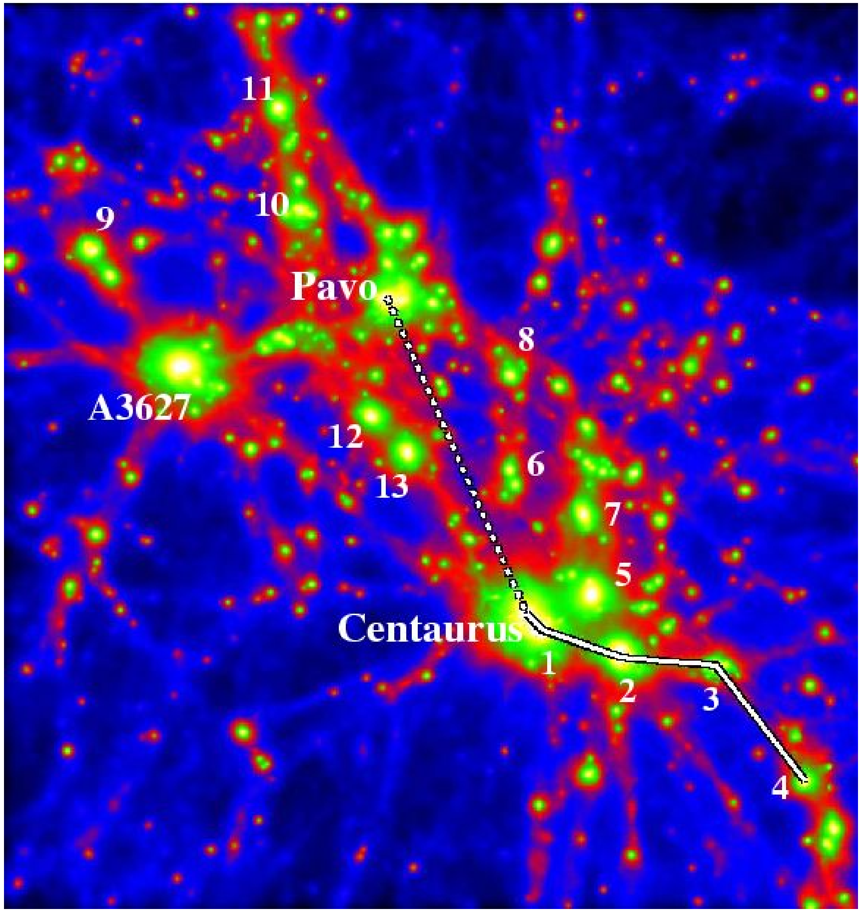

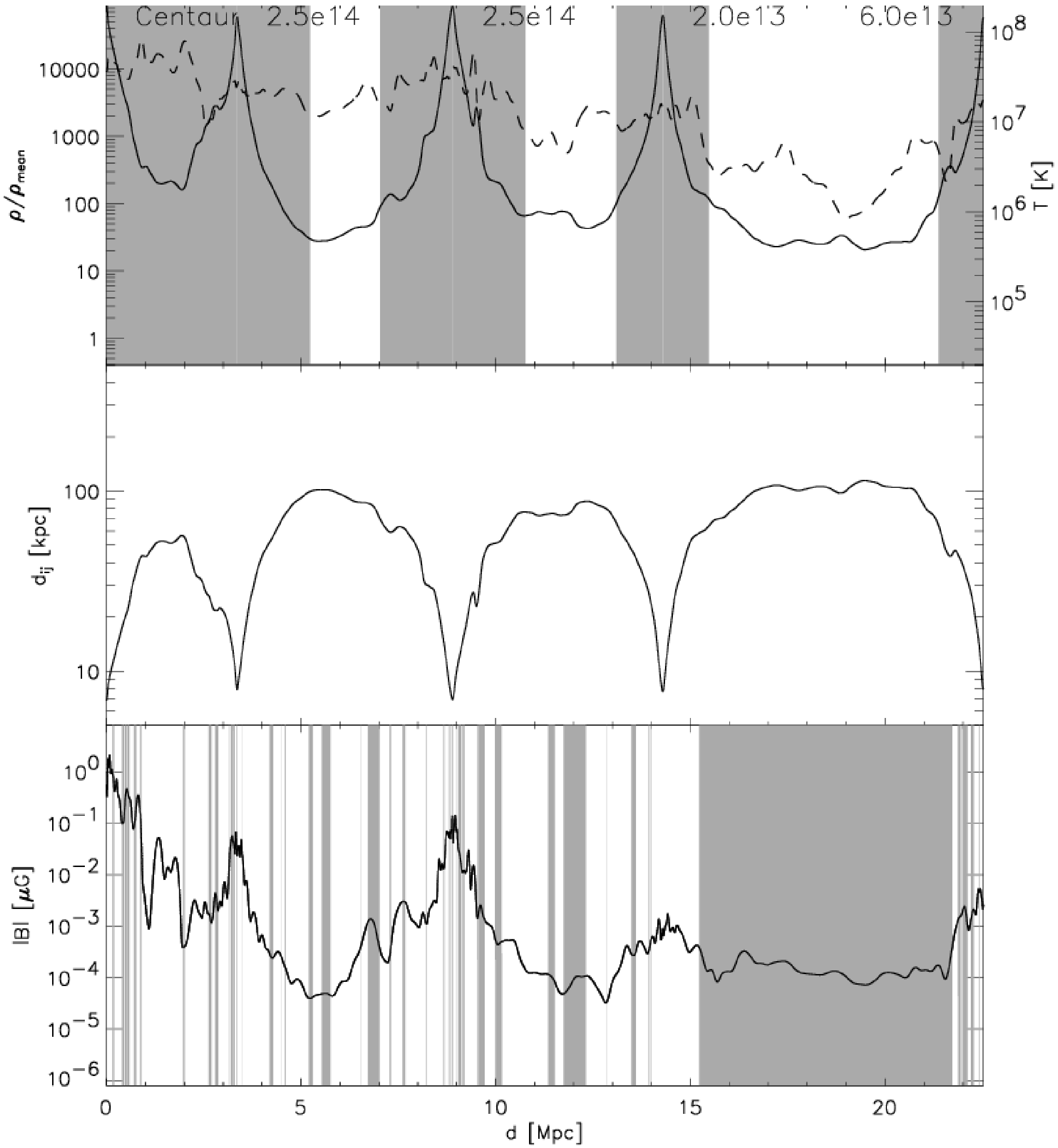

Dolag, Grasso, Springel & Tkachev (2004)

The simulated magnetic field in clusters of galaxies is in good agreement with rotation measurements and radio power-temperature correlations

COMPARISON WITH DATA ON RM AND RADIO POWER

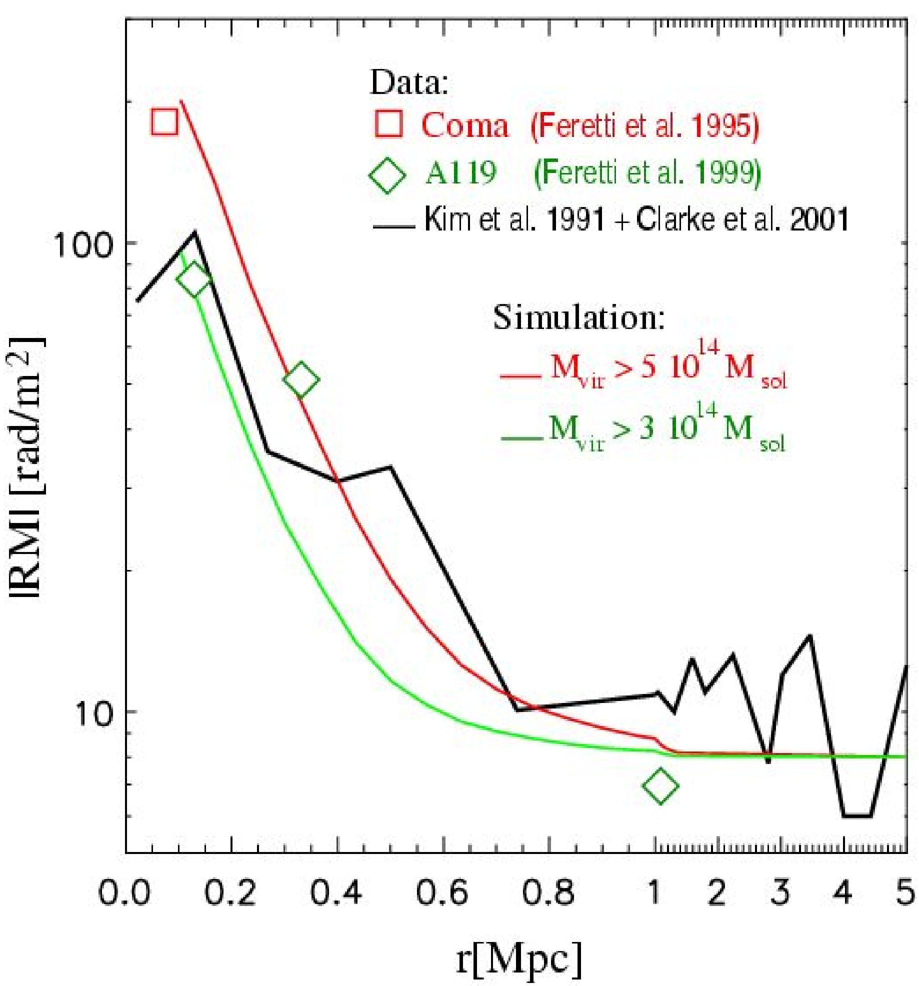

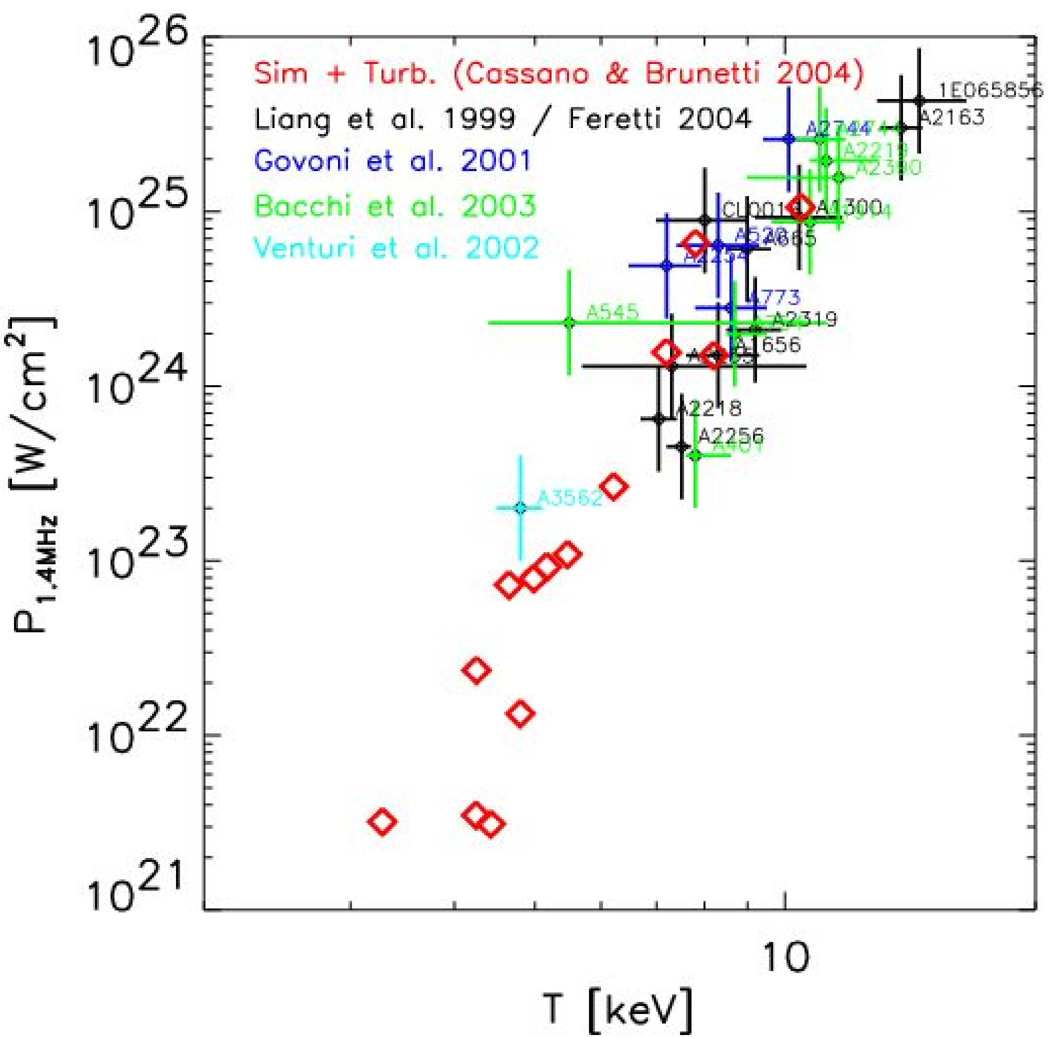

The magnetic field is strongly amplified in clusters of galaxies thanks to shear flows, establishing a correlation between B and cluster size

MAGNETIC FIELD AS A FUNCTION OF OVERDENSITY AND CLUSTER TEMPERATURE

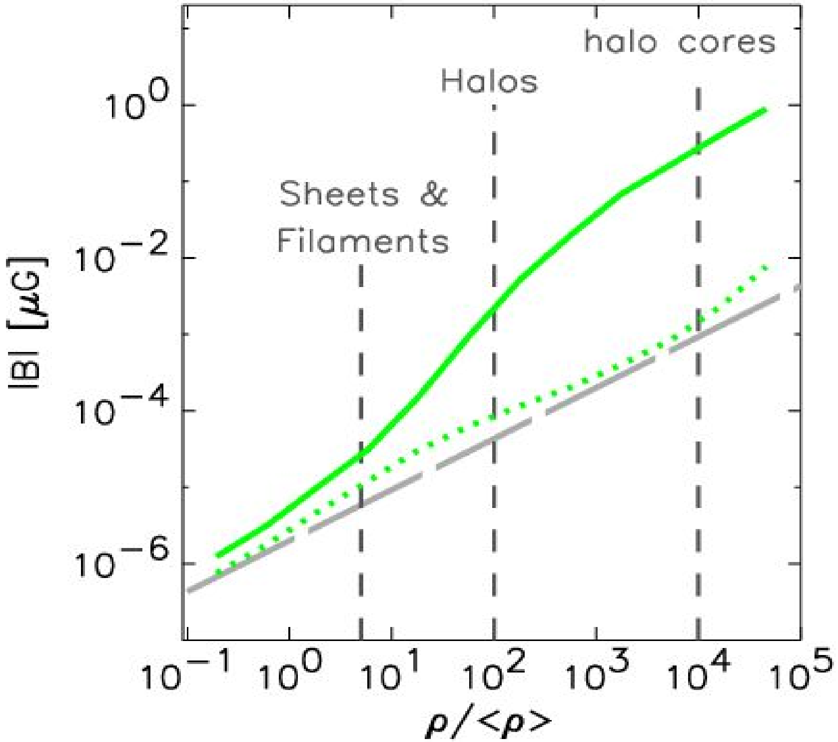

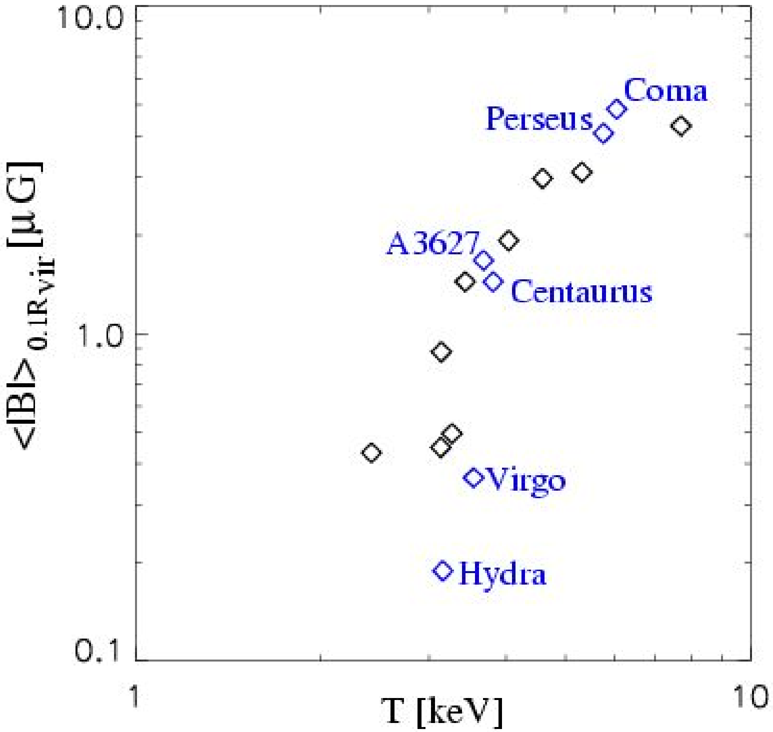

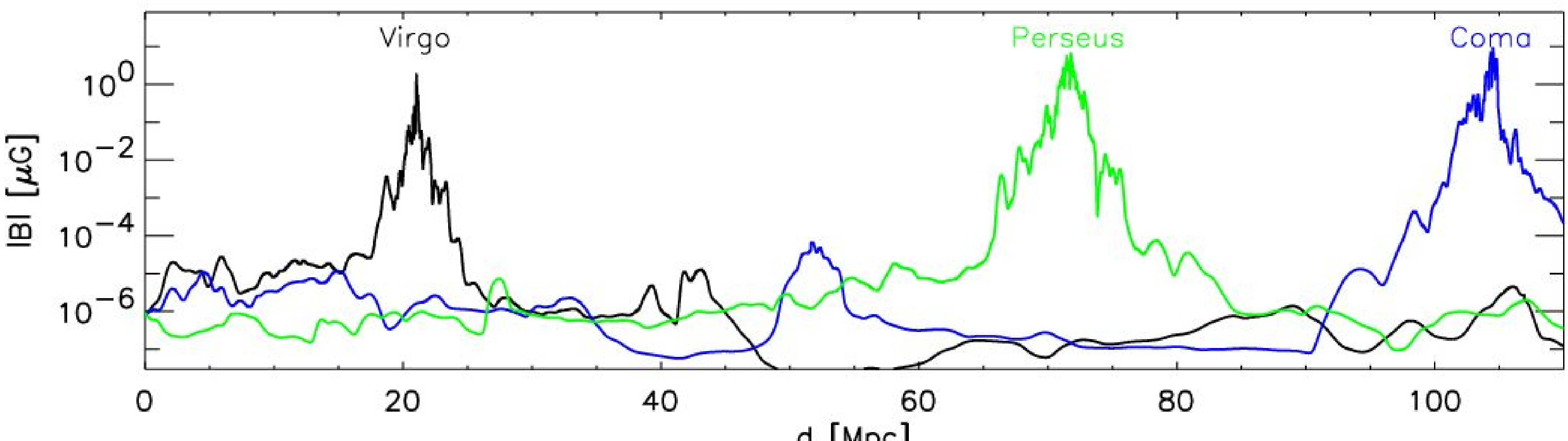

Weak magnetic fields are ubiquitious in the universe

DEFLECTION MAP OF UHECR IN THE LOCAL UNIVERSE

Deflection angles for protons with arrival energies 4 x 10^{19} eV,
within a radius 110 Mpc around the Galaxy

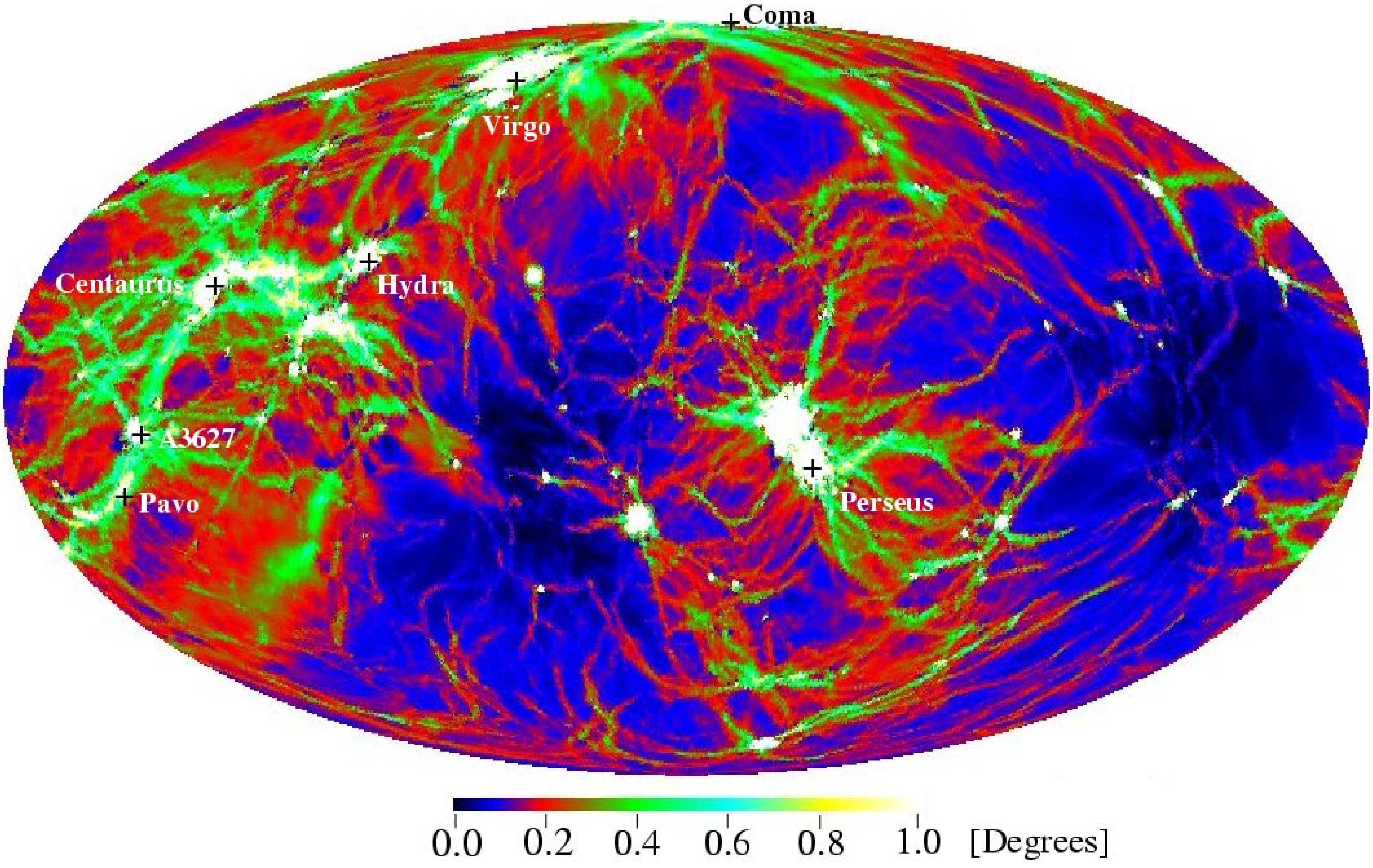

Weak magnetic fields are ubiquitious in the universe

DEFLECTION MAP OF UHECR IN THE LOCAL UNIVERSE

Deflection angles for protons with arrival energies 4 x 10^{19} eV, within a radius 25 Mpc around the Galaxy

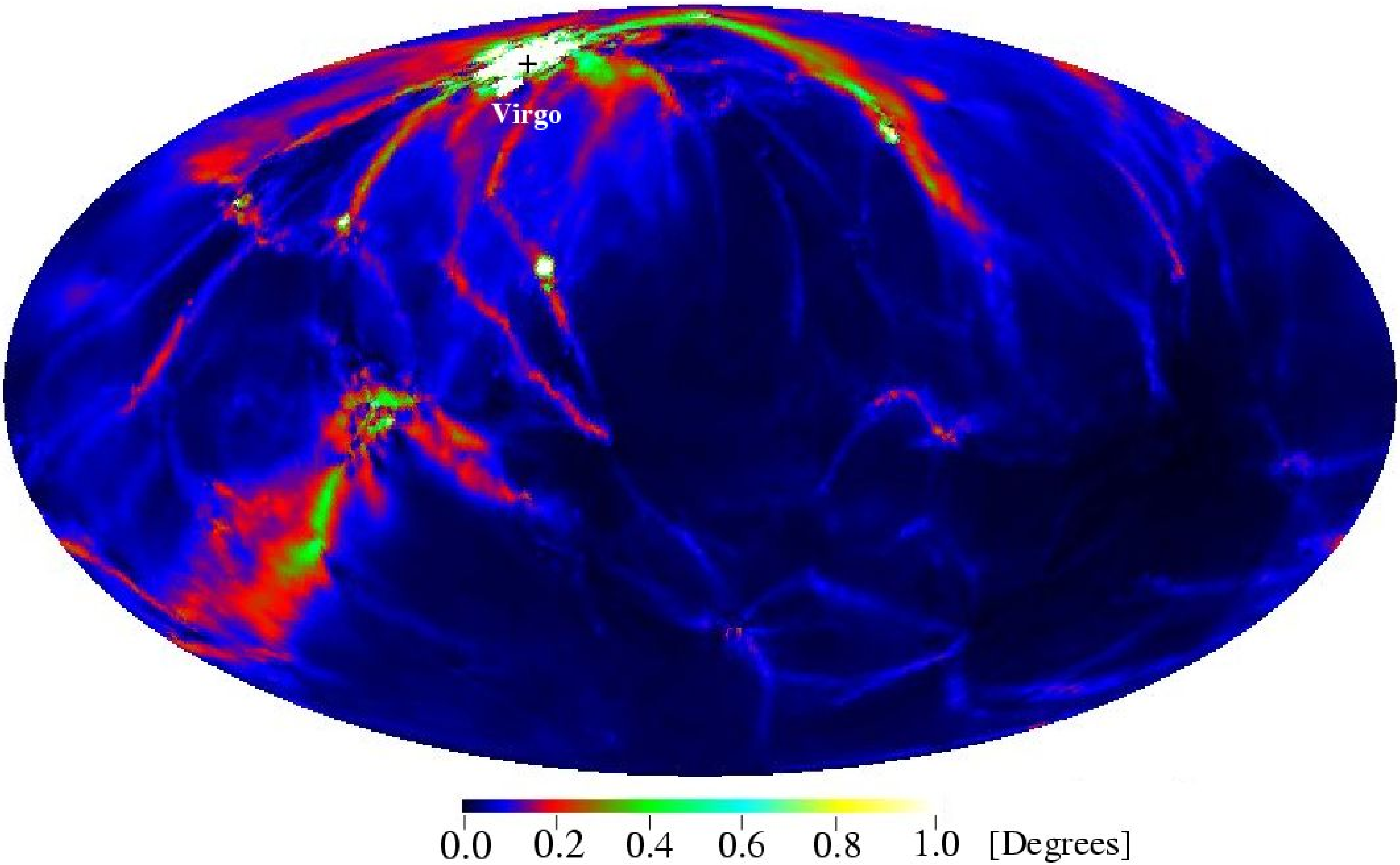

Deflection angles stay small for large fractions of the sky out to cosmological distances – astronomy with UHECR arrival directions may be possible

CUMULATIVE FRACTION OF SKY ABOVE A DEFLECTION ANGLE

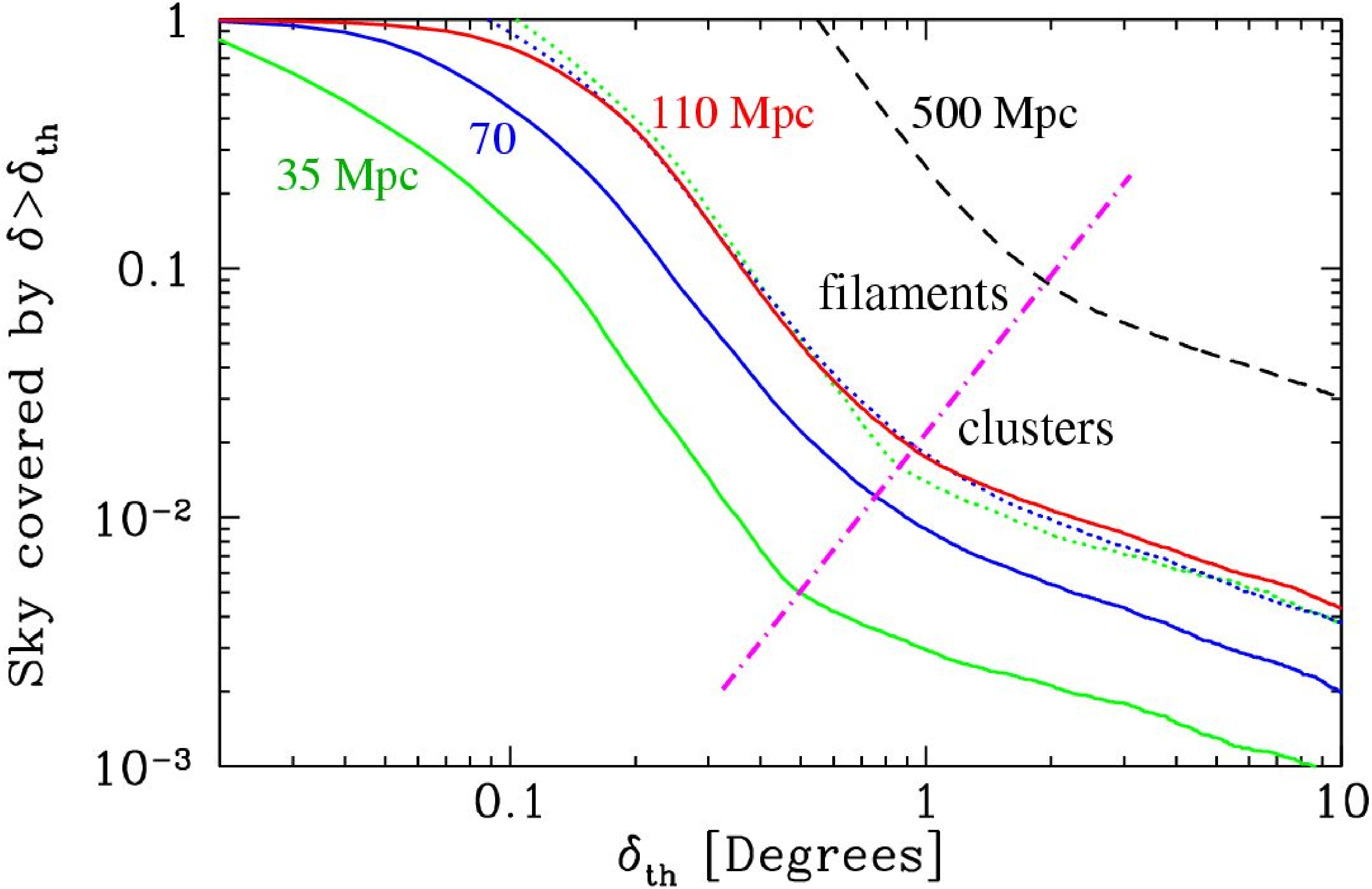

Conclusions I

- We have implemented new numerical methods which allow us to carry out large, high-resolution cosmological simulations of galaxy formation that track the growth of galactic supermassive black holes.

- The growth of black holes is self-regulated by AGN feedback. The relation between final black hole mass and halo size follows the Magorrian relation.

- Mergers of galaxies exhibit a complex interplay between starbursts and nuclear AGN activity. In a major merger, star formation and accretion can be terminated on very short timescales, with the black hole driving a strong quasar outflow.

- Remnants in galaxy mergers with black holes are relatively gas-poor, have low diffuse X-ray emission, show no star formation activity any more, and have close to perfect $r^{1/4}$ surface brightness profiles, even for gas-rich mergers.

- In major mergers, the BHs reach separations below 100 pc fairly quickly after galaxy coalescence. If hydrodynamical effects are indeed efficient in shrinking the binary further, the BHs should merge rapidly thereafter.

- Remnants of mergers with elliptical galaxies redden quickly. This may be related to the observed bimodal color distribution of galaxies.

Conclusions II

- Cosmological simulations of galaxy formation using sub-resolution models for the ISM are quite successfull. They allow a direct study of the effects of galactic winds and outflows, with the generation of winds being treated phenomenologically.

- Our simulation technique converges well for all first order properties of the Lyman-α forest, but full numerical convergence of the model predictions for metal-enrichment and heating of the IGM requires high resolution.

- Despite substantial influence on the star formation history, galactic outflows leave the Lyman-α forest essentially unaffected, even though they provide substantial metal enrichment and heating of the low-density IGM.

- About ~25% of the volume are heated and enriched with metals by redshift 3. The line-width distribution is not significantly modified by this heating. Without the inclusion of winds, the IGM stays pristine. Metals are not transported out of halos by merger processes.

Conclusions III

- Magnetic fields in clusters can be well reproduced with SPH MHD simulations starting from a primordial seed field.

- The cosmic magnetic fields is expected to produce sizable deflections of UHECR only over a small fraction of the sky. Pointing of UHECR sources should be possible.